*Instituto Andaluz de Ciencias de la Tierra (CSCI-UGR)*

*Departamento de Mineralogía y Petrología (Universidad de Granada)*

# "Variabilidad climática en el Mediterráneo Occidental durante el último ciclo glacial: impacto en la evolución cultural humana en el Sur de la Península Ibérica. "

"*Climatic variability in the Western Mediterranean during the Last Glacial cycle: impact on human cultural evolution in southern Iberia peninsula*"

Memoria presentada por el Licenciado en Ciencias Geológicas D. Francisco José Jiménez Espejo para optar el Grado de Doctor por la Universidad de Granada.

Esta Tesis Doctoral ha sido dirigida por la Dr. Francisca Martínez Ruiz, Investigadora Científica del CSIC en el Instituto Andaluz de Ciencias de la Tierra (CSIC-UGR)

En Granada, a Enero de 2007

Vº.Bº. del Director

El Doctorando

Fdo. Francisca Martínez Ruiz

Fdo. Francisco José Jiménez Espejo

Editor: Editorial de la Universidad de Granada
Autor: Francisco José Jiménez Espejo
D.L.: Gr. 71- 2007
ISBN: 978-84-338-4224-4

*Instituto Andaluz de Ciencias de la Tierra (CSCI-UGR)*

*Departamento de Mineralogía y Petrología (Universidad de Granada)*

# Variabilidad climática en el Mediterráneo Occidental durante el último ciclo glacial: impacto en la evolución cultural humana en el Sur de la Península Ibérica.

*"Climatic variability in the Western Mediterranean during the Last Glacial cycle: impact on human cultural evolution in southern Iberian peninsula"*

**Francisco José Jiménez Espejo**

Tesis Doctoral

Granada, 2007

**Francisco José Jiménez Espejo**
Instituto Andaluz de Ciencias de la Tierra (CSCI-UGR)
Departamento de Mineralogía y Petrología-Universidad de Granada. Facultad de Ciencias
Avda.Fuentenueva s/n, 18002-Granada(España)
e-mail: fjjspejo@ugr.es

# CONTENTS


**ABSTRACT / RESUMEN** ..... vi

**I. INTRODUCTION AND OBJECTIVES** ..... **1**

**I.1 Introduction** ..... **3**

**I.2 Objectives** ..... **8**

**II. MATERIALS AND SITE SETTING** ..... **11**

**III. METHODS** ..... **21**

**III.1. Core analyses** ..... **23**

III.1.1. Core description ..... **23**

III.1.2. Smear slides ..... **23**

III.1.3. Magnetic susceptibility ..... **23**

III.1.4. XRF-Scanner ..... **24**

**III.2. Core sampling** ..... **26**

III.2.1. U-channels ..... **26**

III.2.2. Discrete sampling ..... **26**

**III.3. Mineralogical analyses** ..... **27**

III.3.1. X-ray Diffration (XRD) ..... **27**

III.3.1.1. Bulk sample preparation ..... **27**

III.3.1.2. Separation of clay fraction ..... **28**

III.3.1.3. X-Diffraction anayses ..... **29**

III.3.1.4. Qualitative mineral study ..... **30**

III.3.1.5. Semi-cuantitative mineral study ..... **30**

III.3.2. FE-SEM ..... **31**

III.3.3. HR-TEM ..... **32**

**III.4. Geochemical analyses** ..... **32**

III.4.1. X-ray Flourescence (XRF) ..... **32**

III.4.2. ICP-MS ..... **33**

III.4.3. Atomic Absortion (A.A.) ..... **34**

III.4.4. Total Organic Carbon (TOC)..... **35**

III.4.5. Biogenic silica..... **36**

III.4.6. Isotope analyses..... **36**

**III.5. Statistical analyses ..... 36**

**III.6. Dating $^{14}C$ ..... 36**

**IV. PALEOENVIRONMENTAL CHANGES IN THE WESTERN MEDITERRANEAN SINCE THE LAST GLACIAL MAXIMUM: HIGH RESOLUTION MULTIPROXY RECORD FROM THE ALGERO–BALEARIC BASIN**, Jimenez-Espejo, F.J., Martinez-Ruiz, F., Sakamoto, T., Iijima, K., Gallego-Torres, D., Harada. N. ..... **41**

**IV.1. Introduction ..... 42**

IV.1.1. Oceanographic setting ..... **43**

**IV.2. Materials and setting ..... 45**

IV.2.1. Site description ……..…… **45**

IV.2.2. Age model and sedimentation rate ……..…… **45**

IV.2.3. Mineralogy …… **46**

IV.2.4. Geochemical Analyses …… **47**

IV.2.5. U, Mn, and Fe redox proxies ……..…… **48**

IV.2.6. Ba excess as a productivity proxy in the WMS ..... **49**

**IV.3. Results ..... 50**

IV.3.1. Barite and Total Organic Carbon(TOC) ..... **50**

IV.3.2. Oxygen and Carbon isotope Stratigraphy ..... **52**

IV.3.3. Mineralogy and major and trace elements ..... **54**

**IV.4. Discussion..... 55**

IV.4.1. Sea surface conditions as determined by stable isotopes **55**

IV.4.2. Paleo-redox conditions and diagenetic processes in the Algero-Balearic basin ..... **56**

IV.4.3. The last redox-event (LRE): paleoceanographic implications ..... **57**

IV.4.4. Pre-Holocene productivity in the Algero-Balearic basin **57**

IV.4.5. Holocene productivity ..... **59**

IV.4.6. Eolian input ..... **60**

IV.4.7. Detrital proxies during the YD ..... **60**

**IV.5. Conclusions ..... 61**

**V. CLIMATE AND OCEANOGRAPHIC VARIABILITY IN THE WESTERNMOST MEDITERRANEAN SINCE THE LAST GLACIAL MAXIMUM: DETRITAL INPUT, VENTILATION AND PRODUCTIVITY FLUCTUATIONS,** Jiménez-Espejo, F.J., Martínez-Ruiz, F., Gonzalez-Donoso, J.M., Linares,D., Romero, O., Rueda-Ruiz, J.L., Sakamoto, T., Gallego-Torres, D., Ortega-Huertas, M. ..... **65**

**V.1. Introduction ..... 66**

**V.2. Site setting ..... 69**

V.2.1. Oceanographic setting ..... **69**

V.2.2. Core location ..... **70**

V.2.2.1. Core sampling ..... **71**

V.2.2.2. Age model ..... **72**

V.2.2.3. Mineralogy ..... **73**

V.2.2.4. Geochemical analyses ..... **73**

V.2.2.5. Isotopic measurements ..... **75**

**V.3. Results ..... 77**

V.3.1. Ba excess and TOC ..... **77**

V.3.2. Oxygen and Carbon isotope and SST variations …….. **79**

V.3.3. Mineralogy and major and trace elements …… **80**

**V.4. Discussion ……. 82**

V.4.1. Sea surface conditions …….. **82**

V.4.2. Paleoproductivity conditions …….. **84**

V.4.3. Fluvial input and nutrient supply …….. **85**

V.4.4. Paleo-ventilation reconstruction ……. **87**

V.4.4.1. LGM and H1 ……...…… **88**

V.4.4.2. H1 through YD ……... **90**

V.4.4.3. The Holocene …….. **91**

**V.5. Conclusions ……... 92**

**VI. CLIMATE FORCING AND NEANDERTHAL EXTINCTION IN SOUTHERN IBERIA: INSIGHTS FROM A MULTIPROXY MARINE RECORD,** Jiménez-Espejo, F.J., Martínez-Ruiz, F., Clive Finlayson, C., Adina Paytan, A., Tatsuhiko Sakamoto, T., Ortega-Huertas, M., Finlayson, G., Koichi Iijima, K., Gallego-Torres, D., Fa, D. **…….. 97**

**VI.1. Introduction ……. 98**

**VI.2. Materials and methods …….. 100**

VI.2.1. Site description and sedimentation rate ……... **100**

VI.2.2. Mineralogical and geochemical analyses ……. **101**

**VI.3. Results …….. 103**

VI.3.1. Paleoproductivity proxies …….. **103**

VI.3.2. Sea surface conditions obtained through stable isotopes …….. **104**

VI.3.3. Detrital and redox proxies …….. **106**

**VI.4. Discussion …… 108**

VI.4.1. Continental and marine env. in the WMS during MIS 3 **108**

VI.4.2. Ba excess as a climatic stability proxy ……... **109**

VI.4.3. Conditions during intervals of high Ba excess variability …….. **111**

VI.4.4. The role of climatic variability for archaic populations . **115**

VI.4.5. The southern Iberian Neanderthal habitat ……... **118**

VI.4.6. The end of the southern Iberian Neandertahals …….. **119**

VI.4.7. To what extent were climatic conditions really influential? ……. **121**

**VI.5. Conclusions ……. 122**

**VII. THESIS CONCLUSIONS ……. 127**

**VIII. AGRADECIMIENTOS …… 131**

**IX. REFERENCES …… 137**

**APPENDIX……... 157**

**ANNEXES**

**Annexe 1. "Filtration method" for semi-quantitative powder X-ray Difraction analysis of clay minerals in marine sediments.** Iijima, K., Jiménez-Espejo, F.J., Sakamoto, T., (2005).

**Annexe 2. Late survival of Neanderthals at the southernmost extreme of Europe.** Finlayson, C., Giles Pacheco, F., Rodríguez-Vidal, J., Fa, D., Gutiérrez López, J.M., Santiago Pérez, A., Finlayson, G., Allue, E., Baena Preysler, J., Cáceres, I., Carrión, J.S., Fernández-Jalvo, Y., Gleed-Owen C., Jiménez-Espejo, F.J., et al., (2006).

**ABSTRACT**

This study uses a multiproxy approach in order to reconstruct paleoclimate and paleoceanographic conditions and further understand the evolution of climate responses in the western Mediterranean during the last glacial cycle. In addition, the impact of the climate conditions on human cultural evolution in southern Iberia is also analyzed. The westernmost Mediterranean basins are studied, the Algero–Balearic basin and the Alboran sea basin, both key areas for further understanding of the relationships between the North Atlantic and the eastern Mediterranean basins. Selected marine cores are analyzed at high resolution and geochemical and mineralogical data are used as proxies for climate variability reconstruction.

In the Algero–Balearic, sediments from ODP Site 975 are analyzed and different proxies are used to establish a sedimentary regime (detrital elements, mineral composition), primary marine productivity (Ba proxies, TOC), sea surface conditions (stable isotopes) and oxygen conditions (trace metal ratios). Obtained data evidence that fluctuations in detrital element concentrations were mainly the consequence of wet/arid oscillations. Productivity appears to have been greatest during cold events, Heinrich 1 and the Younger Dryas. In contrast, the S1 time interval is not as marked by increases in productivity as it does in the eastern Mediterranean. Within this basin, a significant redox event is reported as a consequence of the major oceanographic circulation change occurring in the western Mediterranean at 7.7 ky BP. This circulation change led to reventilation as well as to diagenetic remobilization of redox-sensitive elements and organic matter oxidation. Comparisons between the paleoceanographic reconstruction for this basin and those from other Mediterranean basins support the hypothesis that across the Mediterranean there were different types of responses to climate forcing mechanisms.

A transect along the Alboran sea basin allows the reconstruction of the westernmost Mediterranean past oceanography. This reconstruction is also based on plancktonic oxygen isotope profiles, sea surface temperatures, and geochemical composition of marine sediments. This transect includes cores were collected at a key depth for detecting changes in the Mediterranean Outflow Waters (MOW) and redox conditions. Geochemical proxies confirm significant paleoproductivity, ventilation and detrital input fluctuations. Isotopes and sea surface temperature obtained by modern analogue techniques also show rapid cooling and warming within this time period. The comparison of Alboran sea records with those from the Algero-Balearic basin evidence strong gradient along the western Mediterranean. In the Alboran sea, productivity was always higher than in the Algero-Balearic basin, and fluvial input played an important role during wet periods such as the Bolling-Allerod and Early Holocene and also during the first part of YD and. Redox proxies evidence the changes in circulation patterns, and suggest that the main strength of the MOW was supplied by the eastern Mediterranean waters. A north-south gradient in the eastern Alboran is recognized, mainly promoted by the LIW flow. Low ventilation conditions prevailed until the time period between 7.9 and 7.2 ky cal BP, when probably started the current circulation pattern. The end of sapropel S1 deposition in the EMS around 6.2 ky cal BP is also recognized in southern Alboran cores indicating the high sensitivity of this area to LIW changes.

Finally, paleoclimate records from the western Mediterranean are used to further understand the role of climatic changes in the replacement of archaic human populations inhabiting South Iberia. Ba excces at ODP Site 975 is used to characterize marine productivity and then relate it to climatic stability. In addition, sedimentary regime and oxygen conditions at the time of population

replacement are also reconstructed. Climatic/oceanographic variations correlate well with Homo spatial and occupational patterns in Southern Iberia. It is demonstrated that low ventilation (U/Th), high river supply (Mg/Al), low aridity (Zr/Al) and low values of Baexcess coefficient of variation, may be linked with Neanderthal hospitable conditions. This piece of evidence further support recent findings which claim that Neanderthals populations continued to inhabit southern Iberia between 30 to ~28 ky cal BP and that this persistence was due to the specific characteristics of South Iberian climatic refugia.

**RESUMEN**

Esta Tesis incluye un estudio multidisciplinar mediante el cual se han reconstruido las condiciones paleoclimáticas y paleoceanográficas así como la evolución de las distintas respuestas climáticas en el Mediterráneo Occidental durante el último ciclo glacial. Además de ello, también se analiza el impacto que la variabilidad climática ha tenido en la evolución cultural humana en el Sur de la Península Ibérica. Se estudian las cuencas más occidentales del Mediterráneo, la cuenca Algero-Balear y la del mar de Alborán, ambas regiones clave para el entendimiento de las interconexiones Atlántico-Mediterráneo. Se han seleccionado distintos testigos de sedimentos marinos, que se han analizado a muy alta resolución utilizando indicadores mineralógicos y geoquímicas para la reconstrucción de la variabilidad climática.

En la cuenca Algero-Balear se han analizado sedimentos del sondeo 975 del "Ocean Drilling Program" y se han utilizado diversos indicadores del régimen sedimentario (elementos detríticos y composición mineralógica), productividad (contenido en Ba y materia orgánica), condiciones paleoceanográficas en la columna de agua (isótopos estables) y de oxigenación (relaciones de elementos traza). Los resultados obtenidos ponen de manifiesto fluctuaciones en la concentración de elementos y fases de origen detrítico como consecuencia de oscilaciones en la humedad y aridez. En cuanto a la productividad, se demuestra que fue mayor durante periodos fríos, eventos Heinrich y "Younger Dryas". Por el contrario, el intervalo de tiempo correspondiente al depósito del sapropel más reciente en el Este del Mediterráneo no corresponde a ningún incremento en la productividad. En esta cuenca si se registra un importante evento de reoxidación a los 7.7 miles de años como consecuencia del cambio en la circulación que en este momento tiene lugar. Este evento también condujo a la removilización de diversos elementos traza, así como a la oxidación de la materia orgánica. La comparación del registro estudiado en esta cuenca con los de otras cuencas

mediterráneas sugiere la existencia de marcadas diferencias en las respuestas climáticas a lo largo del Mediterráneo.

En la cuenca del Mar de Alborán se ha analizado un transecto Este-Oeste para la reconstrucción paleoceanográfica de esta cuenca. Dicha reconstrucción se basa igualmente en perfiles de isótopos estables, temperaturas de aguas superficiales y composición química de los sedimentos. Los testigos se han recuperado a distintas profundidades para el estudio de los patrones de circulación y de las condiciones de oxigenación. Los distintos indicadores utilizados ponen de manifiesto oscilaciones importantes en la productividad, ventilación del fondo y aporte detrítico a la cuenca. Las temperaturas de aguas superficiales señalan las principales oscilaciones climáticas de este periodo. La comparación de los perfiles obtenidos en la cuenca del mar de Alborán y la Algero-Balear indica que existen importantes gradientes a lo largo del Mediterráneo Occidental. En la cuenca del mar de Alborán la productividad fue siempre más elevada y aquí el aporte fluvial jugó un papel importante en dicha productividad en periodos húmedos como el "Bolling-Allerod" y el comienzo del Holoceno, así como al comienzo del "Younger Dryas". Los indicadores de oxigenación ponen de manifiesto cambios muy significativos en la circulación y oxigenación a lo largo del intervalo estudiado. Señalan además, que las aguas procedentes del Este del Mediterráneo también han sido un motor importante en la corriente de salida del Mediterráneo. Este hecho unido a la influencia atlántica ha dado lugar a gradientes Norte-Sur en esta cuenca. De hecho en las regiones del Sur de Alborán se reconocen eventos acaecidos en el Este del Mediterráneo como el depósito del sapropel más reciente. En general, hasta los 7.9-9.2 miles de años las condiciones de ventilación en esta cuenca fueron más reducidas, y a partir de este periodo aumentó la ventilación y se establecieron los patrones actuales de circulación.

Finalmente, los registros paleoclimáticos del Oeste del Mediterráneo también se utilizan para conocer el impacto que la variabilidad climática ha tenido en la evolución

cultural humana en el Sur de la Península Ibérica. En el caso de la cuenca Algero-Balear, las variaciones del contenido en Ba y por tanto en productividad se han usado como indicador de estabilidad climática, definiéndose distintos eventos climáticos de acuerdo a su coeficiente de variación. Igualmente se han usado indicadores del régimen sedimentario para reconstruir las condiciones en el periodo de remplazamiento de poblaciones en el Sur de Iberia. Así, se demuestra que condiciones de oxigenación reducidas, un alto aporte fluvial y valores bajos del coeficiente de variación del contenido en Ba se relacionan con las condiciones más favorables para las poblaciones de Neandertales. Ello demuestra que dichas poblaciones pudieron sobrevivir en el Sur de Iberia hasta los 28.000-30.000 años y que su extinción estuvo fuertemente condicionada por cambios medio ambientales.

# I. Introduction and Objectives

## I.1 INTRODUCTION

At present it is extensively known that climate change is one of the greatest environmental problems facing current society (e.g., Kyoto Protocol, 1997; UN-Nairobi climate change conference, 2006). Action Programmes and investments to address climate change have recently increased as its effects are becoming a major concern for most of countries (http://www.mma.es/portal/secciones/cambio_climatico/). Subsequently, a huge amount of research is devoted to the understanding of the climate system and global change. A vast amount of information is now available online through numerous websites of climate research Programmes and involved Institutions, as well as through the many projects dedicated to investigate causes and effects of the climate change (e.g., www.ipcc.ch/, www.igbp.net/, www.greenfacts.org/studies/climatechange/links/index.htm, www.itas.fzk.de/Zeng/InfUm/Infume.htm). Other than scientists, general public is becoming increasingly aware of climate effects. Decades ago global change was still a conjecture but some of its consequences such as reducing Arctic ice and permafrost, increasing occurrence of catastrophic events (dryness, storms, floods, etc.), increasing $CO_2$ concentration in the atmosphere, global warming caused by human activities, etc. are now well-documented (e.g., Andersen et al., 2004; Moreno Rodriguez et al., 2005). Effects on present human societies have encouraged a great part of climate research focused on present climate, however, the understanding of the climate system at larger scales than instrumental and historical data requires natural archives providing a record of past climate changes (Roberts, 1998; Wilson et al., 2000; Burroughs, 2005). Paleoclimate is therefore a key objective of climate studies for further understanding of the climate system. Different international Programmes (e.g., www.pages.unibe.ch; www.esf.org/publication/154/holivar.pdf), scientific projects as well as specialized scientific journals provide broad information of current research on past global changes. In spite of such amount of data and research, the synergic interactions of the climate system remain a complex challenge for the scientific community (e.g., Bond et al., 1993; Hong et al., 2003; Nederbragt et al., 2005, Rio et al., 2006).

In addition to the uncertainties of future consequences of the climate change, the evolution of the Earth's atmosphere, oceans, biosphere and cryosphere as well as past climate changes (extreme climates, rapid climate changes, climate responses of marine productivity, ocean circulation etc.) are not yet fully understood. In this regard, paleoclimate data may provide the important and necessary constraints on the functioning of the climate system and a comprehensive overview of the climate variability. At the same time, paleoclimate research can help to characterize Earth's past climate, including the forces that drive climate change and the sensitivity of the Earth's climate to those forcings. In addition, it will also contribute to the improvement of climate system models and predictions (www.ncdc.noaa.gov/paleo/paleo.html; Kageyama et al., 2005). Information derived from paleoarchives is the unique tool to extend the instrumental record and characterize how the climate system varies naturally in response to changing conditions and variable forcings. Paleorecords also provide the way to quantify how rapidly climate will respond to these forcings and what the impacts of climate change on ecosystems will be (Potts et al., 1996; Peñuelas and Fillella, 2001, Zavaleta et al., 2003). Description of climate variability can be now attained with a high degree of accuracy from different natural paleo-proxies such as tree-ring chronologies, stable isotopic thermometry, and a large suite of geochemical and sedimentological indicators obtained from ice and sediment archives (both continental and marine) (e.g., Thompson, et al., 1998; de Menocal et al., 2000; Martrat et al., 2004; Moberg et al., 2005). Natural archives provide different time scale resolution for climate variability, being both resolution and continuity of the records the essential points to consider in paleoclimate research (Dansgaard et al., 1993; Bond et al., 1997; Shackleton et al., 2000; Mayewski et al., 2005). Regarding this, marine records and paleoceanographical proxies have revealed as excellent tools for paleoclimate reconstructions (e.g., Hayes et al., 2005; Robinson et al., 2006; Cacho et al., 2006). Marine sediment records allow unravelling the responses of the different climate subsystems- atmosphere (eolian input fluctuations to marine basins), lithosphere (sedimentary regime), oceans (ocean ventilation rates, circulation and water oxygenation) and biosphere (productivity, plankton and benthos response)- to climate

variability (Elderfield et al., 2004). In fact, marine sediments contain a summary of all processes involved in sediment origin (Fig. I.1), thus providing information on such processes.

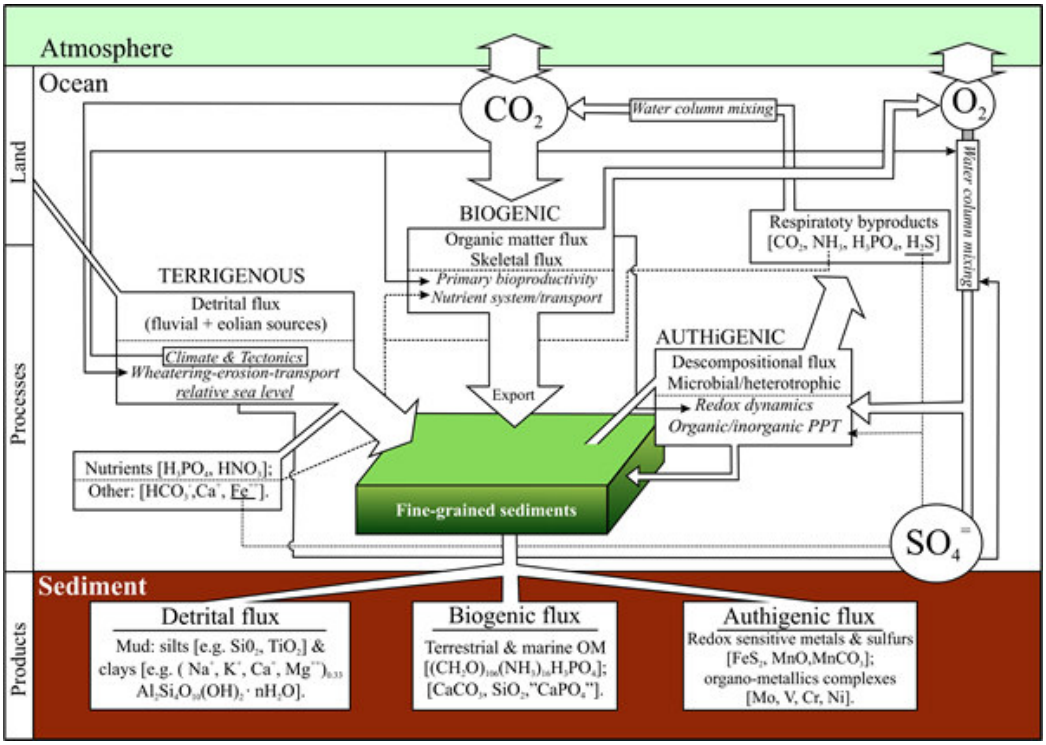


**Fig. I.1**. Conceptual model for the origin of mixed detrital-biogenic facies relating the three major inputs to the processes that control them. Controlling factors are shown in italics. Large and medium scale arrows represent fluxes of key components. Thin arrows illustrate relationships between major controlling factors and depositional processes and/or feedback. Dashed thin arrows apply to major nutrient fluxes only. Dotted thin arrows apply to major authigenic fluxes only. Modified from Sageman, (2004).

The database generated by climate proxies contains evidence of repeated large and regionally extensive changes in atmospheric and oceanic temperatures throughout time (e.g., Bianchi and McCave, 1999; Alley et al., 2002; Moreno et al., 2005b). Given the wide range of the geological time scales and spatial sensitivity of different regions, it is now known that certain time periods and time scales provide more useful information for understanding patterns of current climate variability. Similarly, highly sensitive

regions may provide more valuable paleoclimate information. Taking this into consideration and aiming to the understanding of the climate system and climate responses, this research was designed to analyze paleoarchives that may provide significant information on the factors that govern the spatial and temporal patterns of climate variability. The impact of such variability on ecosystems is also analyzed, with special interest on the impact of climate variability on human cultural evolution. In this context, the time period spanning the last glacial cycle, is considered to be the best time interval for such objectives since it is directly related to our present climate, and also because during this interval significant climate changes occurred at different time scales: decadal (NAO variability) to centennial (Little Ice Age, the Medieval Warm Period) to millennial scales (Heinrich Events, Bond cycles, Younger Dryas, 8.2 cold event). In terms of spatial scale, this research focuses in the Westernmost Mediterranean, because of its oceanographic and hydrographic characteristics is considered to be an excellent natural laboratory. Here high sedimentation rates together with a continuous sedimentation provide exceptional conditions to analyze global and regional climate changes at ultra-high resolution. Additionally, the Iberian Peninsula is particularly sensitive to rapid climatic changes at a decadal to multidecadal scale as currently evidenced by available instrumental data and regional models (Brunet and Lopez, 2001; Brunet et al., 2001). Concerning past climates, this sensitivity has also resulted in exceptional records of past climate changes at decadal to centennial and millennial scales, both during glacial (Dansgaard-Oeschger cycles) and interglacial periods (Cacho et al., 1999; Moreno et al., 2002; Roucoux et al., 2005; Naugthon et al., 2006). These changes have been mainly related to changes in the North Atlantic thermohaline circulation (e.g., Curry and Oppo, 1997; Paterne et al., 1999: Cacho et al., 2002; Sierro et al., 2005; Voelker et al., 2006).

Past climate changes affecting the western Mediterranean and the Iberian Peninsula has also influenced earlier human societies (e.g., Fabregas Valcarce et al., 2003; Finlayson et al., 2004; Mohen, 2006). It is evident that climate and biological evolution have interacted throughout Earth's history. The role of climate in the origin and adaptations of human beings clearly characterizes our past (Potts, 1996; Finlayson,

2005). For instance, the transition from hunting activities to agriculture or domestication has been influenced by significant climate changes such as the "Younger Dryas" (e.g., Dolukhanov, 1997; Weiss and Bradley, 2001; Brooks, 2006; Perry et al., 2006). Similarly, drastic changes in population density or migration of populations may have resulted from climate changes (e.g., Fitzhugh; 1997; Van Geel et al., 2001; Witz and Lemmen, 2003). It has been demonstrated that variations in monsoon activity in the Mediterranean Sea had clear consequences on the development of human civilization (e.g., Bar-Matthews et al., 1999; Cullen et al., 2000; Weiss, 2001; Diamond, 2005; Mohen 2006). The consequences might have been even stronger considering abrupt climate changes. Establishing, hence, the abruptness, amplitude and duration of theses variations can help to understand the evolution de past human societies. In the particular case of the Iberian Peninsula, the transition from hunting-collecting communities from the late glacial to producer communities in the Holocene was mainly driven by climate oscillations. Particular human groups still continued -apparently in concrete ecological niches- as predators contemporaneously to the producers development while other communities occupied similar areas (e.g., Asquerino, 1977; Zvelebil, 1986; Dearing, 2006; Mohen, 2006). This behaviour duality could have been caused by ecological changes in particular areas which prevented the continuity of predator modes forcing in some way the adoption of cattling and/or farming as way of subsistence. A better knowledge of the climate variability, especially that from the period between 9000 and 7000 years BP, would allow an improvement of the understanding of the diversity economy modes as well as explaining the above-mentioned dual ways of subsistence (Sanchez de las Heras et al., 2004).

Despite climate variations being proposed to explain the evolution and changes experiences by past societies, such theory has not been always accepted among archaeologists and historians, and many anthropologists reject climate explanations as being too simplistic. However, it seems out of discussion that climate fluctuations necessarily had social consequences (e.g., Dearing, 2006). In fact, cultures worldwide adopted similar solutions to similar problems, suggesting that human evolution have been a successful response to global environmental changes (e.g., de Menocal, 2001;

Brooks, 2006). Although it is not simple to understand driving mechanisms for human cultural evolution, understanding climate changes and their effects is crucial to understand how humans respond to environmental changes (e.g., Finlayson, 2004). Within this frame, this Thesis aims both the reconstruction of past environmental changes in the western Mediterranean and the advance in the understanding of climate effects on human cultural evolution in the Southern Iberian Peninsula.

Three different result chapters (IV, V and VI) present the main outcome obtained from a multiproxy approach that includes proxies for (*i*) paleoproductivity (Ba proxies and C isotope record), (*ii*) sedimentary regime (detrital elements, clay mineral assemblages), (*iii*) sea surface conditions (sea surface temperatures, oxygen isotope profiles), (*iv*) paleo-oxygen conditions (trace elements ratios) and (*v*) diagenetic evolution of sediment records (trace elements, mineral composition). Chapter IV presents a detailed multiproxy analysis at Site 975 (ODP Leg 161) and provides an excellent record of main climate oscillations affecting the western Mediterranean. Chapter V offers a detailed paleoclimate and paleoceanographic reconstruction of the westernmost Mediterranean, namely the Alboran Sea basin, an exceptional high-resolution archive for reconstructing climate oscillations. Besides, an East-West transect give the necessary information for understanding oceanographic variability, past circulation and Atlantic influence in the Mediterranean. Finally, Chapter VI deals with the impact of climate fluctuations on human cultural evolution and focuses on the impact of environmental changes on *Neanderthal* extinction. Two other published papers indirectly related with the aim of this thesis are included: one of them (Anexe I) deals on methodological techniques, and the other one (Anexe II) related with relevant multidiscplinary studies.

## I.2 OBJECTIVES

As commented in the previous section, climate change is currently one of the most up-to-date subjects in present-day scientific research. Paleoclimate investigations are a key piece of this research, providing the understanding of the climate system at

larger scales than instrumental data. This Thesis goaled within this framework, was motivated by two main facts: first the importance of the western Mediterranean for climate investigations at regional and global scales; and second the profound impact that climate change has had on human cultural evolution. To date, this has been poorly investigated because of the limited connections between archeologist and paleoclimatologists.

In this context, two are the main objectives of this Thesis:

1. The reconstruction of paleoceanographic and paleoclimatic changes spanning the last glacial-interglacial cycle in the western Mediterranean on the basis of geochemical and mineralogical proxies.
2. The evaluation of the impact that climate changes had on human cultural evolution in the Iberian Peninsula.

Regarding the first one, specific objectives are:

1.1. High-resolution analysis of selected marine cores in order to obtain geochemical and mineralogical profiles at millennial-to-centennial scales.
1.2. Identify and time-constrain climate oscillations occurred during the Last Glacial cycle, with special input on abrupt climate changes.
1.3. Analyze and evaluate the response of different climate system components to climate variability:
    i. Ocean response:
        a) marine productivity,
        b) sea surface temperatures,
        c) oxygen conditions, and
        d) circulation patterns.
    ii. Atmosphere response by reconstructing eolian input.
    iii. Lithosphere response by reconstructing sedimentary regime and fluvial input.

1.4. Correlation of the climate oscillations obtained from the studied archives with those from other paleoclimate records such as ice core, continental records, etc.

1.5. Identify and analyze cyclic climate oscillations.

Concerning the second one, the specific objectives are:

2.1. Relate different types and scales of paleoclimatie changes between the marine and terrestrial realms.

2.2. Analyze the possible link between a climate change and an evolutionary event identifying "synchronous" events.

2.3. Evaluate the impact of climate change on the disappearance of past population using *Neanderthal* extinction as case of study.

# II. Materials and site setting

In order to reach the proposed objectives, diverse marine records from the western Mediterranean have been selected. These records were obtained during four different oceanographic cruises:

- Ocean Drilling Program Leg 161
- Training Through Research-Unesco Programe: Cruise 9, Leg 3; Cruise 12, Leg 3; Cruise 14, Leg 2.

The targeted Sites belong to areas of high interest from both paleoceanographic and climatic point of views. These sites were expected to provide a high resolution record of paleoenvironmental conditions during the last glacial cycle as well as the reconstruction of circulation patterns in the westernmost Mediterranean basins.

Leg 161 was the second of two Mediterranean Legs form the ODP with both tectonic and paleoceanographic objectives (www-odp.tamu.edu/ publications/pubs. htm.) During this Leg, the JOIDES Resolution drilled a transect of six sites across the Western Mediterranean, from the Tyrrhenian Sea to the Alboran Sea. Two of these Sites, 975 and 974, in the South-Balearic Margin and Thyrrenian Sea respectively were selected for this study and samples from core 975B-1H and 974A-1H were requested to ODP. Sampling was done at the ODP Core Repository from Bremen (Germany).

TTR-UNESCO Program cruises (http://unesdoc.unesco.org/ulis/index.html), were conducted in the Alboran Sea Basin on board of the R/V Prof. Logachev combining both tectonic and paleoceanographic objectives from several Research Projects of the Andalousian Earth Science Institute (CSIC-UGR). Gravity cores were recovered in a west-east transect that allowed to obtain an exceptional record of climate variability in westernmost Mediterranean as well as establishing variations in the climate responses and circulation patterns (Figure II.1).

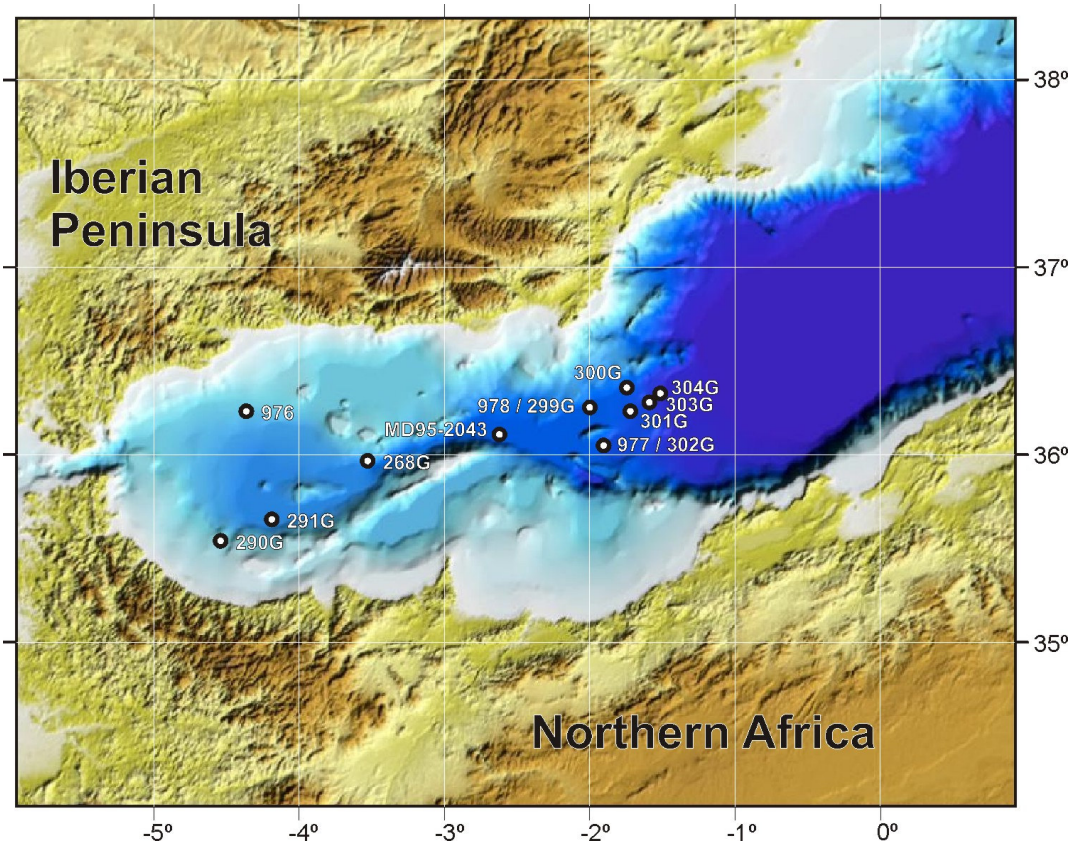


**Fig II.1.** Map showing studied cores and other related sites (ODP 976, ODP 978 and MD95-2043).

Core 974A 1H

ODP Leg 161 hole 974A was recovered in the central Tyrrenian Sea, about 215 km east of Sardinia Island (40º 21,364'N, 12º 08.506'E), on the lower slope of the Sardinian continental margin, in a water depth of 3470m. The total recovery of hole 974A was 9.81 m. The sediments recovered were described as nannofossil-rich clays to silty-clays, with an average carbonate content of 30%. They exhibit local bioturbation and thin to medium colour banding (light olive grey to pale yellowish brown to pale olive) and dark organic-rich layers. Numerous vitric ash beds are also present. (Comas, Zahn, Klaus et al., 1996).

Core 975B-1H

Site 975 is located on the South Balearic Margin between the Balearic Promontory (Menorca and Mallorca islands) and the Algerian-Balearic Basin (38º53.786'N, 4º30.596'E). The site was drilled at the edge of a small basin perched on the east-dipping slope of the Menorca Rise at 2,415 m depth. The total recovery for this core was 415 cm, the studied section was 380 cms. The studied sediments consisted in a nannofossil clay and olive grey calcareous silty clay with moderate colour banding without turbidite presence (Comas, Zahn, Klaus et al., 1996).

Core 977A 1H

ODP Leg 161 Hole 977A is located south of Cabo de Gata in the Eastern Alboran Basin, in a 36-km-wide graben bounded by the Yusuf Ridge and the Maimonides Ridge, at a water depth of 1984 m (36º01.907'N; 1º57.319'W). The recovery was 395 cm of sediments. The sediments were composed of nannofossil clays to silty-clays slightly bioturbated and with a carbonate content between 21 and 61%. This core has variable colours from light olive grey, olive grey to greyish olive (Comas, Zahn, Klaus et al., 1996).

Core 268G

This core was recovered during the TTR-9 campaign and was located to the South of the Djibuti Seamount, in the narrow east-west trend that communicate the West and East Alboran basins (35º 57.814' N, 03º 30.655' W; water depth: 1526 m). The total recovery of core 268G was 330 cm. The first 10 cm consisted in brownish soupy mud. The rest of the core consisted of a homogeneous greyish hemipelagic clayey, with thin foraminifera sandy levels that can be associate to turbidite layer between 290 to 275 cm. (Jimenez-Espejo, 2003)

Core 290G

This core is located in a mud volcano area in the southern margin of the Alboran Sea, close to the Granada mud volcano (35º34.612'N; 4º34.004W; water depth: 854 m). The total recovery of core 291G was 284 cm. The first 12 cm consisted of the usual brownish, soupy foraminifera rich mud. The rest of the core consisted of light olive grey hemipelagic mud, diffusely bioturbated with sparse shell fragments and black spots.

Core 291G

This core is located in the southern margin of the western Alboran basin (35º40.952N, 4º13.970W; Water depth: 1520 m) .The core recovered 351 cm of sediment. The first 2 cm were brown water saturated ooze. The rest of the core consisted of greyish brown mud, diffusely bioturbated, rich in foraminifera becoming light olive clay towards the bottom. This unit was interrupted at 70 cm by a 2 cm thick layer of fine to medium sand, extremely rich in foraminifers. At interval 306-314 cm a planar lamination of clayey silt, silty clay and clayey sand is observed.

Core 299G

It is located in the Eastern Alboran basin to the south of Cabo de Gata in a small east-west trending basin north of the Al-Mansour Seamount (36º13,897'N, 2º03,350W, water depth: 1938 m). The corer retrieved about 469 cm of sediments, predominantly brownish grey mud, with greenish grey clay in the lower 259 cm, and a small amount of silty admixture and foraminifera. Throughout the succession some patches filled with rich water ooze are observed. Between 210-469 cm dark spots and stripes were found. The upper 13 cm is brown structureless water-saturated clayey sediments with a small amount of silty admixture and foraminifera.

Core 300G

This site is located in the East Alboran basin to the south of Cabo de Gata in a small east-west trending basin north of the Al-Mansour Seamount (36º21,532'W; 1º47,501W, water depth: 1860 m). A 458 cm long core of hemipelagic sediments was recovered. The lowermost unit is brown water-saturated structureless mud with a small amount of silty admixture and foraminifera. Most of the core consists of grey clay, brownish in the upper 7 cm, with foraminifera and a small amount of silty admixture. Sediments become more greenish towards the bottom.

Core 301G

This core was located in the south of Cabo de Gata and north of the Al-Mansour Seamount, southward to the core 300G (36º14.813´N 1º45.342´W water depth: 1965 m). The core was 487 cm long. The upper part is brown water-saturated ooze sediments with foraminifera and small amount of silty admixture. The rest of the core is composed by a olive grey hemipelagic mud, brownish in the upper 60 cm, with foraminifera, a small amount of silty admixture and dark spots and stripes throughout the succession.

Core 302G

This site is located south of the Al-Mansour Seamount in a 36 km wide graben that is limited by the Yusuf Ridge to the south and the Maimonides Ridge to the north at the same site as 977 from ODP Leg 161 (36º01,906'N, 01º57,317'W, water depth: 1989 m). 420 cm of hemipelagic mud was collected. There is brownish mud with foraminifera in the upper 14 cm, grey mud between 14 and 164 and greenish grey clayey sediments with small amount of silty admixture, foraminifera, dark spots and rare shell fragments in the lower part of the core.

Core 303G

This core is locate east of the core 301G in a deeper site, following a transect between the Alboran and the Algero-Baleric basin (36º17.429´N, 1º37.380´W water depth 2094 m). The corer retrieved about 461 cm of sediments. There is brownish ooze with foraminifera in the upper 6 cm, medium grey mud with oxidised patch. The lower part is composed by grey clayey sediments with stripes and spots with layers of greenish clays.

Core 304G

This site is located between at the Alboran basin east-dipping slope, connecting with the Algero-Balearic basin (36º19,873'N,1º31,631'W, Depth: 2382 m). 454 cm of hemipelagic sediments were collected. This core consisted of greyish clay, brownish in the upper part, with some silty admixture, and with abundant foraminifera, dark spots and stripes throughout the succession. Oxidized layers are recognized between 30 and 40 cm. The lower part has several greenish, clayey layers. Rare shell fragments occur throughout.

**Table II.1.** Detail of the cores studied in the Alboran, Algero-Baleric and Tyrrhenian basins.

| Station | Latitude | Longitude | Depth (m) | Recovery (m) |
|---|---|---|---|---|
| ODP161-974A-1H | 40º 21,364'N | 12º 08.506'E | 3458 | 9,81 |
| ODP161-975B-1H | 38º53.795'N | 4º30.596'E | 2416 | 4,15 |
| ODP161-977A-1H | 36º01.907'N | 1º57.319'W | 1984 | 3,95 |
| TTR9-268G | 35º 57.814'N | 3º 30.655'W | 1526 | 3,30 |
| TTR12-290G | 35º34.612´N | 4º34004´W | 854 | 2,84 |
| TTR12-291G | 35º40.952´N | 4º13970´W | 1520 | 3,31 |
| TTR14-299G | 36º13.879´N | 2º03.350´W | 1938 | 4,69 |
| TTR14-300G | 36º21.532´N | 1º47.501´W | 1860 | 4,58 |
| TTR14-301G | 36º14.813´N | 1º45.342´W | 1965 | 4,87 |
| TTR14-302G | 36º01.906´N | 1º57.317´W | 1989 | 4,20 |
| TTR14-303G | 36º17.429´N | 1º37.380´W | 2094 | 4,61 |
| TTR14-304G | 36º19.873´N | 1º31.631´W | 2382 | 4,54 |

All listed cores have been routinely analyzed following procedures and methods detailed in the following section. However, only some of them have been selected to accomplish this Thesis. Selection criteria based on the quality of the sediment record and absence of any turbidite layers that could have interrupted the pelagic sedimentation, and also on the evidence provided by analytical data on the suitability of the sites for reaching proposed objectives. Additionally, some of the data are part of work in progress and future publications. Core pictures and description are include in appendix 1.

# III. Methods

This section describes the different methods and techniques used for both mineral and geochemical characterization of the studied sediments. In diagram III.1 we can found a resume of the followed methodology.

## III.1. CORE ANALYSES

### III.1.1 Core description

In order to ensure a correct sampling without any bioturbation or sedimentological disturbance that could affect the paleoclimate interpretation, a detailed description has been carried out on board and also during further sampling in laboratory. On board description paid special attention to colour and lithology changes as well as sedimentary structures. Colours are referred to Munsell Colour Charts. Core photos and close-ups of selected intervals were taken for each core.

### III.1.2. Smear slides

Core description also included smear slide preparation of selected intervals. The sediment was embedded on a glass slide for a petrographic microscopic examination. This helped to a rapid and preliminary sediment characterization and classification, and it was useful for recognizing trends in cored sequences.

### III.1.3 Magnetic susceptibility

Magnetic susceptibility measurements are a non-destructive method of determining the presence of iron-bearing minerals within the sediments. For core ODP 975B-1H, detailed measurements were performed on the Joides Resolution (http://www-odp.tamu.edu/). In the case of TTR cores, it was measured using a Bartington Instruments Magnetic Susceptibility meter with a MS2E1 probe.

**III.1.4. XRF-Scanner**

In the marine geology field and the analysis of marine cores, the XRF-Scanner has recently become a routine analytical method. This method involves several advantages, such as high resolution (up to >1 mm), very fast data recovery compared with others techniques, non-destructive and automatic measurement with <1% quantitative error under favourable conditions. The use of XRF-Scanners is therefore especially useful for high resolution paleoclimate analyses. However, the measure resolution depends on sediment characteristics as for instance bioturbation, lamination etc. In the case of the analyzed cores a 0.5-1 cm resolution has been established because of bioturbation, which could increase noisy information under lower resolution. Three non-destructive XRF-Scanners have been used in this research:

- CORTEX, which is the XRF-Scanner from the Bremen University and located in the ODP Core Repository. This scanner has been widely used and described in many previous works (e.g., Röhl and Abrams, 2000) (Moreno., 2002). This instrument has been used to measure major and trace elements (K, Ca, Ti, Mn, Fe, Cu and Sr) at 1.0 cm resolution in the following cores:

| Core | Section |
|---|---|
| **974A 1H** | 1,2 and 3 |
| **975A 1H** | 1,2 and 3 |
| **975B 1H** | 1,2 and 3 |
| **976B 1H** | 1 and 2 |
| **977A 1H** | 1,2 and 3 |

- The new XRF-Scanner from Bremen University (AAVATECH): also located in the ODP Core Repository. Main components are a Forced air-cooled Oxford 50 Watts X-Ray source with Rhodium anode 125 μm, Be window, Voltage from 4 to 50 kv and current range between 0 to 1 mA. X-detector is a Amptek XR-100CR, 5mm$^2$ 25 μm, Be window, internal Ag collimator, 1.5 inch detector

extension and a MCA8000A Multi channel analyser. This instrument was used, in collaboration with Dr. Oscar Romero, to measure a total of 18 elements (Al, Si, P, S, K, Ca, Ti, Mn, Fe, Co, Ni, Cu, Zn, Rb, Sn, Sr, Zr and Ba) at 1.0 cm resolution in the following cores:

| Core | Section |
|---|---|
| **279G** | 1,2,3,4 and 5 |
| **290G** | 1,2,3,4 and 5 |
| **291G** | 1,2,3,4,5 and 6 |
| **292G** | 1,2,3,4,5 and 6 |

- TATSCANNER F-2: it is the code name of a recently developed original instrument by Dr. T. Sakamoto at the Japan Institute for Research on Earth Evolution (IFREE) of the Agency for Marine-Earth Science and Technology (JAMSTEC) in Yokosuka. Main components are a X-Ray source (5-th times powerful as normal previous sources used) forced air-cooled. Technical data and components of TATSCANNER-F2 are described in Sakamoto et al. (2006). This instrument was used to measure a total of 20 elements (Mg, Al, Si, P, S, K, Ca, Ti, Cr, Mn, Fe, Co, Ni, Cu, Zn, Rb, Sn, Sr, Zr and Ba) at 0.5-1.0 cm resolution in the following cores:

| Core | Section |
|---|---|
| **290G** | 1,2,3,4 and 5 |
| **299G** | 1,2,3,4,5,6,7,8 and 9 |
| **300G** | 1,2,3,4,5,6,7 and 8 |
| **301G** | 1,2,3,4,5,6,7,8 and 9 |
| **302G** | 1,2,3,4,5,6,7 and 8 |
| **303G** | 1,2,3,4,5,6,7 and 8 |
| **304G** | 1,2,3,4,5,6,7 and 8 |

Comparison between XRF-Scanner and analytical techniques for discrete samples (AA, ICP-MS) show a good agreement. Nevertheless, XRF-Scanner data requires control with traditional analysis on discrete samples, with aim to check the quality of XRF-Scanner data or describe complex elemental relationships (Jimenez-Espejo et al., 2006). XRF-Scanner limitations are related with the X-ray absorption by air between sensor and sample (mainly water vapour), the lowest sensibility to light elements, variation in flatness or water content of the sample. Those factors hardly can be avoid, and specially affect light elements such as Al. Errors in Al quantification are expanded during element/Al normalization, and could affect ratio patterns and thus result in unreal observations.

## III.2. CORE SAMPLING

### III.2.1 U-channels

U-channels were taken in TTR cores. Aiming to identify bioturbation or sedimentological disturbances in the U-channels to be studied using Tatscanner, detailed radiographies were done in several core intervals. Used instrument was a SOFTEX M-60, I-0605 tube equipped with Be window, 0.5 x 0.5mm focusing, 50KV, 3mA, at 300 seconds exposure. These analyses demonstrated the presence of some vertical bioturbations that were taken into account for data interpretation (Fig III.1).

### III.2.2 Discrete sampling

Every core was sampled at high resolution, every 1.5 cm for TTR cores and every 2 cm for ODP cores. Sediment samples were divided into two portions, one for mineralogical and geochemical analyses, the other used to separate marine planktonic foraminifers for isotope analyses and dating.

**Figure III.1.** X-ray photography showing a vertical burrow in a core 290G U-channel (top-left)

## III.3. MINERALOGICAL ANALYSES

### III.3.1. X-ray Difraction (XRD)

Bulk and clay mineralogy have been determined by X-ray Diffraction (XRD) using a Philips PW 1710 diffractometer (Dpto. Mineralogía y Petrología-Granada University).

#### *III.3.1.1. Bulk sample preparation*

For bulk mineral analyses, samples were dried at room temperature or using a ventilated heater at 50ºC during 24 hours. Dry samples were homogenized using an

agate mortar and an micromill RETSCH MM 301. Powder samples were packed in Al sample holders for X-ray Diffraction.

### *III.3.1.2. Separation of clay fraction from bulk sediments.*

Separation of the clay fraction were performed following the international recommendations compiled by Kirsch (1991). For clay mineral analyses, the carbonate fraction was removed using acetic acid. The reaction was initiated at a very low acid concentration (0.1 N), and was increased up to 1 N, depending on the carbonate content of each sample. Sediments were also treated by hydrogenperoxide to dissolve organic materials. Clay was deflocculated by successive washing with demineralised water after carbonate removal. For deflocculation of particles, 0.001 mol/l sodium hexametaphosphate solution was added. Clay fraction (<2-μm) was separated by centrifuging at 9000 rpm for 1.3 min, using modified Stoke's law. At least, this procedure has been repeated 4 times in a centrifuge (KUBOTA KS 8000). All extracted clay fractions were washed with pure water for three times to remove dispersing agent. Finally, the clay fraction was smeared onto glass slides to obtain X-ray diffractograms. This procedure improves clay minerals reflections (00l) because c axis of clays is orientated perpendicular to the glass slide.

This procedure has also been compared with a different method, "filtration method", for clay preparation followed in the laboratories of IFREE-JAMSTEC. This method consisted in the addition of 1 ml of 0.5% molybdenite suspension (0.3 μm grain-diameter) as internal standard to 40 mg of clay fraction in tube that preliminarily softly ground in an agate mortar. After addition of 2 ml of pure water, to avoid destruction of clay and molybdenite grains, ultrasonic dispersion of suspension was limited within 1 minute. Nevertheless talc and corundum are frequently adopted as internal standard for quantitative XRD analysis, molybdenite has many advantages such as; acute diffraction peak and substantial intensity with few amount, suitable peak position for clay minerals around 6.15 Å, and uncommon mineral in marine sediments (Quakernaat, 1970). Disadvantages of molybdenite are difficulty to create

powder of ordered particle size and to disperse in water, due to its high flexibility and electric charge. We persevered in development of fine molybdenite fraction and stock suspension. After withdrawal from ultrasonic bath, whole suspension was immediately put into funnel of a vacuum filtration system with Millipore© membrane filter (JHWP04700, 0.45 μm pore diameter). The filter in this examination did not pass through particles. First filtration to drain all fluid was carried out within 5 minutes to avoid grain sedimentation on the filter. If it takes longer, suspension was stirred to keep homogenous. Molybdenite density is heavier than that of common clay minerals, which represents that molybdenite grains will concentrate near the filter, and clay cake homogeneity cannot be ensured. In succession, 1 ml of 0.1 mol/l magnesium chloride solution were followed to replace all free cations with Mg ions, and washed by pure water to remove excess cations and chloride ion. After filtration was completed entirely, "clay cake" on the filter was carefully transferred onto a glass slide. At this time, one drop of pure water was previously put on the slide to remove air bubble between the clay cake and the slide. Finally, the clay cake was dried for 15 minutes at 50 °C with the filter. The filter was slowly removed after it became white from semitransparent. The used instrument was a Mac Science MXP3 HF diffractometer equipped with Cu target (40kV, 20mA, K$\alpha$1=1.54056Å), automatic goniometer and graphite monochromator, by a step scan with 2 seconds of counting time (Iijima et al., 2005).

### *III.3.1.3. X-ray Diffration analyses*

Instruments conditions for X-ray diffractograms were :

| | |
|---|---|
| Radiation: Cu-Ka | Exploration speed: 6º 2Θ/ min |
| Filter: Ni | Voltage: 40 Kv |
| Window slit: 1º | Intensity: 40 mA |
| Slit counter: 0,1º | Sensibility: $5 \cdot 10^3$ |
| Time constant: 0,2 | |

Scans were run from 2–64º 2Θ for bulk-sample diffractograms and untreated clay preparations, and from 2–30º 2Θ for glycolated clay-fraction samples.

### *III.3.1.4. Qualitative mineral study*

*Bulk mineralogy*

The powder bulk sample diffractograms were interpreted using Xpowder software (Martin, 2004). The identification was made using characteristic mineral reflection peak. Position of reflections were corrected using quartz (100) reflection as internal standard. Obtained reflections were compared with data files as PDF (Powder Data File) from the "Joint Committee of Powder Diffraction Standards".

*Clay mineralogy*

For clay identification two glass slides were prepared. One without any treatment, that corresponds to a orientate aggregate (AOA) air dried. Other glass slide was glycolated (EG) with aim to check expansive clays. This treatment consists in the heating of one orientate aggregate until 60ºC during 48 h. in etilenglycol atmosphere. The identification was made in the EG diffratogram comparing with data files PDF. Smectites are easily identified in EG diffractograms because of the expansion that suffered after glycolate treatment. In the case of chlorite and kaolinite the maximum intensity peaks are coincident (7.16Å Kaolinite and 7.10Å Chlorite) and have been identified using the double peak located at 3,58 Å for kaolinite and 3,55Å for chlorite (Moore and Reynolds, 1989).

### *III.3.1.5. Semi-cuantitative mineral study*

Despite the traditional efforts to study clay-rich materials using XRD in a quantitative sense, the highly variable characteristics of clay minerals assemblages are

major obstacle for their quantification (e.g., Aparicio and Ferrell, 2001). Peak areas have been measured in order to estimate semi-quantitative mineral content. The estimation of different clay contents was based in the reflectance intensity of every mineral phase (bulk and clay mineralogy) (Table III.1). Although these data cannot be considered as quantitative, in comparison with elemental contents (e.g. Ca Vs Calcite % see Fig. xx) a high correlation pattern is found with the 4-average tendency line. Data are given in % respect total mineral assemblage. The estimated semiquantitative analysis error for bulk mineral content is 5%; for clay minerals it ranges from 5% to 10%; although semiquantitative analysis aims to show changes or gradients in mineral abundances rather than absolute values.

**Table III.1.** Reflectances and reflections used in the semi-quantitative study.

| Mineral | Reflectance | Reflection (Å) |
|---|---|---|
| Quartz | 1,43 | 3.34 |
| Calcite | 0,09 | 3.03 |
| Clay Min. | 1,05 | 4.45 |
| Feldspars | 1,03 | 3.18 |
| Illite | 0,36 | 10 |
| Smectites | 0,93 | 17 |
| Chlorite+ Kaolinite | 0,98 | 7,1 |

### III.3.2. Field Emission-Scanning Electronic Microscopy (FE-SEM)

The Scanning Electronic Microscope (SEM) was used to analyze mineral phases and characterize mineral morphologies. Secondary electron images of the samples were obtained to get genetic/origin information about minerals. Backscattered vision analysis was used to characterize the "heavy minerals" which appear in the samples.

Selected samples were placed in an aluminium base and covered by a thin carbon layer with aim to secure good conductivity. Used metallizer was a Hitachi UHS. Covert carbon sampled is introduced in a vacuum chamber for his study. Instrument utilized was a Leo Gemini® 1530, a field emission SEM which led a considerable higher magnification than conventional SEM. (Tension 0.1-30 kv; Range zoom: 20-500000x; Resolution: 1 nm). Both instruments are located in the Centro de Instrumentación Científica (CIC) from the University of Granada.

### III.3.3 High Resolution Transmission Electron Microscopy (HR-TEM)

HR-TEM was used to obtain chemical information of the clay minerals found. Samples were prepared in copper and gold grids. A Philips® CM-20 STEM, up to 200 kV accelerating potential and with $Ba_6La$ filament was used. This instrument led a resolution of 1.4/2.7 Ǻ in reticular images, being the resolution in STEM mode up to 50Ǻ. This microscope has an EDX detector and CCD camera to obtain digital images. In order to avoid alkaline volatilization (mainly Na and K) (Nieto et al., 1996) an analytical window of 1 x 1μm was used, with acquisition time between 30 and 200 seconds. Atomic proportions obtained from peak intensity measurements, was transformed into concentrations using natural standards (albite, biotite, espesartine, muscovite, olivine, titanite, MnS and CaS) and procedure described in Cliff and Lorimer (1975).

## III.4. GEOCHEMICAL ANALYSES

### III.4.1. X-ray Fluorescence (XRF)

This technique was used to quantify major elements in discrete sediment samples. Different instruments were used as well as sample preparations techniques. Internal and external standards were used to ensure data comparisons among cores as well as accuracy and reproducibility.

*Sample preparation for XRF analysis*

Two different preparation procedures were used in this study, pressed pellets and fused beads.

Pressed pellets: powder samples were mixed with a binder (wax) into aluminum cups with boric acid backing and pressed. A 50 mm colour homogenous equal density pellets were obtained. Pressed pellets were measured using a XRF analyses were performed using an S4Pioneer Brucker AXS device at the in the Instituto Andaluz de Ciencias de la Tierra (CSIC-UGR) laboratory. The S4 Pioneer is provided with a 4kW excitation source. The fluorescence signal is received by the detector through 4 collimators and 8 diffraction crystals. The interpretation of the resulting data was carried out using the Brucker-designed software SPECTRA plus.

Fussed beads: powder samples were fussed adding lithium tetraborate in a PHILIPS PERL'X3 fuser. A homogenous glass was obtained. This preparation eliminates particle size and mineralogical effects entirely. Beads were measured using a Philips Magix Pro (PW 2400) spectrometer with a Rhodium tube and a 4 kW generator at the CIC (Univ. Granada)..

**III.4.2. ICP-MS**

Inductive Couple Plasma–Mass Spectrometry (ICP-MS) has been used to determine trace element contents. 100 mg of powder samples were dissolved with 2 ml of $HNO_3$ and 3 ml of HF. The resultant dissolution was dried, re-dissolved in 1ml $HNO_3$ and dried again. The residue was dissolved in 4 ml of $HNO_3$ + 96 ml of ultrapure water. 1 ml of this dissolution + 0.5 ml of a 200 ppb of Rh (as an internal standard) + 8.5 ultrapure water was used for the chemical analyses in a Perkin Elmer-Sciex ELAM 5000® ICP-MS. Natural standards with the same sample procedure were used to the calibrate of the analyses. The analyzed elements are: Li, Rb, Cs, Be, Sr, Ba, Sc, V, Cr, Co, Ni, Cu, Zn, Ga, Y, Nb, Ta, Zr, Hf, Mo, Sn, Tl, Pb, U, Th, La, Ce, Pr, Nd, Sm, Eu, Gd, Tb,

Dy, Ho, Er, Tm, Yb y Lu. The instrumental error is ± 2% and ± 5% for elemental concentrations of 50 and 5 ppm respectively.

### III.4.3. Atomic absorption (A.A.)

Major elements (Al, Ca, Mg, K, Mn and Fe) were quantified in some samples using a *Perkin Elmer mod. 5100* Atomic Absorption Spectrometer with a C chamber, mod. 5100 *ZL ZEEMAN* and a FIAS-100 injector, at the CIC (Univ. Granada). Injected samples were the same digested solution used for determination of minor and trace elements in the ICP-MS, and thus, sample preparation equally applies for this analysis. Detection limits is 0.1ppm and analytic error of 2%.

### III.4.4 Total Organic Carbon (TOC)

TOC content was determined using two different methodologies indirectly and directly TOC measurement :

*Indirect method:*

TOC content was obtained by subtraction of the Total Inorganic Carbon (TIC) to the Total Carbon (TC) content:

$$TOC = TC - TIC$$

For TIC determination, the untreated powder sample was weighted in a precision balance and acidified. Obtained $CO_2$ from carbonate dissolution was measured by coulometry (electrolysis). Carbonate was calculated from $CO_2$ content and expressed as calcite ($CaCO_3$). It is assumed that carbonate of the sample represent the TIC content. For TC analysis untreated powder samples are wrapped in tin capsules. Sealed capsules are eating until 1200 ºC in an oven. $CO_2$ generated by combustion was measured and represents the TC. Results are expressed in weight per

cent and analytical reproducibility is >1%. Used instruments was a CM 5200 TC Analyzer (Limnology Department ETH-Zentrum Zurich).

*Direct TOC method:*

- JAMSTEC laboratories: Total organic carbon (TOC) and total Nitrogen content were measured in separate portions of air-dried sediment samples by a CHN analyser (Perkin Elmer 2400 Series 2). Each powder sample processed for TOC was treated with HCl (12N) in a silver cup, until mineral carbon was completely removed. Samples were wrapped after dehydration on a hot plate for 12 hours. Standards and duplicate analyses were used as controls for the measurements, indicating an error under 0.05%.

- University of Bremen laboratories: The sediment sample set for bulk analyses was freeze-dried and ground in an agate mortar. Total carbon contents (TC) were measured on untreated samples. After decalcification of the samples by 6 N HCl, total organic carbon contents (TOC) were obtained by combustion at 1050ºC using a Heraeus CHN-O-Rapid elemental analyzer as described by Muller et al. (1994).

**III.4.5 Biogenic silica**

An automated system was used for determining biogenic silica. This method allows a complete opal recovery, a correction for the non-biogenic silica and not require assumptions with respect to the sediment composition. Untreated powder sample is continuously agitated in an alkaline leaching solution (NaOH 1M) in at hot bath (85ºC) during aprox. 10 min. The alkaline solution is acidified using $H_2SO_4$ (0.088 M) in a hot bath (85ºC). The acidified sample solution is then successively mixed with molybdate, oxalic acid and ascorbic acid reagents. This solution flow through a photometer (SKALAR 6100) and absorbance is measured at a wavelength of 660 nm. The continuous absorbance versus time plot is evaluated according to the extrapolation

procedure of DeMaster (1981) using a strip-chart recorder (LAUMANN DLH 250). A completed methodological description can be found in Muller and Schneider (1993).

### III.4.6. Isotopic analyses

Isotopic analysis ($\delta^{18}O$ and $\delta^{13}C$) in calcium carbonates from monospecific planktonic foraminifer shells (*G. bulloides*) have been made. Approximately 25 specimens were picked from the N125 μm fraction and senescent forms were avoided. Foraminifers were cleaned in an ultrasonic bath to remove fine-fraction contamination, rinsed with distilled water and thoroughly washed in alcohol. Sample was placed in metal cup and crushed. An automatic loader introduced samples on the instruments for $CO_2$ extraction by acidification (pure phosphoric acid 100%) at 90ºC. Three instruments were used: a GV-Instruments Isoprime mass spectrometer located in IFREE-JAMSTEC laboratories Yokosuka, a VG-Prims mass spectrometer located in the ETH-Zentrum-Zurich and a Finnigan MAT 251 mass spectrometer (Isotope Laboratory, Department of Geosciences, University of Bremen, Germany) (analytical reproducibility was ±0.10‰ for both $\delta^{18}O$ and $\delta^{13}C$ based on repeated standards).

## III.5. STATISTICAL ANALYSES

Different parameter (average, moving-average lines, etc) has been used for data interpretation. Specially useful have been Pearson's correlation coefficient (bivariate correlations) between time plot geochemical data. Used software has been SPSS v. 13.0

## III.6. DATING $^{14}C$

Dates were obtained using $^{14}C$-AMS (*Accelerator Mass Spectrometry*) techniques in two laboratories the Leibniz-Labor for Radiometric Dating and Isotope Research (Germany) and Isotope Research and Poznan Radiocarbon Laboratory (Poland). Datation has been reached in calcium carbonates from monospecific planktonic foraminifer shells (*G. bulloides*). Shells where cleaned in metanol in ultrasonic bath, and

later, washed and dried. In order to compare our data with other paleoclimatic records, all $^{14}$C-AMS ages were calibrated to calendar years (cal. BP). For samples from 20 to 0 ky has been used Calib 5.0 software (Stuiver and Reimer, 1993). We used the standard marine correction of 400 yr, as well as the Marine04 calibration curve (Hughen et al., 2004). For samples older than 20 ky, has been used Calpal "Beyond the ghost" version and CALPAL 2005 SFCP as calibration curve.

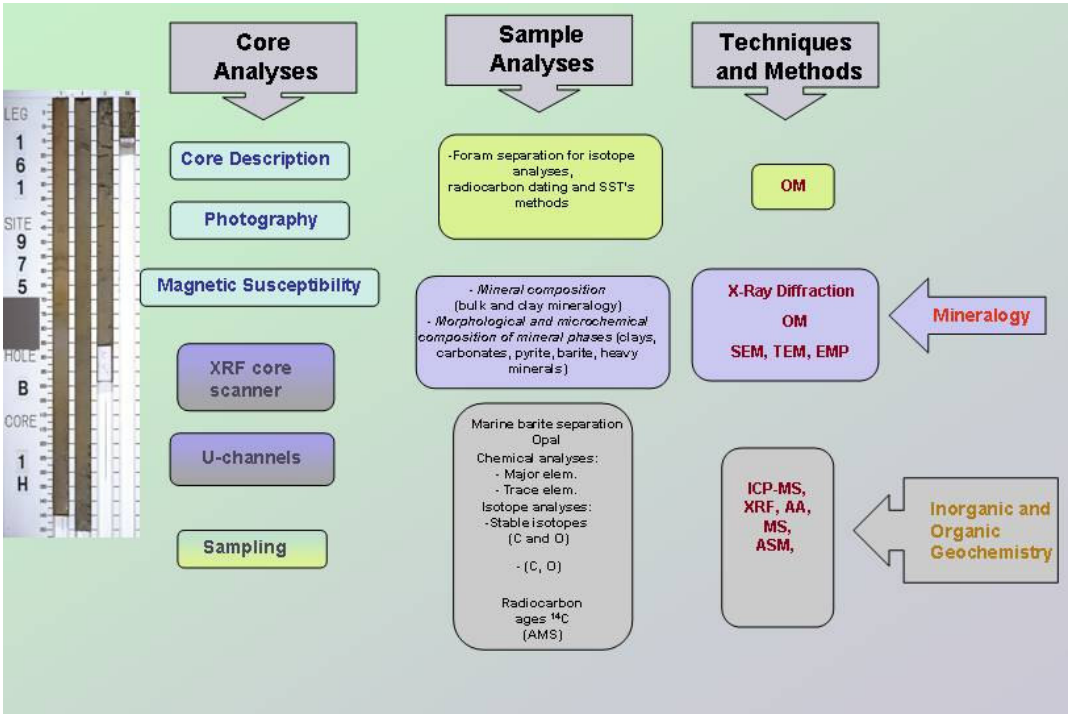


**Diagram III.1.** Followed methodology resume.

# IV. Paleoenvironmental changes in the western Mediterranean since the last glacial maximum: High resolution multiproxy record from the Algero–Balearic basin

# Paleoenvironmental changes in the western Mediterranean since the last glacial maximum: High resolution multiproxy record from the Algero–Balearic basin

Francisco J. Jimenez-Espejo, Francisca Martinez-Ruiz, Tatsuhiko Sakamoto, Koichi Iijima, David Gallego-Torres, Naomi Harada. Palaeogeogr. Palaeoclimatol. Palaeoecol. (2006), doi:10.1016/j.palaeo.2006.10.005

## ABSTRACT

The present study uses a multiproxy approach in order to further understand the evolution of climate responses in the Western Mediterranean as of the Last Glacial Maximum. Sediments from ODP Site 975 in the Algero-Balearic basin have been analysed at high resolution, both geochemically and mineralogicallly. The resulting data have been used as proxies to establish a sedimentary regime, primary marine productivity, the preservation of the proxies and oxygen conditions. Fluctuations in detrital element concentrations were mainly the consequence of wet/arid oscillations. Productivity has been established using $Ba_{excess}$, according to which marine productivity appears to have been greatest during cold events H1 and YD. The S1 time interval was not as marked by increases in productivity as was the eastern Mediterranean. In contrast, the S1 interval was first characterized by a decreasing trend and then by a fall in productivity after the 8.2 ky BP dry-cold event. Since then productivity has remained low. Here we report that there was an important redox event in this basin, probably a consequence of the major oceanographic circulation change occurring in the Western Mediterranean at 7.7 ky BP. This circulation change led to reventilation as well as to diagenetic remobilization of redox-sensitive elements and organic matter oxidation. Comparisons between our paleoceanographic reconstruction for this basin and those regarding other Mediterranean basins support the hypothesis that across the Mediterranean there were different types of responses to climate forcing mechanism. The Algero-Balearic basin is likely to be a key area for further understanding of the relationships between the North Atlantic and the eastern Mediterranean basins.

## IV.1. INTRODUCTION

The Mediterranean has been the focus of intense paleoclimate research. In particular, for North Atlantic circulation, and thus for global climate, mediterranean thermohaline circulation has been of substantial importance (e.g., Johnson et al., 1997; Sierro et al., 2005). In addition, the Mediterranean has been especially sensitive to climatic change, such as Dansgaard-Oeschger (D/O) and Monsoonal cycles, Heinrich events (H), etc. A multitude of interdisciplinary approaches have led to an enormous quantity of climate data within different time-frames (e.g., Rossignol-Strick, 1985; Cacho et al., 1999; Emeis et al., 2000a; Krijgsman, 2002; Wedealb et al., 2003; Colmenero et al., 2004; Martrat et al., 2004; Moreno et al., 2005). It is now well-known that in the eastern and western Mediterranean basins climatic responses have been significantly different. The eastern Mediterranean has been characterized by the cyclical deposition of sapropels since the Messinian (e.g., Rossignol-Strick et al., 1985; Rohling and Hilgen, 1991; Emeis and Sakamoto, 1998; Emeis et al., 2000b). Although organic rich-layers have also been reported in the West (Comas et al., 1996), the absence of true sapropels clearly distinguishes both regions. To date, no equivalent of the most recent sapropel from the eastern basin (S1, Mercone et al., 2000) has been reported in the westernmost basin (Martinez-Ruiz et al., 2003). However, it is likely that climatic records from basins located near the limit between the eastern and western basins will make it possible to determine the gradients and differences in climate responses. Because it is situated in the central part of the western Mediterranean, the Algero-Balearic basin is a key location for the understanding of such differences and circulation patterns during the last glacial cycle. This basin is largely isolated from direct continental/river discharge and from tectonic activity, thus providing a unique record for climate-related responses at centennial/millennial scale (Comas et al., 1996).

A multiproxy approach of this record has been performed at ODP Site 975. Regarding circulation, this site enables the monitoring of the history of eastbound inflowing Atlantic waters and westbound outflowing Mediterranean waters (Fig. IV.1). ODP core 975B-1H was sampled for high-resolution geochemical and mineralogical

analyses. Reconstruction of climatic responses have been made by using a number of proxies: Ba and Ba/Al ratios as paleo-productivity proxies (e.g., Dymond et al., 1992; Paytan, 1997) and, U and other redox sensitive elements as proxies for paleo-redox conditions and ventilation processes. Moreover, redox sensitive elements have also provided data regarding post-depositional diagenetic processes. Sedimentary regime conditions have been established based on interpretations of detrital elements and bulk and clay mineralogy.

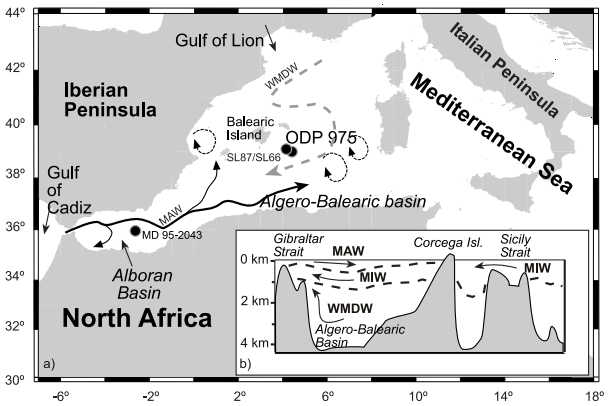


**Figure IV.1.** a) Map of the western Mediterranean showing the location of the studied core, ODP Site 975 and other related cores. West longitudes are negative. Arrows represent the main oceanographic currents. Black line indicates the Modified Atlantic Water (MAW). Dotted lines correspond to eddies. Dashed line represents the Western Mediterranean Deep Water (WMDW). b) Cross section showing main currents (MIW: Mediterranean Intermediate Water). Arrows indicate flow direction. Modified from Cramp and O'Sullivan (1999).

## Oceanographic setting

At present the western Mediterranean Sea (WMS) dynamic is driven by frontal and turbulent regimes, rather than by thermohaline processes linked to atmospheric seasonality. Eddies thus play a major role in the exchange of water masses (Millot, 1999). The Balearic Channels are important passages for meridional exchanges between

the cooler, more saline waters of the northern basins (Gulf of Lion), and the warmer, fresher waters of the southern basins (Alboran and Algero-Balearic basins) (Pinot et al., 2002). Surface water is composed of inflowing Atlantic water progressively modified by air-sea interaction and is referred to in the literature as Modified Atlantic Water (MAW) (Fig. IV.1). Below the MAW flows the Mediterranean Intermediate Water (MIW) (Cramp and O'Sullivan, 1999). The deepest levels are filled with the Western Mediterranean Deep Water (WMDW), which is formed via deep convection in the Gulf of Lion (Fig. IV.1) (Benzohra and Millot, 1995). The production of WMDW is controlled by wind strength, initial density of source waters, and the circulation patterns (Pinardi and Masetti, 2000). North-westerlies constitute the major driving force for deep water formation, as well as for enhanced thermohaline circulation (Millot, 1999; Cacho et al., 2000).

Concerning marine productivity, the Mediterranean Sea is an oligotrophic area (Cruzado, 1985). However, one of the highest productivity level is located in the westernmost Mediterranean and is associated with upwelling activity and the hydrological structures of surface waters (Morel, 1991). Organic nutrients are brought to the WMS by Atlantic inflow (Dafner et al., 2001), whereas mineral nutrients are mainly of eolian and fluvial origin, though they sometimes come from deep Mediterranean waters. Eolian input is especially important for Fe, N and other nutrient elements (Gomez, 2003). Phosphate, which is mainly of fluvial origin, is the limiting nutrient for primary production in the Mediterranean sea (Krom et al., 1991). A physical-biological coupling has been described for the Algero-Balearic southern margin, being that primary production displays a rapid response to the dynamic conditions (Lohrenz et al., 1988; Moran et al., 2001) associated with frontal and eddy circulation.

## IV.2. MATERIALS AND METHODS

### IV.2.1. Site description

ODP Site 975 is located on the Southern Balearic Margin between the Balearic Promontory (Minorca and Majorca islands) and the Balearic Abyssal Plain (38º 53.795' N 4º 30.596' E; 2,416 meters below sea level, see Fig. IV.1). Sediments at this site consist of nannofossil or calcareous clay, nannofossil or calcareous silty clay, and slightly bioturbated nannofossil ooze (Comas et al., 1996). The upper 150 cm of core 975B-1H were sampled continuously every 2 cm. Sediment samples were divided into two portions, one dried and homogenized in agate mortar for mineralogical and geochemical analyses, the other used to separate marine planktonic foraminifers.

### IV.2.2. Age model and sedimentation rate

The age model for the sampled interval is based on five $^{14}$C-AMS dates (accelerator mass spectrometry) recorded in monospecific planktonic foraminifers (Table IV.1) (Leibniz-Labor for Radiometric Dating and Isotope Research). The validity of the model is also strengthened by stable isotope stratigraphy and major biostratigraphic variations. In order to compare our data with other paleoclimatic records, all $^{14}$C-AMS ages were calibrated to calendar years (cal. BP) using Calib 5.0 software (Stuiver and Reimer, 1993). We used the standard marine correction of 400 yr, as well as the Marine04 calibration curve (Hughen et al., 2004). Linear extrapolation between radiocarbon ages may therefore result in spurious differences in age among time-parallel markers. Thus, we have compared our stable isotopic curve with other paleo-SST records in the WMS, where $\delta^{18}O_{G.\ bulloides}$ fluctuations are synchronous with those of SST at millennial timescale (Cacho et al., 2001).

The linear sedimentation rates (LSR) of late Holocene sediments are 4.4 cm/ky (2,050-0 cal. yr BP), approximately half of the older sediments sampled at this location: 7.7 cm/ky at 7,500-2,050 cal. yr BP, 7.0 cm/ky at 13,250-7,500 cal. yr BP and 7.8 cm/ky

at 20,000-13,250 cal. yr BP. These LSR values are slightly higher than the ones corresponding to the Algero-Balearic basin (e.g., Martinez-Ruiz et al., 2003; Weldeab et al., 2003). They are twice the sedimentation rates estimated for open marine eastern Mediterranean Sea (EMS) ODP sites (Emeis et al., 1996) and five-fold lower than those of the Alboran basin (Comas et al., 1996). Temporal resolution of samples taken from the core is ~400 to 175 yr, which makes it possible to distinguish millennial/centennial climate oscillations.

**Table IV.1.** Results of AMS $^{14}C$ carbon dating of single planktonic foraminifer *G. bulloides* (>125 μm) taken from ODP core 975B-1H. Calibration has been made using Calib 5.0 software.

| Lab. code | Sample Description | Core depth | Conventional Age | Calibrated age |
|---|---|---|---|---|
| KIA 27327 | 975B / 1 / 8 - 10, 1.0 mg C | 9 cm | 2,455 + 30 / -25 BP | 2,049 ± 54 cal BP |
| KIA 27328 | 975B / 1 / 50 - 52, 1.0 mg C | 51 cm | 7,070 + 40 / -35 BP | 7,519 ± 42 cal BP |
| KIA 27329 | 975B / 1 / 90 - 92, 0.9 mg C | 91 cm | 13,330 ± 60 BP | 15,201 ± 135 cal BP |
| KIA 27330 | 975B / 1 / 130 - 132, 0.8 mg C | 131 cm | 15,870 ± 80 BP | 18,768 ± 67 cal BP |
| KIA 27331 | 975B / 2 / 45 - 47, 1.0 mg C | 190 cm | 19,460 ± 110 BP | 22,512 ± 114 cal BP |

[a] Reservoir effect 400 years. (One sigma ranges)

### IV.2.3. Mineralogy

Bulk and clay mineral compositions were obtained by X-ray diffraction (XRD). For bulk mineral analyses, samples were packed in Al sample holders. For clay mineral analyses, the carbonate fraction was removed using acetic acid. The reaction was initiated at a very low acid concentration (0.1 N), and the concentration was increased to 1 N, depending on the carbonate content of each sample. Clay was deflocculated by successive washing with demineralised water after carbonate removal. The <2-μm fraction was separated by centrifugation at 9000 rpm for 1.3 min. The clay fraction was smeared onto glass slides for XRD. Separation of the clay fraction and preparation of samples for XRD analyses were performed following the international recommendations compiled by Kirsch (1991). X-ray diffractograms were obtained using a Philips PW 1710 diffractometer with Cu-K◎ radiation and an automatic slit. Scans were run from 2–64º 2◎ for bulk-sample diffractograms and untreated clay

preparations, and from 2–30º 2◎ for glycolated clay-fraction samples. Resulting diffractograms were interpreted using Xpowder software (Martin, 2004). Peak areas have been measured in order to estimate semi-quantitative mineral content. Representative samples were also prepared following the "filtration method" using internal standard (MoS) (Quakernaat, 1970; Iijima et al., 2005). The estimated semiquantitative analysis error for bulk mineral content is 5%; for clay minerals it ranges from 5% to 10%; although semiquantitative analysis aims to show changes or gradients in mineral abundances rather than absolute values.

Morphological studies on selected samples were performed by means of field emission scanning electron microscopy (FESEM), whereas quantitative geochemical microanalyses of the clay minerals were obtained by transmission electron microscopy (TEM) using a Philips CM-20 equipped with an EDAX microanalysis system. Quantitative analyses were obtained in scanning TEM mode only from the edges using a 70-Å diameter beam and a scanning area of 200 x 1000 Å. In order to avoid alkali loss, a short counting time (30 s) was selected, thus providing better reproducibility for alkali contents (Nieto et al., 1996).

**IV.2.4. Geochemical analyses**

Total organic carbon (TOC) and total nitrogen content were measured by a CHN analyzer in separate portions of air-dried sediment samples (Perkin Elmer 2400 Series 2). Each powder sample was treated with HCl (12N) in a silver cup, until mineral carbon was completely removed. Samples were then wrapped after dehydration on a hot plate for 12 hours. Standards and duplicate analyses were used as controls for the measurements and indicate an error of less than 0.05%.

Major element measurements (Mg, Al, K, Ca, Mn and Fe) were obtained by atomic absorption spectrometry (AAS) (Perkin-Elmer 5100 spectrometer) with an analytic error of 2%. K, Ca, Ti, Mn, Fe, Cu and Sr have also been quantified using an X-Ray Fluorescence scanner (University of Bremen). The XRF-core scanner was set to

determine bulk intensities of major elements on split sediment sections (Jansen et al., 1998; Rölh and Abrams, 2000) at intervals of 1 cm with an accuracy in standard powder samples of over 0.20 % (wt). A depth correction was performed to compare AAS and XRF-scanner data. This comparison indicates a high correlation between such techniques. An average for Ti was obtained from XRF-core scanner data in order to normalize Ti to Al contents. This average will be referred to as $Ti_{mean}$ /Al. Analyses of trace elements including Ba were performed using inductively coupled plasma-mass spectrometry (ICP-MS) following HNO3 + HF digestion. Measurements were taken in triplicates by spectrometry (Perkin-Elmer Sciex Elan 5000) using Re and Rh as internal standards. Variation coefficients determined by the dissolution of 10 replicates of powdered samples were higher than 3% and 8% for analyte concentrations of 50 and 5 ppm, respectively (Bea, 1996).

Stable carbon and oxygen isotope ratios of calcareous foraminifers were analysed to establish the stratigraphic framework of core 975B-1H. Approximately 25 specimens of *Globigerina bulloides* were picked from the >125 μm fraction and senescent forms were avoided. Foraminifers were cleaned in an ultrasonic bath to remove fine-fraction contamination, rinsed with distilled water and thoroughly washed in alcohol. Stable isotopes were measured using a GV-Instruments Isoprime mass spectrometer. Analytical reproducibility of the method is $\pm$0.10‰ for both $\delta^{18}O$ and $\delta^{13}C$ based on repeated standards.

**IV.2.5. U, Mn, and Fe as redox proxies**

Several element/Al ratios have been selected as redox proxies (e.g., Mn/Al, Fe/Al and U/Al). This selection is based on the fact that manganese and iron oxides are solid phase electron acceptors that are able to reflect paleo-redox conditions. Fe displays a complex redox pattern involving a sequence of burial, dissolution, remobilisation and reprecipitation. Fe content is limited by water column pyrite formation and scavenging, and also by siliciclastic flux and the presence or absence of water column hydrogen sulphide (Lyons et al., 2003). Enrichments in Mn and Fe could

be promoted by the diffusion of $Mn^{2+}$ and $Fe^{2+}$ in pore waters from anoxic to oxic layers in which such cations are immobilized. These Fe/Al and Mn/Al enrichments are usually distanced as a result of differences in thermodynamics and kinetic processes (e.g., Thomson et al., 1995; Martinez-Ruiz et al., 2000; Rutten and de Lange, 2003). Patterns in Mn and Fe complement the behaviour of U. When pore water nitrates vanish in sediments beneath the redoxcline, U (VI) dissolved in pore water is reduced to immobile U (IV) and precipitates (Anderson, 1982; Barnes and Cochran, 1990; Mangini et al., 2001). In anoxic conditions U becomes immobile, while reduced Mn and Fe can be dissolved in pore water. These oscillations in redox-sensitive element/Al ratios are related to Eh-pH gradients and changes in bottom redox conditions (Mangini et al., 2001). As regards other redox proxies, trace metals display high affinity to Mn and Fe oxi-hydroxides and are common in post-oxic and anoxic pore waters where they are reduced and dissolved. On reaching an oxidative front, these elements can precipitate into other solid phases (Klinkhammer et al., 1982). Organic substances and changes in clay minerals also contribute to this mobilization (Balistrieri and Murray, 1986).

### IV.2.6. Ba excess as a productivity proxy in the WMS

Although the use of Ba excess as a proxy has been extensively discussed, recent studies have suggested that it should be applied with greater caution, given that barium requires pore water sulphate concentrations of >15mM in order to ensure the absence of sulphate reducing sediments (Paytan et al., 1996; McManus et al., 1998a; Eagle et al., 2003), and thus of subsequent barite dissolution or Ba remobilisation (Brumsack, 1986; McManus et al., 1998b). Ba content also depends on sediment provenance, sedimentation rates, Ba cycling within sediments (Mercone, 2001; Eagle Gonneea and Paytan, 2006) and lateral transport (Sanchez-Vidal et al., 2005). Another major limitation of the Ba excess signal is that the processes governing its production/accumulation and preservation do not vary over time. Nevertheless, Ba can be considered as a robust proxy for paleoproductivity reconstructions in Mediterranean basins, since Ba, Ba/Al ratios, Ba excess and/or barite accumulation

rates have been reliably used by many studies to compare surface productivity changes in the WMS and EMS (e.g., Dehairs et al., 1987; Emeis et al., 2000a; Martinez-Ruiz et al., 2000; Martinez-Ruiz et al., 2003; Weldeab et al., 2003; Paytan et al, 2004), and no indications for barite dissolution have been observed at this site.

## IV.3. RESULTS

### IV.3.1. Barite and Total Organic Carbon (TOC)

TOC content is under 0.5%, and $C_{org}$/N ratio values oscillate between 2 and 6, thus suggesting a marine provenance (Meyers, 1994). Depth profiles show a progressive down-core decrease in TOC. Maximum TOC is found in sub-surface samples (0.45%) where organic matter is presently undergoing degradation (Fabres, 2002). Although TOC content shows no major variations along the core, a slight increase followed by a marked drop is observed between the last deglaciation and the Younger Dryas (YD). Minimum TOC content (0.2 %) is reached during the Holocene transition (Fig. IV.2).

FESEM analyses show the presence of barite crystals with morphologies corresponding to typical marine barite (1-5 μm in size with round and elliptical crystals). Detrital elements and Ba peaks display an absence of correlation which also suggests that this barite is of authigenic origin. The Ba content derived from marine barite (Ba excess) has been obtained by subtracting the amount of terrigenous Ba from the total Ba content (e.g., Dymond et al., 1992; Eagle et al., 2003). It is used here as the excess associated with crustal phases and is calculated as:

$$(Ba_{excess}) = (\text{total-Ba}) - Al(Ba/Al)_c$$

where total-Ba and Al are concentrations and $(Ba/Al)_c$ is the crustal ratio for these elements. In this study, a value of $(Ba/Al)_c = 0.002$ has been used, estimated by Weldeab et al. (2003) for the Balearic Sea on the basis of surface sediments and current

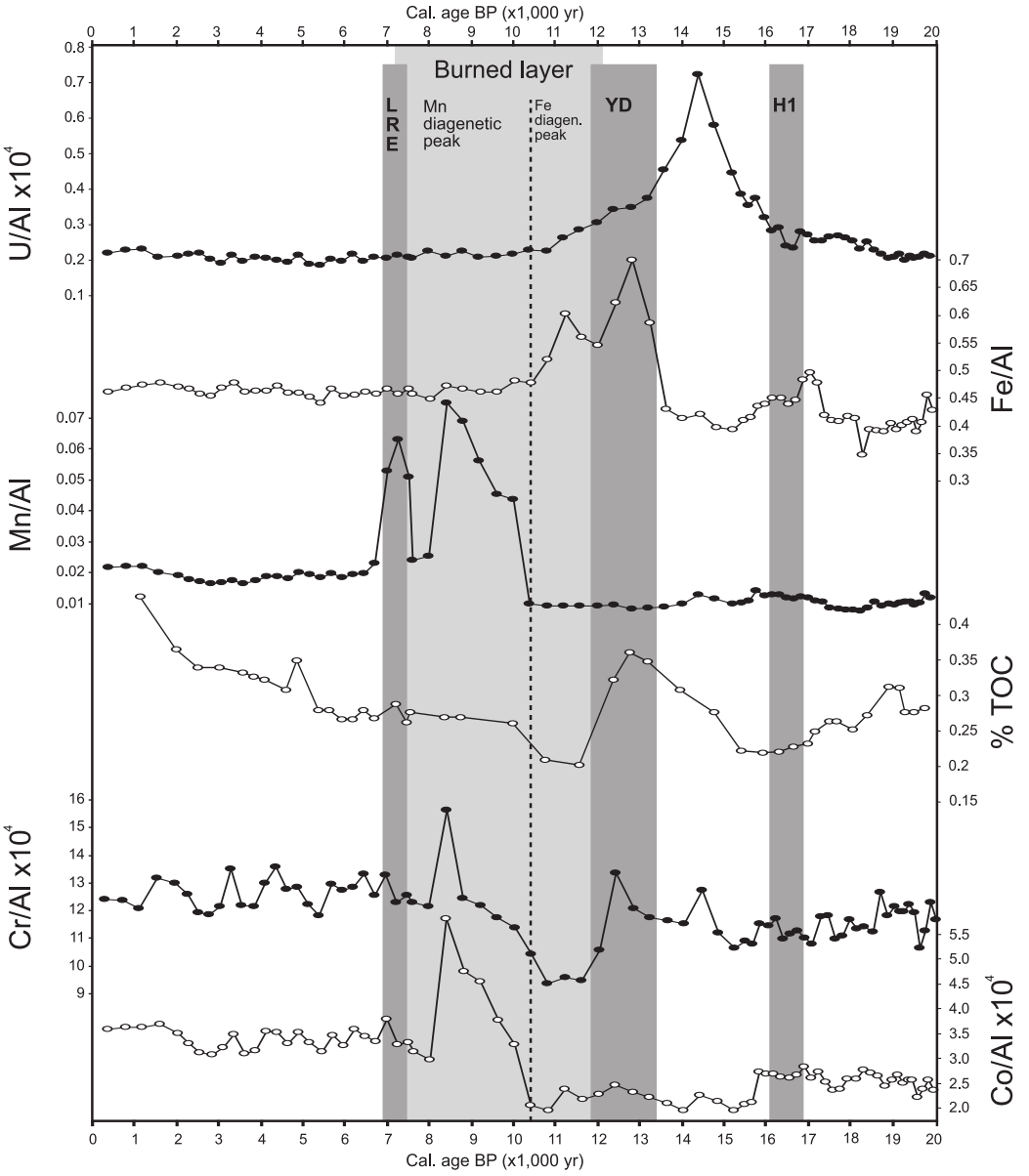


**Figure IV.2.** Total organic carbon wt. (%) (TOC) and elemental/Al ratios according to age plotted as redox proxies. The dark-grey vertical bar indicates the last redox event (LRE) in the Algero-Balearic basin, Younger Dryas (YD) and Heinrich 1 event (H1). Light-grey vertical bar indicates the "burned layer" that evidence re-oxidation processes.

oligo-trophic conditions. It is assumed that the $(Ba/Al)_c$ ratio of the terrigenous matter remains constant over the period studied. Al is found mainly in aluminosilicates, although it should be kept in mind that this ratio may undergo slight variations. In

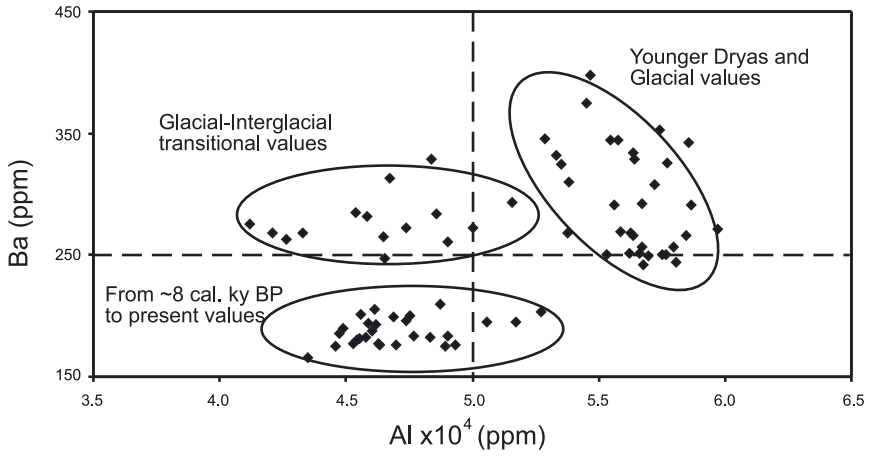


**Figure IV.3.** Ba versus Al (x10$^4$) content (ppm) in samples from the analyzed time interval.

fact, three regions can be distinguished by comparing Ba and Al content (Fig. IV.3). A first region of glacial and YD values, (20 to 15 cal. ky BP and 12.3 to 11.1 cal. ky BP), a second region of between 8.2 to 0 cal. ky BP values, and a final region of glacial-interglacial transitional values. This grouping suggests differences in detrital Ba and different $(Ba/Al)_c$ values, although it does not substantially affect the use of $Ba_{excess}$ as a paleoproductivity proxy. On the other hand, the $Ba_{excess}$ enrichment area included the interval between 18.5-18 cal. ky BP and ~8.0 cal. ky BP within which maximum $Ba_{excess}$ content is observed at 16.5-16 cal. ky BP (Fig. IV.4). $Ba_{excess}$ and TOC do not display similar trends when compared as paleoproductivity proxies. Only one maximum TOC peak during the YD onset coincides with higher values in $Ba_{excess}$.

### IV.3.2. Oxygen and Carbon isotope stratigraphy

Variations in $\delta^{18}O_{G.\ bulloides}$ in the WMS support significant climate oscillations since the Last Glacial Maximum. Maximum glacial-interglacial amplitude of $\delta^{18}O_{G.\ bulloides}$ in core 975B-1H lies between 3.84‰ and 0.69‰, with a total oscillation of 3.15‰. The latter value is between that of the Alboran basin (~2.5 ‰) and the Levantine basin located at the EMS (3.5-4 ‰) (Emeis et al., 2000b). Deglacial warming began between 17.5 and 18 cal. ky BP, displaying thereafter a stable trend (Fig. IV.4). No major cold

**Figure IV.4.** Core ODP 975B-1H age profiles of: (a) relative quartz concentration (%); (b) Mg/Al ($x10^4$) ratio; (c) Zr/Al ($x10^4$) ratio; (d) Ti mean/Al ($x10^4$) ratio; (e) K/Al ($x10^4$) ratio; (f) relative calcite concentration (%); (g) Ba content (ppm); (h) Al content ($x10^4$) (ppm); (i) Ba/Al ($x10^4$) ratio; (j) Ba excess (ppm); (k) $\delta^{18}O$ *G. bulloides* (‰) and (l) $\delta^{13}C$ *G. bulloides* (‰) 3-period moving average. Ti mean, is an average value obtained from the XRF-scanner. Grey vertical bars indicate the last redox event (LRE) in the Algero-Balearic basin, Younger Dryas (D/O stadial 1) and Heinrich 1 event (D/O stadial 2). Grey-dashed bars represent sapropel S1 (S1a and S1b) time intervals. D/O interstadials and 8.2 cold event are also represented.

reversals have been recognized during the last deglaciation. At the end of the YD and H1 cold events, there were sharp signal decreases that may be representative of short warm periods and/or depleted $\delta^{18}O$ surface currents. After these decrease, $\delta^{18}O_{G.\ bulloides}$ returns to deglaciation warming pattern values. Warming continues into the early Holocene until ~7 cal. ky BP. As of the latter date, the isotopic record displays a cyclical fluctuation pattern whose values are situated between 0.69 ‰ and 1.39 ‰. Values of $\delta^{13}C_{G.\ bulloides}$ were found to be highly variable. The maximum amplitude of $\delta^{13}C_{G.\ bulloides}$ is between –0.5 ‰ and –1.38 ‰, with a total oscillation of 0.88 ‰ $\delta^{13}C_{G.\ bulloides}$ undergoes sudden increase/decrease shifts which do not significantly correlate with the last glacial-interglacial transition.

### IV.3.3 Mineralogy and major and trace elements

A complete mineralogical analysis has been performed for a correct interpretation of geochemical data. The sediments sampled at Site 975B are predominantly composed of clay minerals (10-45%), calcite (30-70%) and quartz (10-30%), with low quantities of dolomite and feldspar (<5%). We have also identified accessory minerals, such as zircon, rutile, apatite and biotite, as well as authigenic minerals, such as anhydrite-gypsum, pyrite, Mn and Fe oxi-hydroxides. Clay mineral assemblages consist of illite (50-80%), smectite (20-40%) and kaolinite + chlorite (15%-40%). Additional clay minerals, such as sepiolite, palygorskite and illite/smectite (I/S) mixed layers were also identified using TEM.

Figure IV.4 shows the distribution of selected profiles of major and trace element ratios. Elemental concentrations have been normalized to Al. This normalization assumes that Al concentrations in sediments are contributed by alumino-silicates (e.g., Calvert, 1990). High correlation between Al and quartz contents in the analysed interval also corroborates this idea. We detected no grain sorting leading to quartz and heavy mineral enrichments which are associated with turbidites (Wehausen and Brumsack, 1999).

Several element/Al ratios have been used as redox proxies. At the top of the core (<10 cmcd) there is lightly higher in Mn/Al, while a marked double peak can be seen between ~7 to ~10 cal. ky BP (Fig. IV.2). Before this time, Mn/Al content shows low values within a linear and regular pattern. The most significant Mn/Al enrichment is related to other redox sensitive element/Al ratios, thus indicating the high affinity between these trace metals and Mn oxides. An increase in the Fe/Al ratio consecutively mirrors the double Mn/Al peak. The U/Al ratio displays a linear and regular pattern with one distinct enrichment peak.

## IV.4. DISCUSSION

### IV.4.1. Sea surface conditions as determined by stable isotopes

Oscillations in $\delta^{18}O_{G.\ bulloides}$ in the WMS are mainly due to changes in SST (Cacho et al., 1999) and to external fresh water input (Sierro et al., 2005). The first sharp decrease in $\delta^{18}O_{G.\ bulloides}$ was reached around 16 cal. ky BP, and is associated with negative $\delta^{13}C_{G.\ bulloides}$ values and increases in productivity. This pattern of proxies has been attributed to Atlantic currents enriched in iceberg melt waters (Sierro et al., 2005). Nevertheless, according to our age model, the most significant increase in $\delta^{18}O_{G.\ bulloides}$ is located at the end of H1 and could be related to the sharp warming which took place at the end of this cold event (Cacho et al., 2002a). Another sharp increase in $\delta^{18}O_{G.\ bulloides}$ reaching Holocene values occurred at the end of the YD. These warmings arose in

Northern Europe later than they did in the areas surrounding the ODP 975B site. They have also been detected around the Iberian margin (Bard et al., 1987) and Mediterranean basins (Cacho et al., 2001), and interpreted in relation to rapid polar front northward movements.

The $\delta^{13}C_{G.\ bulloides}$ values are highly variable (Fig. IV.4), a fact which could reflect the complexity of the hydrographic processes involved in this region. Changes in $\delta^{13}C_{G.\ bulloides}$ do not follow major climatic/oceanographic oscillations. Decreasing peaks appear during H1 and YD cold events and could be related to a fertilized Atlantic inflow (Rogerson et al., 2004). The lowest $\delta^{13}C_{G.\ bulloides}$ values were attained during the Holocene and could indicate the existence of gyre activities. The latter may have promoted isotopic exchanges with the atmosphere (Broecker and Maier-Reimer, 1992).

**IV.4.2. Paleo-redox conditions and diagenetic processes in the Algero-Balearic basin**

The Saharan aerosols represent the primary source of Mn in the Algero-Balearic basin (Guieu et al., 1997). Mn distribution within the basin is, however, mainly controlled by bottom-water oxygen conditions (Yarincik et al., 2000). In the uppermost section of core 975B-1H, a slight enrichment in Mn content could be seen as corresponding to current oxic/post oxic limits (Marin and Giresse, 2001; Fabres, 2002). A Mn/Al double peak appears above this enrichment. Minimum TOC values are observed at the lowest Mn double peak boundary coinciding with a relative maximum in the Fe/Al ratio (Fig. IV.2). This pattern can be accounted for by a redox front promoted by better ventilated deep water covering a sediment which had formed under lower ventilation conditions. Reoxygenation led to hydrogenic deposition or precipitation of the upper Mn/Al peak (Van Santvoort et al., 1996; Thompson et al., 1995). Following this event, an oxidant front began to penetrate downwards through the sediment column. The redox front blocked the upward diffusion of $Fe^{2+}$ and $Mn^{2+}$, thus forming the lower Mn/Al peak and an upper Fe/Al enrichment (e.g., Rutten et al., 1999). This front is also responsible for an organic matter oxidation, i.e., the "burned layer" (Fig. IV.2), and for significant alterations in the original uranium content

distribution. Sedimentation rate and TOC concentrations control the burn-down depth. According to the model of Jung et al. (1997) a burn-down depth of >20 cm is expected in these conditions (TOC <1% and LSR=5-7 cm/ky). Thus, the latter results fit well with our estimated burn down depth (24 cm), while they also account for the differences between the $Ba_{excess}$ and TOC records.

Similar relationships between Mn, Fe and U have been found in Atlantic (Mangini et al., 2001) and eastern Mediterranean basins and have been interpreted as indicating the penetration of a redox front in which the upper Mn peak represents the uppermost position of the redoxcline (Van Santvoort et al., 1996; De Lange et al., 1999). All of the above-mentioned observations involve the presence of a postdepositional redox front in core 975B-1H. We propose that this last redox event (LRE) was originated by the redoxcline when it reached the ocean floor at 7.5 – 7.0 cal. ky BP.

**IV.4.3. The last redox-event (LRE): paleoceanographic implications**

A major oceanographic change, dated at 7.7 cal. ky BP in the Alboran Sea (Perez-Folgado et al., 2003), has been identified from faunal assemblage changes in the WMS. This is related to the progressive increase in Atlantic inflow (Rohling et al., 1995) and consequent deepening of the nutricline and pycnocline (Flores et al., 1997). The LRE recognized in the Algero-Balearic basin has been dated at between 7.5 and 7.0 cal. ky BP and could be linked with this event. Nevertheless, detrital proxies are markedly affected during this event (Fig. IV.4). These observations suggest scavenging processes and/or synchronous climatic/oceanographic changes. The LRE could represent a recent intensification in thermohaline circulation and/or the first moment in which WMDW fills its deep basins. The cause of these regional variations and the origins of current circulation patterns in the WMS have yet to be clarified. This change may have been caused by variations in surface thermohaline conditions in the WMS which, in turn, are linked with changes in the Atlantic inflow (Rohling et al., 1995) and in the Evaporation/Precipitation ratio (De Rijk et al., 1999; Myers and Rohling, 2000).

### IV.4.5. Pre-Holocene productivity in the Algero-Balearic basin

Productivity cannot be described on the basis of the TOC content at Site 975. TOC content was altered by postdepositional oxidation (see section 4.2), although part of the glacial TOC signal was preserved. The latter signal displays an increase in the vicinity of 15.2 cal. ky BP, which is prior to the deposition of the last organic rich layer (ORL) in the Alboran Sea basin (14.5 to 9.0 cal. ky BP) (Cacho et al., 2002b). Moreover, the Alboran Sea ORL does not coincide with our $Ba_{excess}$ enrichment (~18 to ~8.0 cal. ky BP) and, therefore, no correlation can be observed between the Algero-Balearic basin and the Alboran Sea ORL.

Productivity interpreted on the basis of the $Ba_{excess}$ proxy was highest during the last deglaciation, displaying a maximum peak at 16.5-16 cal. ky BP and a smaller one at the beginning of the YD (Fig. IV.4). Previous research using core 975B-1H has indicated increases in water productivity during the glacial period and a slight enhancement during sapropel formation in the EMS (e.g., Capotondi and Vigliotti, 1999). Although the highest primary productivity in the Alboran basin was reached during the D/O warm interstadial at 28 to 50 ky (Moreno et al., 2004), at Site 975 we found an inverse signal corresponding to the most recent D/O cycles (Fig. IV.4). This discrepancy can be explained by the presence of a high isotopic-temperature gradient located between the Morocco and Portugal margins during the YD event and prior to 16 ky. Such a gradient can be accounted for by the presence of the Azores front in the Gulf of Cadiz (Rogerson et al., 2004), which may have created a highly fertilized inflow jet of Atlantic water. It is possible that this jet penetrated into the westernmost WMS basins. Prior to 16 ky, productivity generated by progressive increases in melt water during the last deglaciation could have been further enhanced by this jet inflow. The Azores Front is, however, associated with vigorous upwelling (Alves et al., 2002) and a light $\delta^{13}C_{G.\ bulloides}$ (Rogerson et al., 2004), although the $\delta^{13}C_{G.\ bulloides}$ signal at Site 975 is only slightly affected. The highest $Ba_{excess}$ content during the YD is reached at the beginning of this cold event and may be related to increases in taxa using an r-strategist approach (Young, 1994; Sprovieri et al., 2003). A rise in productivity during the YD has also been

recorded at ODP Hole 976C, located in the Alboran basin (Martinez-Ruiz et al., 2004). An eastward displacement of the Alboran gyres and a relatively wet YD have also been proposed as an explanation for increased productivity in the easternmost Alboran basin (Barcena et al., 2001).

### IV.4.6. Holocene productivity

At the nearby SL87/KL66 sites, productivity inferred on the basis of biogenic Ba and accumulation rates have been related to glacial (high productivity) and interglacial (low productivity) phases during the late Pleistocene. No increases have been observed in productivity during EMS sapropel deposition (Weldeab et al., 2003). However, in ODP 975B no major decreases in $Ba_{excess}$ occurred at the beginning of the current interglacial period. Early Holocene $Ba_{excess}$ presents values similar to those of the glacial period and the most important decrease in $Ba_{excess}$ took place between 8.5 and 8.0 cal. ky BP. This fall could be related to the faunal change associated with critical increases in Atlantic inflow at 7.7 cal. ky BP (Rohling et al., 1995; Flores et al., 1997) and/or with the 8.2 cal. ky BP cold event reported in other areas of the Mediterranean (e.g., De Rijk et al., 1999; Ariztegui et al., 2000; Sprovieri et al., 2003). The fact that the interval between both events is so short makes it difficult to attribute this fall in productivity to either the earlier or the later event. It is, however, clear that this decrease in $Ba_{excess}$ preceded the LRE, thus indicating that 8.2 may in fact be the most influential event.

The 8.2 cal. ky BP cold event interrupted the deposition of sapropel S1 in the EMS. Wet climate and reduced surface water salinities have been reported in the EMS for the sapropel S1 deposition period (e.g., Combourieu-Nebout et al., 1998; Ariztegui et al., 2000; Myers and Rohling, 2000). The sequences arising from this hiatus have been described as intervals S1a and S1b (Ariztegui et al., 2000). In the WMS, we found high $Ba_{excess}$ values during the period equivalent to the S1a deposition, but low values

during S1b. The origin of this divergence is probably linked with the establishment of varying climatic conditions in the WMS and EMS. Following the 8.2 cold event, the EMS returns to wet climatic conditions. In the WMS, however, there is an expansion towards a hot and dry summer Mediterranean climate (Jalut et al., 2000). This may imply a decrease in runoff over all WMS borderlands. Such a marked difference in the climatic conditions affecting both basins, along with the Atlantic/Nile influence, could account for such a large gap in paleoproductivity during S1b deposition between the WMS and EMS.

**IV.4.7. Eolian input**

At present, the main source of detrital material for the Algero-Balearic basin is the Sahara Desert. Sahara dust is characterized by high quartz, Ti and Zr content (Guieu and Thomas, 1996). In core 975B-1H, $Ti_{mean}$/Al and Zr/Al display different degrees of correlation depending on the period in question. The $Ti_{mean}$/Al signal shows a clear response during the YD, but Zr/Al ratio is not significantly affected by this cold and arid event. Zr/Al values were lowest during the S1 sapropel deposition time interval, thus suggesting humid conditions, whereas a positive peak is observed in $Ti_{mean}$/Al. These discrepancies in eolian proxies may indicate either a different source area and/or varying sensitivities to wind speed. In particular, we observed that, during the last 5 cal. ky BP, there was a progressive increase in Zr/Al that was perhaps coetaneous to the beginning of the arid period in the Saharan. This most recent rise in Zr/Al is mirrored by the increase in the $Ti_{mean}$/Al ratio, although to a lesser extent.

On the other hand, palygorskite and fibrous minerals have been related to arid conditions and eolian input in the WMS (Prospero, 1985; Molinaroli, 1996; Foucault and Melieres, 2000). No palygorskite or fibrous clay minerals were detected in core 975B-1H samples which are time equivalent to the S1 sapropel deposition. This also suggests that surrounding margins were influenced by wet conditions and low eolian input. Palygorskite and fibrous minerals (sepiolite, crisotile and kaolinite) are observed

following S1 deposition. This suggest enrichment in clay minerals with fibrous morphologies during periods of increased eolian deposition.

### IV.4.8. Detrital proxies during the YD

The highest Mg/Al and K/Al ratio values were reached during the YD (Fig. IV.4). These proxies are associated with fluvial input. The YD is nevertheless considered both a cold and dry period (e.g., Renssen et al., 2001). An intra-YD warm/wet event could promote this high detrital river supply, as long as it is kept in mind that fluvial supply is mainly related to landscape stability and vegetation cover, and not only to increase/decrease in runoff. A strong seasonality during YD (Allen et al., 1996) and/or a significant difference in aridity between northern and southern WMS margins can also contribute to these patterns. Hence, the YD event in the WMS may have developed a particular signal that distinguishes it from other northern hemispheric climatic records.

It is possible that this highest detrital ratio is associated with the short warm event dated at (~12,250 cal. yr BP) and already documented in the Gulf of Cadiz, Alboran Sea and Tyrrhenian Sea (Cacho et al., 2001). In various central European continental records, bi-modal phases have also been reported during YD (Goslar et al., 1993; Walker, 1995; Brauer et al., 2000), whereas there are some southern Iberian Peninsula lake records which do not develop a signal during the YD cold spell (Carrion, 2002).

## IV.5. CONCLUSIONS

Geochemical and mineralogical proxies show evidence of significant paleoenvironmental changes occurred in the western Mediterranean during the last 20 ky. A redox event (LRE) was established and dated between 7.5 and 7.0 cal. ky BP. This event has deeply influenced both TOC preservation and redox element distribution within these sediments. It has also been related to the beginning of recent frontal

circulation in the WMS. Detrital-element profiles also display significant variations which coincide with this LRE. Such variations cannot be accounted for by only increases in Atlantic inflow and would appear to imply scavenging and/or atmospheric changes. Productivity has been characterized by $Ba_{excess}$ and presents fluctuations that can be related to the Atlantic inflow and fresh water input. This productivity was higher during glacial periods and reached its maximums during the YD and ~16 cal. ky BP. A significant productivity decrease started between 8.5 and 8.0 cal. ky BP which has been related to the 8.2 cal. ky BP cold event. Ba profiles support therefore significant productivity differences between the western and eastern Mediterranean at time of S1 sapropel deposition. Thus, comparison of the Algero-Balearic with other Mediterranean basins supports the hypothesis that across the Mediterranean there were different types of responses to climate forcing mechanism. Consequently, this area represents a key location for further understanding of the relationships between the North Atlantic and the eastern Mediterranean basins.

# IX. References

# Climate and oceanographic variability in the westernmost Mediterranean since the Last Glacial Maximum: detrital input, ventilation and productivity fluctuations.

Francisco J. Jiménez-Espejo, Francisca Martínez-Ruiz, José M. González-Donoso, Dolores Linares, Óscar Romero, José Luis Rueda Ruiz, Tatsuhiko Sakamoto, David Gallego-Torres, Miguel Ortega-Huertas. (Submitted to Earth and Planetary Science Letters)

## ABSTRACT

By presenting sea surface temperatures, planktonic oxygen isotope profiles and geochemical composition of marine sediments, we offer here a multi-parameter reconstruction of the Western Mediterranean oceanography since the Last Glacial Maximum. Selected cores were collected at key depths for detecting changes in the Mediterranean Outflow Waters and redox conditions. Comparison of Alboran sea records with those from the Algero-Balearic basin evidence strong gradient along the western Mediterranean. Productivity was always higher in the Alboran Sea, where fluvial input influenced marine productivity during wet periods such as the Bølling-Allerød, the early Younger Dryas and the early Holocene. Ventilation proxies evidence a significant sensibility of the western Mediterranean to Atlantic and eastern Mediterranean oceanographic variations. These proxies suggest that the main strength of the Mediterranean Outflow Waters was supplied by the eastern Mediterranean waters and that the Levantine Intermediate Water-Western Mediterranean Deep Water redoxcline during Last Glacial Maximum was located deeper than they today. Low ventilation conditions had been associated to weakness in deep and intermediate currents. A definitive interruption of low ventilation conditions, which probably marked the start of the current circulation pattern, occurred between 7.9 and 7.2 ky cal BP. The end of sapropel S1 deposition in the eastern Mediterranean around 6.2 ky cal BP is also recognized in southern Alboran cores indicating the high sensitivity of the area to the Levantine Intermediate Water changes. A north-south gradient in the eastern Alboran is recognized, mainly promoted by intense LIW flow, river/coastal influence and sea level.

## V.1. INTRODUCTION

Extensive paleoclimatic research in the Mediterranean during the last few decades has demonstrated the exceptional nature of Mediterranean records for paleoceanographic and paleoclimatic reconstructions at regional and global scale (e.g., Rosssignol-Strick, 1985; Cacho et al., 1999; Emeis et al., 2000; Krijgsman, 2002; Martrat et al., 2004; Sierro et al., 2005; Cacho et al., 2006). Additionally, high sedimentation rates in different regions have also allowed for high-resolution records of climate variability at millennial and centennial scales (e.g., Moreno et al, 2005). This is the case of the Alboran Sea basin, where an elevated detrital supply has resulted in exceptional sediment marine archives. Its connection with the NE Atlantic adds further interest to this region because saline Mediterranean Outflow Waters (MOW) may significantly affect North Atlantic circulation, and thus global climate (Johnson, 1997; Sierro et al., 2005; Rogerson et al., 2006). Over time, variations of the thermohaline circulation in the western Mediterranean have greatly influenced temperature and productivity gradients. In fact, the existence of strong gradients from the Gulf of Cadiz through the Tyrrhenian Sea has been documented in terms of sea surface temperatures (SSTs) and carbonate isotope records (Cacho et al., 2001). However, even though a large set of climate data is available, many aspects of the paleoceanographical evolution of the western Mediterranean since the Last Glacial Maximum (LGM) remains controversial; e.g., the precise influence of Atlantic waters on past circulation in the Mediterranean, spatial and temporal importance of marine productivity fluctuations and the variations of intermediate waters along the western Mediterranean basins. In the eastern Mediterranean geochemical proxies have been extensively used for reconstructing sapropel deposition including productivity and oxygen variations (e.g., Wehausen and Brumsack 1999; Martinez-Ruiz et al., 2000; Emeis et al., 2003; Robinson et al., 2006; Reitz et al., 2006). In the western Mediterranean, by contrast, less research has been devoted to both productivity and ventilation fluctuations, with few studies addressing fluvial and eolian input fluctuations in terms of sediment composition (Moreno et al., 2002; Wedealb et al., 2003; Moreno et al., 2005).

Within the aforementioned framework, this paper attempts to reconstruct detrital supply, marine productivity variations and redox conditions in the western Mediterranean since the LGM, thus improving our understanding of the western Mediterranean sea (WMS) past oceanography. With this objective, a multiproxy approach has been taken in four selected marine records from the Alboran Sea and Algero-Balearic basins. These cores have been collected between 1,500 and 2,500 mbsl, known to be a key depth for detecting changes in the MOW and redox conditions (Reitz et al., 2006; Rogerson et al., 2006). The reconstruction of climatic variability and climatic/oceanographic responses has been made as follows: Ba excess is used as a paleoproductivity proxy; modern analogue techniques in planktonic foraminifera assemblages are used to calculate paleotemperatures, while stable isotope (C and O) composition in *Globigerina bulloides* serves as sea surface proxy; Mg/Al, Si/Al, Zr/Al, K/Al are, in turn, used as detrital proxies. U/Th and other redox sensitive ratios have also provided data regarding changes in ventilation and/or diagenetic processes.

**Paleoenviromental proxies**

The use of Ba as a paleoproductivity proxy has been discussed in great detail in many recent papers (e.g., Gonnea and Paytan, 2006), and it has been suggested that barium proxies should be applied with caution. Barium requires enough pore water sulphate concentration to ensure the absence of sulphate reducing sediments (Paytan et al., 1996; McManus et al., 1998; Eagle et al., 2003), and subsequent Ba remobilisation (Brumsack, 1986; McManus et al., 1998). Moreover, Ba content is also dependent on sediment provenance, sedimentation rates, Ba cycling (Mercone, 2001; Eagle Gonneea and Paytan, 2006) and lateral transport (Sanchez-Vidal et al., 2005). Further limitations of Ba proxies are the variations in the processes affecting its production/accumulation and preservation with time. However, some other geochemical proxies may shed light on the reliability of Ba proxies, such as the Ba/Al ratio profiles themselves. Diagenetic Ba peaks are relatively easy to identify in the geochemical record since they are typically far different from broad Ba profiles derived from enhanced productivity. Additionally, morphological analyses of barite crystals separated by sequential

leaching procedures are evidence of diagenetic or authigenic origin. In general, previous work in the western Mediterranean (e.g., Martinez-Ruiz et al., 2003; Moreno et al., 2004), as well as our own data available for this study, has revealed that Ba content can also be used as reliable proxy for productivity in the western Mediterranean. Furthermore, Ba proxies can be integrated with other paleoceanographical proxies, to shed further light on productivity fluctuations.

Regarding isotope stratigraphy the framework for interpretation of stable isotope data has been well explained by different authors (e.g., Rogerson et al., 2004). Previous studies indicate that $\delta^{18}O_{G.\ bulloides}$ oscillations in the WMS are related mainly with sea surface temperatures (SST) (Cacho et al., 1999) and $\delta^{18}O$ from the Atlantic input (Sierro et al., 2005). Comparison of the variation in $\delta^{18}O$ of the same species between records has been interpreted as showing a difference in environmental conditions, mainly related with changes in temperature and the freshwater cycle (Rogerson et al., 2004; Sierro et al., 2005). Sea surface water paleotemperature estimates are based on the best modern analogue techniques (squared chord distance, squared dissimilarity coefficient and the inverse distance squared weighting function MATSCH2IDW), which have already provided good results in previous studies in the area in question (e.g. González-Donoso et al., 2000; Serrano et al., 2007).

In terms of chemical composition several element ratios can be used as redox proxies (Mn/Al, Fe/Al and U/Th). The use of these ratios is based on their capacity to change their oxidation state in relation to oxygen availability in the environment. Patterns in Mn and Fe complement the behaviour of U (Mangini et al., 2001). Under anoxic conditions U becomes immobile, while reduced Mn and Fe can be dissolved in pore water. Nevertheless, when oxidant conditions reach the sediment, Mn and Fe precipitate as oxi-hydroxides, and U changes into a soluble valence state. This promotes a characteristic manganese peaks than has been described throughout the Mediterranean (e.g., Thomson et al., 1995; Mangini et al., 2001; Jimenez-Espejo et al., 2006; Reitz et al., 2006). However, high sedimentation rates have been reached in the Alboran basin, preventing the development of redox fronts and the use of these redox

relationships. Studies in the eastern Mediterranean sea (EMS) demonstrate that even under high sedimentation rates, single Mn/Al peaks could indicate the presence of ventilation changes (Reitz et al., 2006). These Mn/Al peaks are only well developed in areas where oxic/dysoxic interfaces in the water column contact the bottom topography, turning the location and depth of the core into a key factor for recording these variations in ventilation (e.g., Calvert and Pedersen et al., 1996; Reitz et al., 2006).

The use of several element/Al ratios in order to define changes in the composition of terrigenous detrital matter is based on the relationship between different minerals and their sources. This is the case for Ti/Al and Zr/Al ratios that are related to the presence of heavy minerals, mainly supplied by the Sahara aerosols (e.g., Guieu and Thomas, 1996), and the case of Mg/Al and K/Al ratios, in the EMS, where have been related with variations in Nile river discharge (Wehausen and Brumsack, 1998). In any case, the use of Mg/Al, K/Al, Si/Al as detrital proxies requires a profound understanding of the area, because these elements could be provided by different sources.

## V.2. SITE SETTING

### V.2.1 Oceanographic setting

The semi-enclosed Mediterranean Sea connects with the NE Atlantic ocean through the westernmost Alboran basin. The Alboran basin is surrounded by abrupt physiography drained by mountain rivers. Despite the relatively small size of river basins, recent studies indicate that these rivers are highly important as sediment feeders to the marine environment, and in promoting flood events that result in large suspended plumes dispersed along the Alboran Sea (Liquete et al., 2005). In contrast, the Algero-Balearic basin is more isolated from direct continental/river discharge and from tectonic activity, being the coarse fraction dominated by the supply of submarine canyons (Comas, Zahn, Klaus et al., 1996; Zuñiga et al., 2006).

The surface water of the WMS is composed of inflowing Atlantic water, progressively modified by air-sea interaction, thus giving rise to Modified Atlantic Water (MAW) (Millot, 1999). The intermediate waters flow below the MAW. These are mainly composed of the Levantine Intermediate Water (LIW) generated in the EMS (Cramp and O'Sullivan, 1999). The deepest levels are made up of Western Mediterranean Deep Water (WMDW), which is formed via deep convection in the Gulf of Lion (Benzohra and Millot, 1995). The genesis of WMDW has been attributed to several factors, such as wind strength, initial density of source waters, circulation patterns, freshwater input and greenhouse warming (Rohling and Bryden, 1992; Bethoux et al., 1998; Millot, 1999; Pinardy and Massetti, 2000). WMDW has been well correlated with North Atlantic water evolution and the NAO index (Rixen et al., 2005). However, recent studies indicate that anomalous atmospheric conditions could generate WMDW, even under zero NAO index (López-Jurado et al., 2005).

### V.2.2. Core location

Four cores spanning the last 20 ky have been analysed (Fig. V.1, Table V.1). Alboran basin cores (300G, 302G and 304G) were collected during the Training Through Research (TTR) Cruise 14, Leg 2, while core ODP 975B-1H was recovered during the ODP Leg 161 in the Algero-Balearic basin (Comas, Zahn, Klaus et al., 1996). Results on this last core have been earlier published (Jimenez-Espejo et al., 2006).

**Table V.1.** Core data: location, water depth, studied interval and linear sedimentation rate.

| Core | Location | Water depth (m) | Estudied interval (cm) | Linear Sedim. rate* (cm/kyr) |
|---|---|---|---|---|
| **Alboran basin** | | | | |
| TTR14-300G | 36º 21,532 N,1º 47,507 W | 1 860 | 266 | 13.3 |
| TTR14-302G | 36º 01,906 N, 1º57,317 W | 1 989 | 335 | 16.75 |
| TTR14-304G | 36º 19,873 N, 1º 31,631 W | 2 382 | 291 | 14.55 |
| **Algero-Balearic basin** | | | | |
| ODP161-975B | 38º53.795'N, 04º30.596'E | 2 416 | 150 | 7.5 |

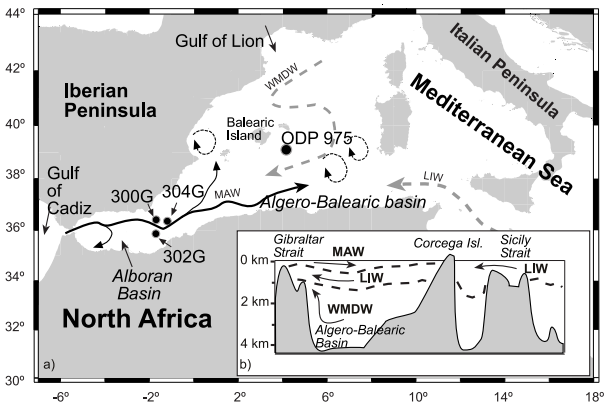


**Figure V.1.** Map of the western Mediterranean showing the location of the studied cores, TTR-300G, TTR-302G, TTR-304G and ODP 975B. Arrows represent the main oceanographic currents. Black line indicates the Modified Atlantic Water (MAW). Dotted lines correspond to eddies. Dashed line represents the Western Mediterranean Deep Water (WMDW) and the Levantine Intermediate Water (LIW). Arrows indicate flow direction. Modified from Cramp and O´Sullivan (1999).

Lithologies from the Alboran cores correspond to greyish olive nannofossil clay and nannofossil-rich silty clay with highly homogenous colouration. Sediments from the Algero-Balearic basin consist of nannofossil or calcareous clay, nannofossil or calcareous silty clay, and slightly bioturbated nannofossil ooze (Comas, Zahn, Klaus et al., 1996).

### V.2.3. Core analyses and age model

#### *V.2.3.1. Core analysis*

Magnetic susceptibility was routinely measured on board during cruises (Comas, Zahn, Klaus et al., 1996, Comas and Ivanov,. 2006). Further analyses were carried out on U-channels that were run at different resolutions (between 0.5 and 1 cm)

with an X-Ray Fluorescence scanner (TATSCAN-F2) (Sakamoto et al., 2006). Alboran basin cores were sampled continuously every 1.5 cm, and core 975B-1H every 2 cm. Sediment samples were divided into two portions, one dried and homogenized in agate mortar for mineralogical and geochemical analyses, the other used to separate marine planktonic foraminifers.

*V.2.3.2. Age model*

The age model is based on 10 $^{14}$C-AMS dates (accelerator mass spectrometry) recorded in monospecific planktonic foraminifers (Table V.2) (Leibniz-Labor for Radiometric Dating and Isotope Research and Poznan Radiocarbon Laboratory). In order to compare our data with other paleoclimatic records, all $^{14}$C-AMS ages were calibrated to calendar years (cal. BP) using Calib 5.0 software (Stuiver and Reimer, 1993). We used the standard marine correction of 400 yr and the Marine04 calibration curve (Hughen et al., 2004). Nevertheless, linear extrapolation between radiocarbon ages may therefore result in spurious differences in age among time-parallel markers. For this reason, the age model was checked, comparing it with other well-dated records in the WMS (Cacho et al., 2001). The validity of the model is also strengthened by stable isotope stratigraphy and major biostratigraphic variations, and further supported by correlation of geochemical profiles.

**Table V.2.** Results of AMS 14C carbon dating of single plancktonic G. bulloides (>125 mm) taken from cores 300G, 302G and 975B-1H. Calibration has been made using Calib 5.0 software.

| Lab. code | Sample Description | Core depth | Conventional Age (BP) | Calibrated age (cal BP) |
|---|---|---|---|---|
| Poz-14597 | 300G/ 2 / 17-19 | 75 cm | 6470 $\pm$ 40 | 6910 $\pm$ 80 |
| Poz-14188 | 300G / 3 / 54-56.5 | 168 cm | 11690 $\pm$ 60 | 13150 $\pm$ 65 |
| Poz-12157 | 300G / 4 / 6-7.5 | 179 cm | 11890 $\pm$ 60 | 13950 $\pm$ 65 |
| Poz-14190 | 302G / 5 / 8-10 | 225 cm | 11950 $\pm$ 50 | 13350 $\pm$ 60 |
| Poz-14186 | 302G / 7 / 53-55 | 374 cm | 20480 $\pm$ 100 | 23990 $\pm$ 160 |
| KIA 27327 | 975B / 1 / 8 - 10 | 9 cm | 2,455 + 30 / -25 BP | 2,049 $\pm$ 54 |
| KIA 27328 | 975B / 1 / 50 - 52 | 51 cm | 7,070 + 40 / -35 BP | 7,519 $\pm$ 42 |
| KIA 27329 | 975B / 1 / 90 - 92 | 91 cm | 13,330 ± 60 BP | 15,201 $\pm$ 135 |
| KIA 27330 | 975B / 1 / 130 - 132 | 131 cm | 15,870 ± 80 BP | 18,768 $\pm$ 67 |
| KIA 27331 | 975B / 2 / 45 - 47 | 190 cm | 19,460 ± 110 BP | 22,512 $\pm$ 114 |

Sedimentation rates at the Alboran sites are much higher than those estimated for the Algero-Balearic area (Table V.1). Sedimentation rates in the Alboran basins oscillate between approx. 10 cm/ky during the late Holocene, and up to 20 cm/ky during some pre-Holocene periods. Temporal resolution is ~200 to ~50 yr for Alboran sites and ~400 to ~175 yr for the Algero-Balearic site (Jimenez-Espejo et al., 2006).

*V.2.3.3. Mineralogy*

Bulk and clay mineral compositions were obtained by X-ray diffraction (XRD). For bulk mineral analyses, samples were packed in Al sample holders. For clay mineral analyses, the carbonate fraction was removed using acetic acid. Separation of the clay fraction and preparation of samples for XRD analyses were performed following the international recommendations compiled by Kirsch (1991). X-ray diffractograms were obtained using a Philips PW 1710 diffractometer with Cu-K⊚ radiation and an automatic slit. Resulting diffractograms were interpreted using Xpowder software (Martin, 2004). Peak areas have been measured in order to estimate semi-quantitative mineral content.

Morphological studies of mineral phases, such as barite, from selected samples were performed by means of field emission scanning electron microscopy (FESEM, Leo Gemini-1530). Quantitative geochemical microanalyses of the clay minerals were obtained by transmission electron microscopy (TEM) using a Philips CM-20 equipped with an EDAX microanalysis system.

*V.2.3.4. Geochemical analyses*

Major element measurements (Mg, Al, K, Ca, Mn and Fe) (Fig. V.2) were obtained by atomic absorption spectrometry (AAS) (Perkin-Elmer 5100 spectrometer) with an analytical error of 2% and by X-Ray Fluorescence (XRF) using a S4 PIONEER. Major element profiles have also been obtained using a non-destructive X-Ray Fluorescence scanner (TATSCANNER-F2, IFREE/JAMSTEC). The XRF-core scanner

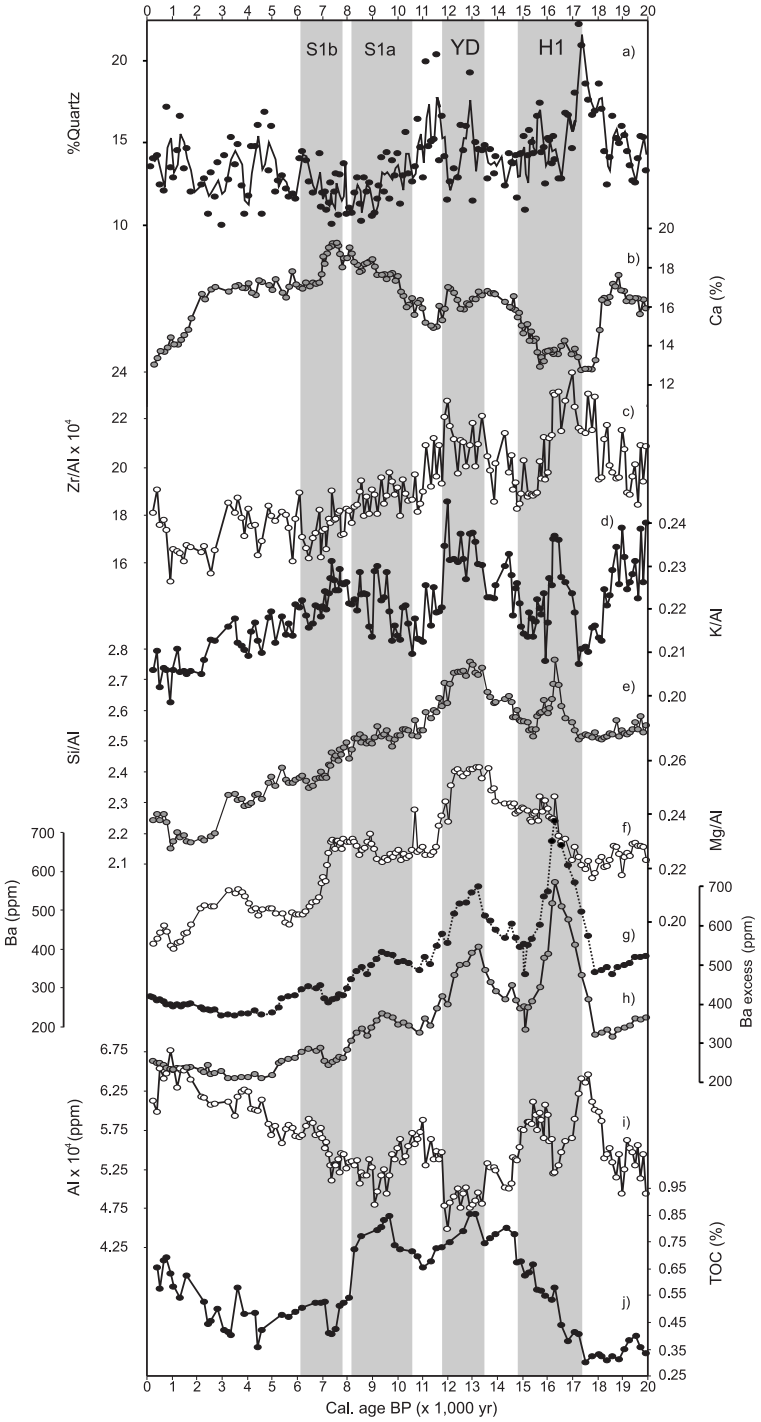


**Figure V.2.** Core TTR-300G age profiles of : (a) relative quartz concentration, 3-period moving average (%); (b) Ca (wt. %) (c) Zr/Al (x$10^4$) ratio; (d) K/Al ratio (e) Si/Al ratio (f) Mg/Al ratio (g) Ba (ppm) (h) $Ba_{excess}$ (ppm) (i) Al x $10^4$ (ppm) (j) Total organic carbon wt. (%) (TOC).Grey vertical bars indicate Heinrich 1 event (H1), Younger Dryas (YD) and sapropel S1 (S1a and S1b) time intervals.

was designed to determine bulk intensities of major elements on split sediment sections (Sakamoto et al., 2006) at intervals between 0.5 and 1 cm with an average accuracy of 0.1% (wt) for standard powder samples of the Geological Survey of Japan.

Comparison of AAS, XRF and XRF-scanner data indicates concordance between techniques. Analyses of trace elements were performed using inductively coupled plasma-mass spectrometry (ICP-MS) following HNO3 + HF digestion. Measurements were taken in triplicates by spectrometry (Perkin-Elmer Sciex Elan 5000) using Re and Rh as internal standards. Variation coefficients determined by the dissolution of 10 replicates of powdered samples were higher than 3% and 8% for analyte concentrations of 50 ppm and 5 ppm respectively (Bea, 1996).

Samples from core 300G were also used to measure Total Organic Carbon (TOC) and Nitrogen. After decalcification on the samples 6 N HCl, both were obtained by combustion at 1050ºC using a Heraeus CHN-O Rapid elemental analyzer as described by Müller et al., 1998. Isotope and TOC data from core 975B-1H have been published previously in Jimenez-Espejo et al. (2006).

*V.2.3.5. Isotopic measurements*

For isotope stratigraphy, stable carbon and oxygen isotope ratios of calcareous foraminifers from core 300G was also obtained (Fig. V.3a, b). Approximately 25 specimens of *G. bulloides* were picked from the >125 μm fraction and senescent forms were avoided. Foraminifers were cleaned in an ultrasonic bath to remove fine-fraction contamination, rinsed with distilled water and thoroughly washed in alcohol. Stable isotopes were measured using a Finnigan MAT 251 mass spectrometer (Isotope Laboratory, Department of Geosciences, University of Bremen, Germany). All $\delta^{18}O$ data given are relative to the PDB standard. Analytical reproducibility of the method is approx. +0.07‰ for both $\delta^{18}O$ and $\delta^{13}C$.

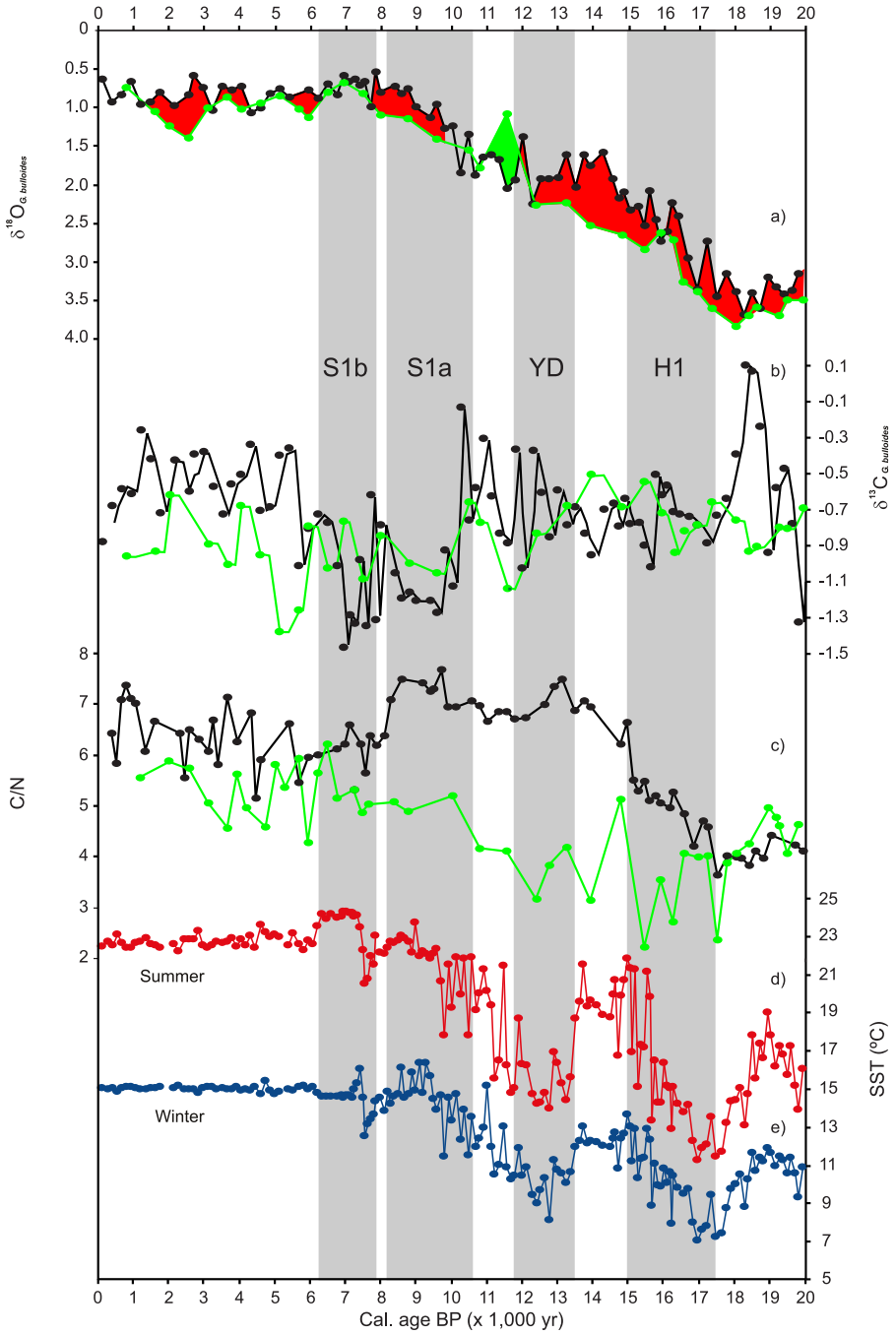


**Figure V.3.** Age profiles (a) Offset of $\delta^{18}O$ between the *G. bulloides* record of TTR-300G (black) and the *G. bulloides* record of ODP 975B (green). (b) $\delta^{13}C$ *G. bulloides* in of TTR-300G (black) and ODP 975B (green) cores. (c) C/N ratio in of TTR-300G (black) and ODP 975B (green) cores. SST's core 300G(d) Summer temperatures (red) (e) Winter temperatures (blue). Grey vertical bars indicate Heinrich 1 event (H1), Younger Dryas (YD) and sapropel S1 (S1a and S1b) time intervals.

## V.3. RESULTS

### V.3.1. Ba excess and TOC.

FESEM analyses of barite crystals from Ba-enriched intervals demonstrate sizes and morphologies corresponding to typical marine barite (1-5 ◎m in size with round and elliptical crystals). Detrital elements peaks (e.g. Al, Zr and K) and Ba maximums display an absence of correlation (Fig V.2) which also suggests that this barite is of authigenic origin. The Ba content derived from marine barite (Ba excess) was obtained by subtracting the amount of terrigenous Ba from the total Ba content (e.g., Dymond et al., 1992; Eagle et al., 2003). It is used here as the excess associated with crustal phases, and is calculated as:

$$(Ba_{excess}) = (\text{total-Ba}) - Al(Ba/Al)_c$$

where total-Ba and Al are concentrations, and $(Ba/Al)_c$ is the crustal ratio for these elements. In this study, we used a value for $(Ba/Al)_c = 0.002$, as estimated by Wedealb et al. (2003), in the Algero-Balearic basin. For Alboran cores, which have a different detrital supply, $(Ba/Al)_c = 0.0033$ was used, as estimated by Sanchez-Vidal et al. (2005) on the basis of current conditions. Al is found mainly in aluminosilicates and it is assumed that the $(Ba/Al)_c$ ratio of terrigenous matter remains constant over the period studied.

In spite of differences in relative amounts of $Ba_{excess}$, all cores show the same pattern of variations (Fig. V.4). Three major enrichment time intervals can be distinguished: ~18 - ~15.3 cal. ky BP; ~13.5 - ~11.3 cal. ky BP, and 10.4 - ~8.2 cal. ky BP. Highest $Ba_{excess}$ content is observed at ~16.1 cal. ky BP (Fig. V.4). Although no data of sediment bulk density are available for Mass Accumulation Rate (MAR), considering the higher LSR in the Alboran basin, we assume that the Ba-MAR was also significantly higher in this area, as compared to the Algero-Balearic basin. The lowest values are reached during the Holocene, after a two-step decrease in $Ba_{excess}$ in the Alboran basin, and only after a single-step decrease in the Algero-Balearic basin (Fig. V.4). TOC

content is less than 0.9% at core 300G and less than 0.5% at core 975B-1H. $C_{org}$/N ratios oscillate between 3.6 and 7.7 at the Alboran Sea core, thus suggesting a mainly marine provenance (Meyers, 1994). TOC variations are sensitive to major climatic changes, with a major drop ~8.0 cal. ky BP. C/N and TOC content follows a high correlation ($r > 0.9$) at core 300G.

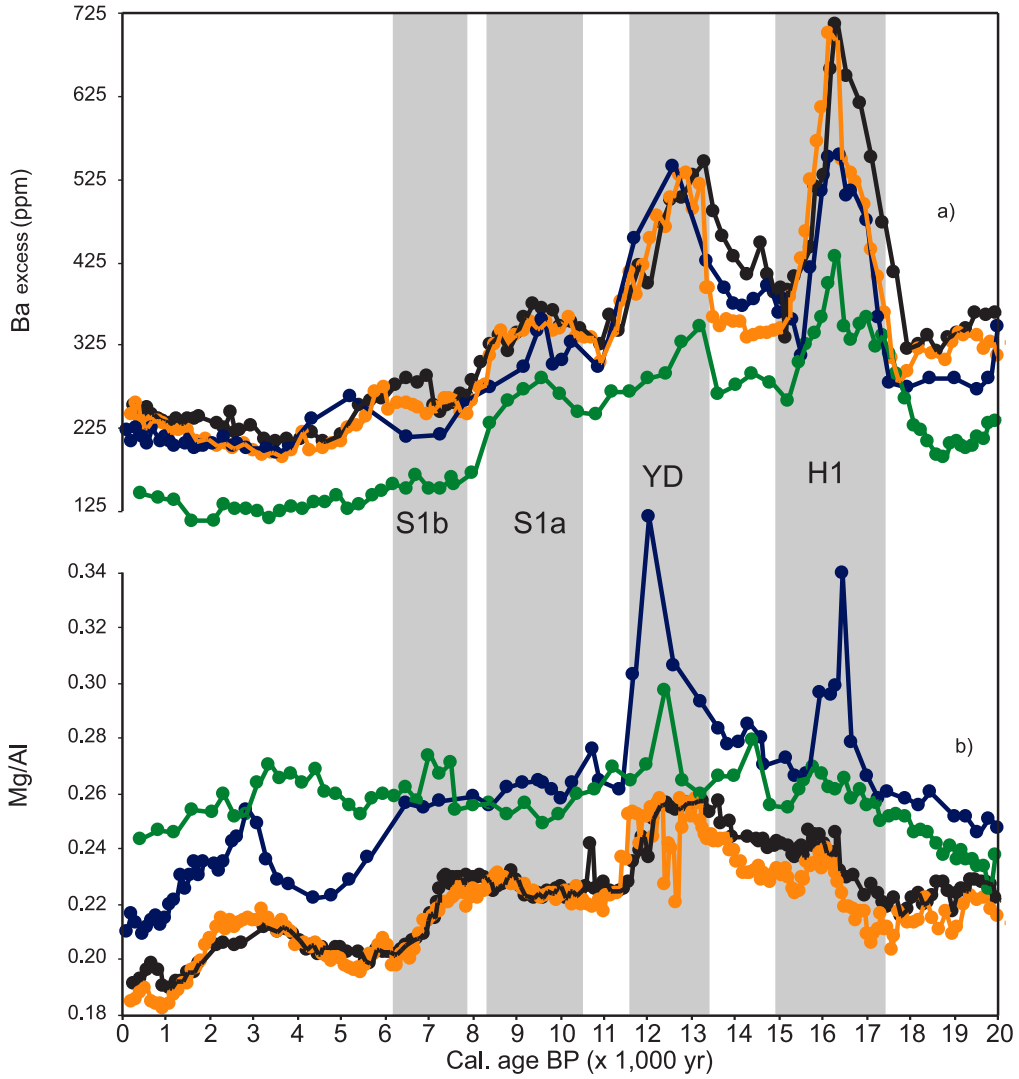


**Figure V.4.** (a) $Ba_{excess}$ (ppm) age plotted comparison among cores. ODP 975B values x 1.5 (b) Mg/Al ratio age plotted comparison among cores. (TTR-300G: black; TTR-302G: orange; TTR-304G: blue; ODP 975B: green). Grey vertical bars indicate Heinrich 1 event (H1), Younger Dryas (YD) and sapropel S1 (S1a and S1b) time intervals.

**V.3.2. Oxygen and carbon isotope and SST variations.**

Oxygen and Carbon isotope composition has been analysed in sediment samples from core 300G and has been compared with that of ODP 975B (Jimenez-Espejo et al., 2006). Maximum glacial-interglacial amplitude in the Alboran core ranges from 3.69‰ to 0.55‰ and lies between 3.84‰ and 0.69‰ for the Algero-Balearic basin, with a total oscillation of 3.14‰ and 3.15‰ respectively. Although $\delta^{18}O$ shows a high correlation (r = 0.92) among cores, some discrepancies are observed. The deglacial period in both cores started at ~18 cal. ky BP, with a continuous increasing trend of $\delta^{18}O$ that stopped during the Younger Dryas (YD). Increase continued in the Alboran Sea until ~7.8 cal. ky BP, but in the Algero-Balearic basin it finished at ~7.0 cal. ky BP. Nevertheless, slight time discrepancies could be also attributed to age model differences.

Values of $\delta^{13}C$ are highly variable in the Alboran Sea basin, and suggest a partial climatic link response. Following the tendency values from this core, three time periods can be distinguished: highly variable values during the last deglaciation, light values during the early Holocene and heavy values during the late Holocene. Minimum values is reached at ~7 cal. ky BP and few significant heavy peaks are found at ~18.3, ~10.2 and ~7.7.

Futher insight on the reconstruction of past sea surface conditions was obtained from paleo-SST obtained from foraminifera plancktonic assemblages in core TTR-300G. The calculated SST indicate cyclical and/or abrupt changes in surface conditions. Usually SST variations are related with major climatic events, nevertheless, few of them could be related to regional factors (e.g., between 8 to 7 ky cal BP). Oscillation of about 7 ºC occurred during the last deglaciation. The lowest SST were reached during the Heinrich 1 event (H1). Bølling-Allerød (B-A) and YD are well constrained by SST variations. Late Holocene values are marked by a highly stable pattern around 23ºC for summer and 13ºC for winter temperatures. Those observations are in agreement with other paleo-SST records in the WMS (Cacho et al., 2002; Perez-Folgado et al., 2003)

### V.3.3 Mineralogy and major and trace elements

The Alboran Sea basin sediments are richer in detrital elements, and are composed of clay minerals (30-60%), calcite (25-50%) and quartz (10-20%), with low quantities of dolomite and feldspar (<5%). In all analysed sediments, accessory minerals such as zircon, rutile, apatite and biotite, as well as authigenic minerals, such as anhydrite-gypsum, pyrite, Mn and Fe oxi-hydroxides have also been identified. Clay mineral assemblages in the Algero-Balearic basin consist of illite (50-80%), smectite (20-40%) and kaolinite + chlorite (15-40%). Clay mineral assemblage from the Alboran Sea sediments are richer in illite (65-85%) and usually poorer in smectites (10-20%) and kaolinite + chlorite (10-25%). Additional clay minerals, such as sepiolite, palygorskite and illite/smectite (I/S) mixed layers were also identified. Analysed sediments from the Algero-Balearic basin are predominantly composed of clay minerals (10-45%), calcite (30-70%) and quartz (10-30%), with low quantities of dolomite and feldspar (<5%) (Jimenez-Espejo et al., 2006).

Geochemical profiles of selected major and trace element ratios are shown in figures V.2 and V.5. Elemental concentrations have been normalized to Al. This normalisation assumes that Al concentrations in sediments are contributed by alumino-silicates (e.g., Calvert, 1990). High correlation between Al and quartz content in the analysed interval also corroborates this idea. No grain-sorting processes or relevant turbidites were recognized throughout the intervals studied. Selected sensitive redox trace elements ratios (Mn/Al and U/Th) display different relationships according to the paleoceanographic evolution. The high values of Mn/Al enrichment in the uppermost section of the core (<10 cmcd) are not represented on the plot because they are off the scale. Relevant timing discordances appears in Mn/Al and U/Th time plot ratios between cores. Mn/Al follow a complex pattern, only partially related with climatic oscillations (Fig V.5). This could be linked with Mn provenance source, detrital and diagenetical. Probably diagenetical phenomena explain Mn/Al enrichments during the last deglaciation, while detrital input could explain Late Holocene Mn/Al increase.

In another hand, low U/Th values were reached during LGM and Late Holocene and, in general, enrichments were reached during H1 and YD and Early Holocene.

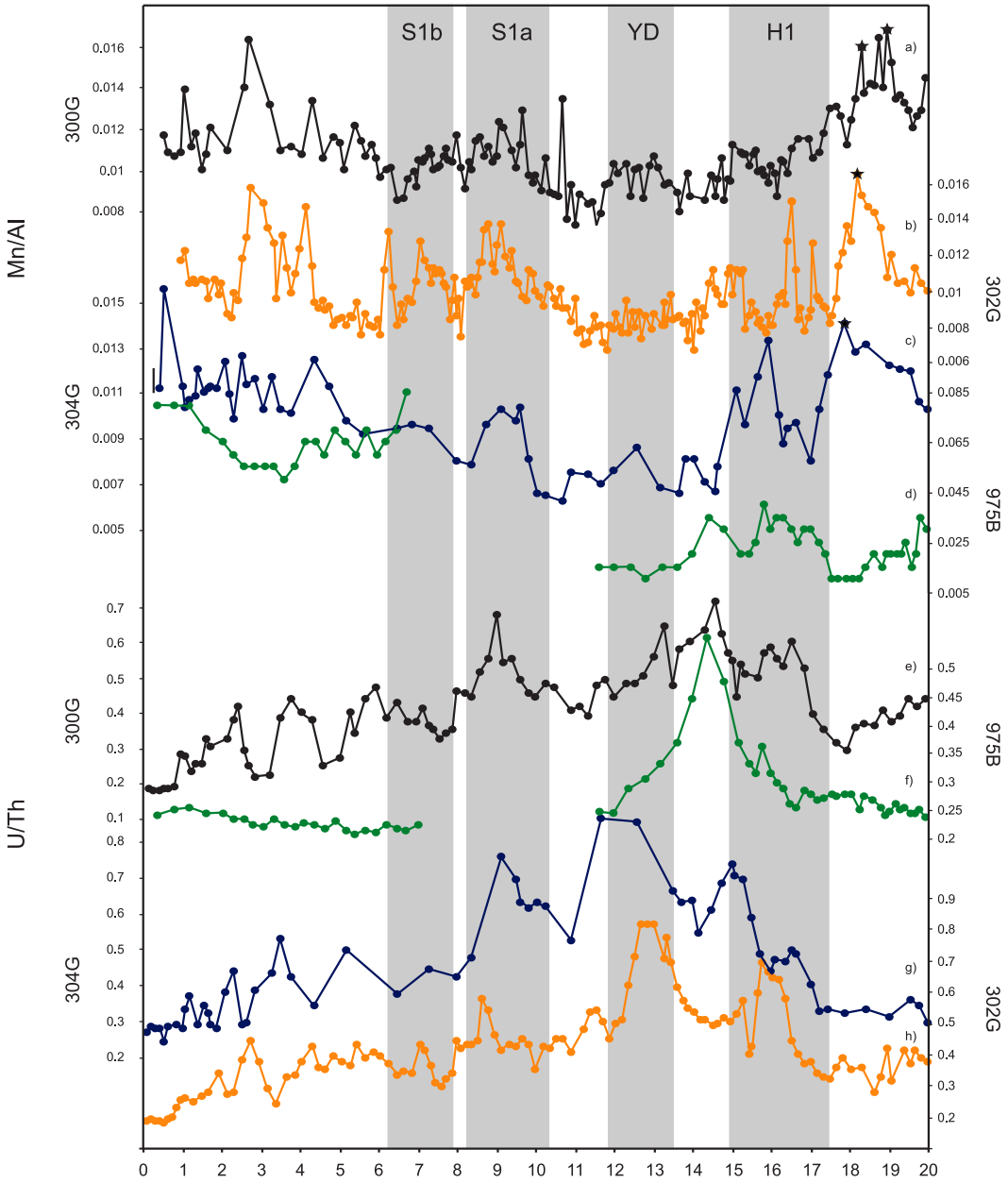


**Figure V.5.** (a) Mn/Al ratio age plotted comparison among cores. (b) U/Th ratio age plotted comparison among cores. Grey vertical bars indicate Heinrich 1 event (H1), Younger Dryas (YD) and sapropel S1 (S1a and S1b) time intervals. (TTR-300G: black; TTR-302G: orange; TTR-304G: blue; ODP 975B: green).

## V.4. DISCUSSION

### V.4.1. Sea surface conditions

During the LGM we found a marked $\delta^{13}C$ isotopic offset, and time points with similar $\delta^{18}O$ values (at 19.8, 19.4 and 18.3 ky cal BP) (Fig V.3a, b). These events, coincident with sharp SST coolings (at 19.8 and 18.3 ky cal BP, see Fig V.3d, e), might be related with the input of cold Atlantic waters penetrating the WMS and reaching the Algero-Balearic basin . The lighter (19.8 ky cal BP) and heavier (18.3 ky cal BP) $\delta^{13}C_{G.\ bulloides}$ values recorded in the Alboran Sea compared with those observed in the Argelo-Balearic basin suggest a variable $^{12}C$ resupply in the Alboran area, and suggest variations in the nature of Atlantic input, as well as the presence of upwelling phenomena in the westernmost Alboran and/or Gulf of Cadiz (Rogerson et al., 2004). At the end of the LGM (~18.0 ky cal BP), a $\delta^{18}O$ isotopic offset can be seen between cores 300G and 975B, while the $\delta^{13}C$ offset almost disappears (Fig. V.3c). The isotopic increase is not mirrored by the SST, however, which shows a cold trend. This suggests that changes occurred early during the last deglaciation were probably related with variations in the characteristics of Atlantic input rather than with climatic changes in this area. (Sierro et al., 2005).

During H1, a narrow $\delta^{18}O$ offset and very stable $\delta^{13}C$ values are observed. The beginning of this cold event is characterised by a decrease in the SST, similar to the one that took place at ~17.0 cal. ky BP, reaching the lowest temperature values estimated for the Alboran Sea in the last 20 cal. ky BP (~7 ºC and ~11 ºC for winter and summer SST respectively). Nevertheless, there was no $\delta^{13}C$ offset. This fact suggests homogeneous cold surface waters occupying both areas, promoted by an intense Atlantic input. A weakened WMDW promoted by the Atlantic input in turn highly enriched by iceberg meltwater at 16.0 ky cal BP has been previously described (Sierro et al., 2005).

After 16 cal. ky BP a stable deglaciation pattern is followed in both basins, and there is an enhancement of the C/N ratio and $\delta^{18}O$ offset between cores. A priori, the light $\delta^{18}O$ observed in the Alboran Sea might be related to the progressive increase in salinity and oxygen isotopes values that the Atlantic input underwent when entering the WMS (Sierro et al., 2005; Cacho et al., 2006), and/or to differential freshwater/coastal influence. During the YD, $\delta^{18}O$ follows a flat pattern and the offset disappears. The SST were lower than those reached during the LGM. $\delta^{13}C$ values become very unstable in the Alboran basin during the YD, which resembles a complex hydrographic setting, probably promoted by similar mechanisms to those proposed above for the glacial period. At the end of YD, a unique situation in the WMS is observed. At 11.5 cal. ky BP there is a large isotopic offset between cores, and an unusual situation is reached, where 975B $\delta^{18}O$ values exceed those from the 300G core. The SST oscillations involve a warming, especially during summer, larger than 5ºC in less than 200 years. This implies a strong east-to-west isotopic gradient that could, in turn, reflect a high temperature contrast, with the warmest waters being in the Algero-Balearic area.

During ~10.0 to ~8.0 cal. ky BP, a new isotope offset between both areas has been established. This period shows stable SST and high $\delta^{13}C$ values that could indicate steady hydrographical conditions. These conditions ended between ~7.7 and ~7.2 cal. ky BP, when a major foraminiferal faunal turnover took place (Perez-Folgado et al., 2003), along with a major oceanographical change giving rise to the current setting of eddies and frontal circulation pattern of the WMS (Rohling et al., 1995). During this transitional period, the lowest $\delta^{13}C$ values were reached in the Alboran Sea. This higher rate of $^{12}C$ supply to surface waters in the Alboran basin compared with the Algero-Balearic basin was probably related a intense vertical water mixing and/or gyres activity. The SST described during this transitional period relevant oscillations (>3ºC), that imply major changes in surface waters. After 7.0 cal. ky BP, the reducing offset of $\delta^{18}O$ and C/N indicates a weak modification of the Atlantic input along both basins. SST values remain very stable, in contrast, $\delta^{13}C$ becomes highly variable after this date, probably reflecting the complex hydrographical pattern established in both areas.

### V.4.2. Paleoproductivity conditions

In terms of marine productivity, the WMS is mostly oligotrophic, although in the westernmost Mediterranean, mesotrophic levels related with current mixing (e.g., Almeria-Oran front) and upwelling also occur (Reul et al., 2005). Organic nutrients are brought to the WMS by the Atlantic inflow (Dafner et al., 2001), whereas mineral nutrients are mainly of aeolian and fluvial origin. Phosphate, which is mainly of fluvial origin, is the limiting nutrient for primary production in the Mediterranean Sea (Krom et al., 1991).

Redox sensitive element distribution rules out major diagenetical influence on the Ba record in both basins for the analysed time interval (Jimenez-Espejo et al., 2006; this study). The TOC record is substantially affected by reoxidation fronts in the Algero-Balearic basin (Jimenez-Espejo et al., 2006). The opposite is true for the Alboran Sea basin. In spite of this, TOC correlation with $Ba_{excess}$ content is poor, as it is during abrupt climatic events (eg. H1). This suggests that the preserved sediment TOC signal partially reflects productivity but is affected by preservation. The earliest $Ba_{excess}$ enrichment to take place during the last 20 ky was in the Algero-Balearic basin around 18.6 cal. ky BP occurred slightly later mirrored in the Alboran Sea basin. The establishment of cold conditions during H1 and the input of a highly fertilized Atlantic jet inflow (Rogerson et al., 2004; Sierro et al., 2005) probably favoured the increase of the marine productivity. The mainly marine origin of TOC, prior to 16 ky cal BP is also corroborated by low C/N values at core 300G.

During the B-A, $Ba_{excess}$ reaches relative low levels in both basins. A productivity offset is established during this period among studied sites in the Alboran Sea basin, showing higher productivity levels in those closer to the margin (Fig V.4a). This is coincident with a $\delta^{18}O$ isotopic offset (Fig. V.3a) and a coetaneous increase in the C/N ratio. Thermohaline intensification that could promote upwelling phenomena has not been described during this period (see section 5.4.2), and Atlantic jet fertilisation was

inactive (Rogerson et al., 2004). Our observations suggest the presence of a freshwater river plume during the B-A that promoted regional productivity differences.

The beginning of the YD is marked by a significant increase in $Ba_{excess}$, which is more pronounced in the Alboran Sea basin. This increase could be caused by different processes, such as a bloom of r-strategist taxa taking advantage of changing conditions (Sprovieri et al., 2003). Nevertheless, previous studies based on diatoms indicate relatively low levels of salinity in surface waters, related with a decrease in salt content of the Atlantic input and increased local river activity in the Alboran margin (Barcena et al., 2001). High Mg/Al ratios in both basins and high C/N values suggest the influence of fluvial activity. It appears that despite arid continental conditions prevailing at that time (Gonzalez-Samperiz et al., 2005), high-loaded river plumes promoted productivity increase until 12.5 ky cal BP, when the productivity started to decrease.

Between ~11 and ~8.2 cal. ky BP the highest $Ba_{excess}$ values in both basins coincide with warmer, wetter climatic conditions in the Mediterranean (Ariztegui et al. 2000). Around 8.2 ky cal. BP marine productivity dropped again (Fig. V.4a). During this period, faunal replacement points to changes at 7.7 ky cal BP (Perez-Folgado et al., 2003), while oxi-redox geochemical proxies (Jimenez-Espejo et al., 2006) suggest further oceanographical variations at ~7.2 ky cal BP. Cores TTR-300G and TTR-302G are sensitive to the 7.7 ky cal BP rapid change, while low $Ba_{excess}$ values were recorded in all cores at ~7.2 ky cal BP, except for core TTR-302G. After those events, the Algero-Balearic basin reaches low $Ba_{excess}$ values that are characteristic of the late Holocene period. Nevertheless a secondary $Ba_{excess}$ enrichment, after the 7.2 event, is observed in the Alboran Sea basin and ended at ~5.4 cal. ky BP.

### V.4.3. Fluvial input and nutrient supply

The previous section describes the variations of marine productivity according to $Ba_{excess}$ content and its relation with fluvial activity. In general, fluvial influence has

been usually underestimated, probably on account of the narrow-drainage river basins that surround the westernmost WMS along with low current rainfall. Enhanced freshwater input might be expected during the wet conditions of the B-A (e.g., Gonzalez-Samperiz et al., 2006), and probably melt water during the early YD (Broecker, 1992). Nevertheless, it was during the Holocene when productivity, apparently, was affected by dry events. A major decrease took place ~8.2 cal. ky BP when cold, dry conditions affected the northern hemisphere (Alley et al., 2005). The minimum $Ba_{excess}$ values reached at 7.2 cal. ky BP could be related with the onset of the present circulation pattern of the Mediterranean Sea (Jimenez-Espejo et al., 2006), and with dry conditions around the WMS (e.g., Wusam et al., 1999). In addition, at 5.4 cal ky BP, arid conditions in the land adjacent to the Tyrrhenian Sea are known (Carboni et al., 2005) as well as aridification periods in North Africa and the Levant (e.g., De Menocal et al., 2000; Jalut et al., 2000; Gasse et al., 2002, Bar-Matthews, 2003). These dryer conditions could be the factor that caused the final decrease in $Ba_{excess}$ in the Alboran Sea.

Fluvial influence could be described by other ratios, such as Mg/Al (e.g., Wehausen and Brumsack, 1998). Three minerals are the main carriers of elemental Mg to the marine sediments: dolomite, smectites and chlorites (Wehausen and Brumsack, 1998; Tipper, 2006). In the analysed sediments, TEM analyses revealed that the most frequent smectite is aluminous-phase (beidellite and I/S illite/beidellite), while Mg rich smectites are rare. Average dolomite content is very low, less than 2%. However, from XRD we can deduce that chlorite content is in excess of 10%. TEM analysis data indicates a chlorite average composition of $(Si_{2.84}Al_{1.16})\ O_{10}\ (Fe_{1.77}\ K_{0.05}\ Al_{1.68}\ Ca_{0.05}\ Mg_{2.29})\ (OH)_8$. These observations suggest that Mg is principally associated with chlorite. Comparing Mg/Al and Si/Al ratios in the Alboran Sea sediments analysed, we obtain a high degree of correlation (r between 0.8 and 0.93) (Fig. V.2e, f). In addition, textural analysis of surface features of the chlorites and quartz grains obtained by SEM indicates features that can be related with abrasive subaqueous actions (Carter, 1984). All the previous observations suggest a similar detrital origin for Mg and Si, mainly supplied by rivers that carry weathering materials (Meybeck, 1987, Tipper, 2006).

In the Alboran Sea basin there was a high-to-moderate correlation between $Ba_{excess}$ and Mg/Al ratio (range = 0.534 - 0.804). However, there was no correlation in the Algero-Balearic basin (r = 0.039). This is interpreted as a high level of sensitivity to river supply in the Alboran basin compared with the Algero-Balearic basin. The Ba content correction ($Ba_{excess}$), along with other analyses (see section 3.1.) show that detrital influence in $Ba_{excess}$ values can be ruled out. All the previous observations suggest a link between atmospheric/fluvial conditions and productivity in the WMS. During wet periods, riverine input of nutrients might have played a primary role in productivity in the Alboran Sea (which is narrower) while only a secondary role in the central WMS. Fluvial discharge could be responsible for enhanced nutrient loads, especially phosphate, and could also have promoted water stratification affecting the composition, mixing and advection of phytoplankton.

This river influence tallies with recent studies, which indicate the high sensitivity of the Mediterranean Sea to freshwater changes (Skliris et al., 2006), and the dynamic evolution of small rivers in spite of their reduced catchment areas (Budillon et al., 2005). In fact, the southern Iberia river systems are very important as sediment feeders to the ocean (Liquete et al., 2005). The narrow continental shelf and the presence of gullies favour sediment transfer from rivers to deeper sedimentary environments (García et al., 2006; Lobo et al., 2006).

### V.4.4. Paleo-ventilation reconstruction

Changes occurring in the intensity, density and flowing depth of the MOW were influenced by the formation of intermediates and deep water masses in the Mediterranean (Rogerson et al., 2005; Sierro et al., 2005; Cacho et al., 2006; Voelker et al., 2006). For the sake of simplicity, in this study we will limit our representation of intermediate waters to the LIW and of deep waters to the WMDW. However, past variations in water masses such as the Tyrrhenian Deep Water, or the Winter Intermediate Water could also have played some role in WMS paleoceanography (Send

et al., 1999). Changes in the WMDW can be inferred from variations in bottom ventilation conditions (Cacho et al., 2006) as well as the location of water mixing surfaces (Reitz et al., 2006). The development of redox fronts could provide information about currents, as described at core 975B-1H (Jimenez-Espejo et al., 2006). Nevertheless, high sedimentation rates in the Alboran basin prevent the formation of redox fronts when more oxic waters reach the sea floor. This observation is corroborated by the absence of diagenetical relationships between Mn/Al and Fe/Al peaks, and correlation with other published data, such as $\delta^{13}C$ in benthic foraminifera (Cacho et al., 2006) (Fig. V.5). With regard to the Fe/Al ratio, the presence of abundant framboidal pyrite established by SEM analyses demonstrates the existence of a microenvironment with oxygen depletion and secondary sulphide deposits. Thus, caution must be exercised when using Fe a input material proxy in the Alboran basins.

*V.4.4.1. LGM and H1.*

Prior to the H1 period, all the cores studied show low U/Th ratios and high Mn/Al values. This could indicate well-ventilated conditions around both basins on account of WMDW strengthening. The single Mn/Al peaks correlate well in all the Alboran cores (Fig. V.5a,b,c,d). A first Mn/Al peak appears at the shallowest core (TTR-300G; 1860 mbsl) at 19.0 ky cal BP, followed by a series of peaks, the last of which is dated at 18.3 ky cal BP (Fig. V.5a,b,c). Consequently, at 18.2 ky cal BP a pronounced Mn/Al peak appears at the next Alboran core (TTR-302G; 1989 mbsl), and finally, at 17.9 ky cal BP, a maximum Mn/Al peak at the deepest site (TTR-304G; 2382 mbsl). This progression of Mn/Al peaks could indicate a redoxcline deepening prior to the H1 event. The redoxcline probably represents the boundary between the LIW and the WMDW, and could be related with the base of the MOW, whose estimated depth in the Gulf of Cadiz was ~2,000 m during the LGM (Rogerson et al., 2006). This could suggest that the main strength of the MOW was supplied by the eastern Mediterranean waters. Other implication is that the LIW-WMDW redoxcline was located deeper than they are today, as well as has been concluded for the MOW base in previous studies (Rogerson et al., 2006; Cacho et al., 2006).

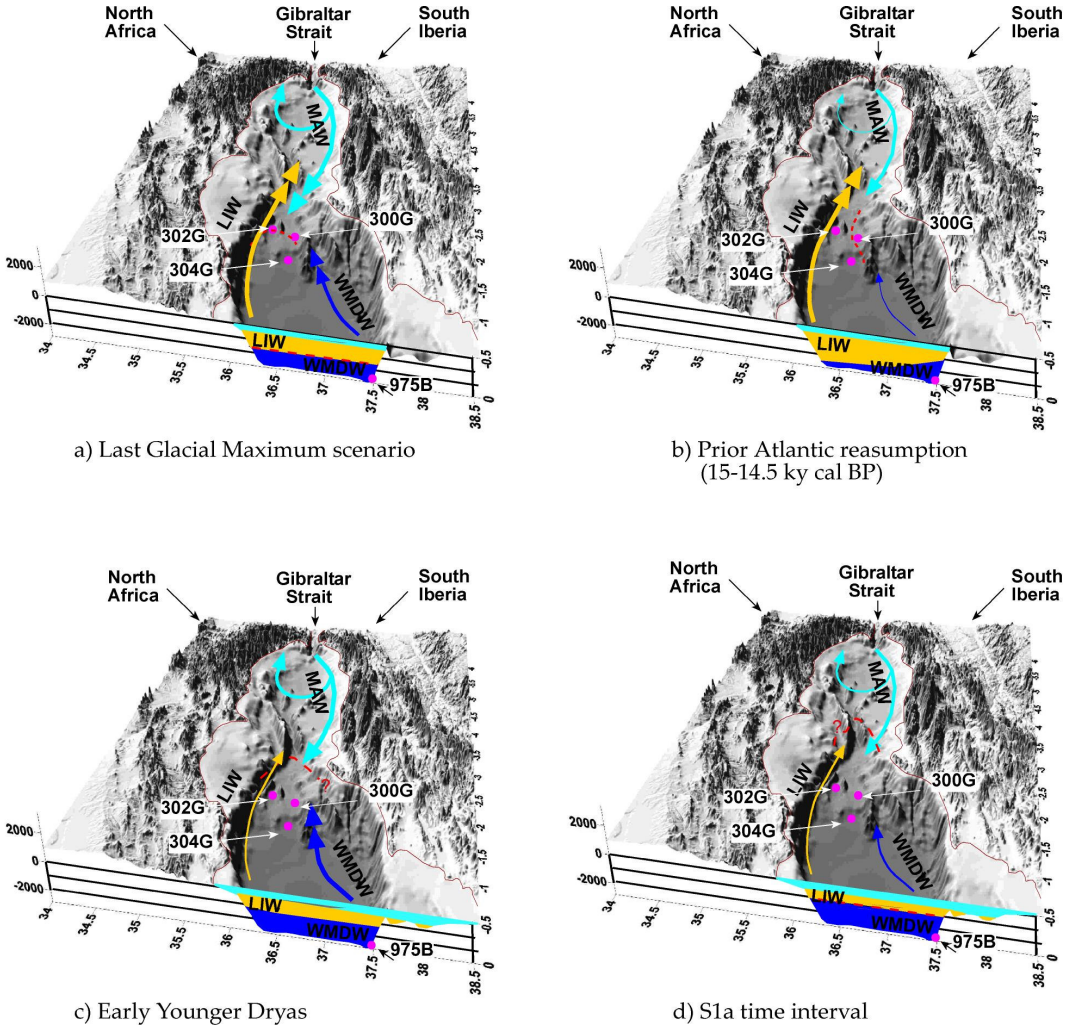


**Figure V.6.** Paleoceanographic scenarios that summarize main currents changes that controlled redox element distribution along Alboran and Algero-Balearic basins(a) Last Glacial Maximum scenario (b) Between H1 and 14.5 ky cal BP (c) Early Younger Dryas (d) S1a time interval.

During H1 a relevant oceanographic change occurred. The increase of the U/Th ratio indicates low ventilation conditions coupled with a weakned WMDW. This could have caused a shallowing of the WMD-LIW redoxcline (also recorded in cores 304G and 302G, Fig. V.6b). The decrease in ventilation reached a critical stage at the culmination of H1 (~16.0 ky cal BP) when fresher Atlantic waters occupied the surface

of the WMS (Sierro et al., 2005; Cacho et al., 2006). During this period, the U/Th ratio of all cores increased in both basins, indicating a weakened WMDW. Nevertheless the southernmost Alboran position, 302G, follows a different trend after 16.0 ky cal BP, and the U/Th ratio progressively decreases. Intense MOW and contourite formation has been described in the Gulf of Cadiz during H1 (Toucanne et al., 2006). It is probable that an intense LIW input sustained the MOW during this event, and the location of core TTR-300G in a preferential pathway for the LIW suggests a slight north-south divergence in the Alboran records.

*V.4.4.2. H1 through YD.*

By the end of H1, the WMDW-LIW redoxcline apparently underwent a process of shallowing and/or attenuation, and did not record in our Mn/Al record during the remaining deglacial period. Surprisingly, the U/Th ratio increased in the northern cores (975B and 300G) until 14.5 ky cal BP (Fig. V.5e,f), suggesting a weakning of the WMDW throughout H1 into Bølling (Fig. V.6c). At 14.6 cal ky BP a major change happened in North Atlantic circulation, consisting of an abrupt intensification of intermediate and deep currents (McManus et al., 2004; Gheriardi et al., 2005). This resumption of Atlantic circulation and/or the associated oceanographic changes apparently triggered an intensification in the formation of the WMDW at 14.5 ky BP, increasing bottom ventilation in the northern cores. Nevertheless, during the B-A, an increase in the U/Th ratio at the southernmost core suggests a significant reduction of the LIW. In order to witness a resumption of this current, we must wait for the YD onset (~12.5 ky cal BP) (Fig. V.6c), when a sharp decrease in the U/Th record at core 302G was recorded (Fig. V.5h). The strength of the LIW probably promoted MOW intensification and the formation of the YD contourite in the Gulf of Cadiz (Faugeres et al., 1984; Voelker et al., 2006). In spite of the formation of WDMW during B-A and YD, its intensity was not high enough in order to avoid low ventilation at the deepest levels of the Algero-Balearic basin (Fig. V.5f). A reduced density gradient between the upper and lower layer, along with the rise in sea level and freshwater input could explain this weakening of WMDW formation (Schönfeld et al., 2000; Rogerson et al., 2005). Well-

ventilated conditions did not reach core TTR-304G until ~11.5 ky cal BP (Fig. V.5g). Afterwards, redox information from core 975B-1H is not representative of the original conditions because it is affected by a redox front (Jimenez-Espejo et al., 2006).

*V.4.4.3. The Holocene*

The high U/Th ratios reached during the Early Holocene in all our cores indicate low oxygenate conditions along both basins (Fig. V.5e,g,h). During this period, humid conditions set in around the Mediterranean, promoting the formation of the last sapropel in the eastern Mediterranean basins between 9.5 and 6.0 ky cal BP (Mercone et al., 2001). Both WMDW and LIW were weak, reaching a ventilation minimum at ~9.0 ky cal BP (Fig V.6d). The cause of this weakness can probably be attributed to high riverine input which, in turn, reduced surface salinity, and affected the formation of intermediate and deep waters (Bethoux and Pierre, 1999). The sensitivity of Mediterranean thermohaline circulation has been confirmed by recent circulation models that reflect thermohaline sensitivity to a variation of 5-10% in the Mediterranean mean freshwater budget (Skliris et al., 2006).

The end of these low ventilation conditions followed a two-step pattern. The first abrupt decrease could be associated with the 8.2 cold event, reported throughout the Mediterranean (e.g. Ariztegui et al., 2000; Sprovieri et al., 2003). This cold event interrupted the formation of sapropel S1 in theEMS, giving rise to two sequences, S1a and S1b (Ariztegui et al., 2000), and probably promoted the formation of deep waters along the Mediterranean. Relative low values in the Mn/Al ratio at this time probably indicate a major change in the position of the oxic/dysoxic interface. A definitive interruption of low ventilation conditions, which probably marked the start of the current circulation pattern, occurred between 7.9 and 7.2 ky cal BP. It seems that the LIW flowed with sufficient strength to bring about well oxygenated conditions in the Alboran cores between 7.9 and 7.2 ky cal BP, despite the fact that sapropel deposition continued. In fact, the offshore formation of the LIW and its intermediate depths could have prevented river influence and maintained low ventilation in the EMS. At 7.2 ky

cal. BP the WMDW abruptly restarted, promoting the development of a redox front at core 975B-1H (Jimenez-Espejo et al., 2006), and changes to the water column in further WMS basins, such as the Tyrrhenian (Carboni et al., 2005). At 7.2 ky cal BP we are probably witnessing the filling of the whole deep area of the WMS by a intense WMDW (Jimenez-Espejo et al., 2006). Nevertheless, this new re-start gave rise to relatively less-oxygenated conditions in the Alboran basin than had been seen in the previous 700 years. Fluvial discharge and atmospheric conditions under a high sea-level stand could explain these intra-Holocene changes.

The end of sapropel S1 deposition in the EMS around 6.2 ky cal BP (Casford et al., 2003) is well marked by the Mn/Al ratio at core 302G (Fig. V.5b), indicating once again the high sensitivity of this core to LIW changes. The most recent U/Th enrichment peaks located at core 300 (Fig. V.5e) seem to describe 1.4 ky cycles between 7.2 ky BP and the subrecent. These cycles have been described for previous periods (Moreno et al., 2005) and could be related with the intensity of the northwesterly winds over the Gulf of Lions and consequent WMDW convection (Cacho et al., 2000).

## V.5. CONCLUSIONS

Sea surface temperatures, oxygen isotope values and geochemical proxies evidence significant climate and oceanographic variations in the westernmost Mediterranean Sea since the LGM. A persistent isotopic and geochemical offset indicates the presence of significant gradients between the Alboran and the Algero-Balearic basins. These gradients mainly resulted from changes in the Atlantic input, eastern Mediterranean currents and fluvial input. Marine productivity, characterized by Ba excess, was higher in the Alboran basin than in the Algero-Balearic basin. The Mg/Al ratio suggests strong effect of riverine input on marine productivity in the Alboran basin during wet periods such as the B-A, Early Holocene and also during the first half of YD.

Sea level, Atlantic input and atmospheric/oceanographic conditions (river/runoff input, wind intensity and sea surface temperature) have modulated the Mediterranean

thermohaline circulation. Changes in the WMDW have been inferred from variations in bottom ventilation conditions. The development of redox fronts and redox proxies provide information about ventilation conditions. Prior to the H1 period, well-ventilated conditions occurred in both basins on account of WMDW strengthening and a redoxcline deepening, which probably represents the boundary between the LIW and the WMDW. During H1, redox proxies indicate low ventilation conditions coupled with a weakened WMDW. The YD is characterized by a strengthened LIW which probably promoted the intensification of MOW. During the early Holocene low oxygen conditions occurred along both Alboran sea and the Algero-Balearic basins. Low ventilation conditions also appear to be associated to weakened WMDW and LIW currents. The end of these low ventilation conditions followed a two-step pattern. The first abrupt decrease could be associated with the 8.2 cold event. This cold event interrupted the formation of sapropel S1 in the EMS and probably promoted the formation of deep waters along the Mediterranean. Afterwards, low ventilation conditions were interrupted between 7.9 and 7.2 ky cal, which probably marked the start of the present-day circulation pattern. During the whole time period studied, our data suggest that the South Alboran area was sensitive to LIW oscillations, and comparisons with studies in the Gulf of Cadiz indicate that enhanced MOW flow was primarily driven by LIW input.

# VI. Climate forcing and Neanderthal extinction in Southern Iberia: insights from a multiproxy marine record

# Climate forcing and Neanderthal extinction in Southern Iberia: insights from a multiproxy marine record

Francisco J. Jiménez-Espejo, Francisca Martínez-Ruiz, Clive Finlayson, Adina Paytan, Tatsuhiko Sakamoto, Miguel Ortega-Huertas, Geraldine Finlayson, Koichi Iijima, David Gallego-Torres, Darren Fa.

Journal Quaternary Science Reviews. (Accepted)

## ABSTRACT

Paleoclimate records from the western Mediterranean have been used to further understand the role of climatic changes in the replacement of archaic human populations inhabiting South Iberia. Marine sediments from the Balearic basin (ODP Site 975) was analysed at high resolution to obtain both geochemical and mineralogical data. These data were compared with climate records from nearby areas. $Ba_{excces}$ was used to characterise marine productivity and then related to climatic variability. Since variations in productivity were the consequence of climatic oscillations, climate/productivity events have been established. Sedimentary regime, primary marine productivity and oxygen conditions at the time of population replacement were reconstructed by means of a multiproxy approach. Climatic/oceanographic variations correlate well with Homo spatial and occupational patterns in Southern Iberia. It was found that low ventilation (U/Th), high river supply (Mg/Al), low aridity (Zr/Al) and low values of $Ba_{excess}$ coefficient of variation, may be linked with Neanderthal hospitable conditions. We attempt to support recent findings which claim that Neanderthals populations continued to inhabit southern Iberia between 30 to ~28 ky cal BP and that this persistence was due to the specific characteristics of South Iberian climatic refugia. Comparisons of our data with other marine and continental records appear to indicate that conditions in South Iberia were highly inhospitable at ~24 ky cal BP. Thus, it is proposed that the final disappearance of Neanderthals in this region could be linked with these extreme conditions.

## VI.1. INTRODUCTION

Human origins and the extinction of archaic populations have been the subject of intense debate in recent decades (e.g., Stringer and Andrews, 1988; Wolpoff, 1989; Brauer, 1992; Harpending et al., 1993; Lahr and Foley, 1998). Many hypotheses have been proposed for the extinction of such populations. Among the latter, research has focussed primarily on Neanderthals (e.g., Flores, 1998; Finlayson, 2004; Horan et al., 2005; Finlayson et al., 2006). The Neanderthal extinction took place mainly during Marine Isotope Stage 3 (MIS3), a period which has been considered highly unstable and which is characterised by conditions not existing in present-day environments (Stewart, 2005). Recent studies have suggested that climatic and environmental factors alone may have caused Neanderthal extinction, given that climatic stability was of crucial importance for their distribution (Finlayson and Giles-Pacheco, 2000; Stewart et al., 2003a; Stewart, 2004a). Climatic variability has been determined by using a number of proxies such as $\delta^{18}O$ (Stringer et al. 2003; Burroughs, 2005). However, the hypothesis based on climatic and environmental factors alone has not been widely accepted, despite the fact that it has been discussed in depth. It is well known that Neanderthal populations were in fact able to successfully adapt to significant climatic fluctuations for approximately 300 ky (Finlayson, 2004). Their adaptability is likely to have involved a profound knowledge of their environment and the capacity to exploit different hab itats, as well as seasonal mobility strategies, occupation of rich biotope areas (Finlayson, 2004; Finlayson et al. 2004), improved tool-making skills and better lithic resource management (Baena et al., 2005). Local extinctions and abandonment were, however, frequent in Neanderthal ecology (Trinkaus, 1995).

Neanderthal extinction is an especially difficult topic since it requires that relevant existing data from a multitude of disciplines be brought together and correlated with an appropriate methodological rigor on which consensus among researchers is highly problematic. The difficulties include: aspects of climatic influence on archaeological records, complex relationships between fossils and climatic conditions, incomplete nearby continental records, biased interpretations of climatic

records, the sources of cultural features, an overemphasis on artefacts, rudimentary excavation techniques, dates obtained through a variety of methods and materials, dating and age models, and the coexistence of different underlying paradigms. The consequence of such a panorama is a highly fragile epistemology (Vega Toscano, 2005). It has been suggested that the late Neanderthal populations survived in Southern Iberia. In general, Southern Iberia has been considered a "cul du sac" (Zilhao, 1996; Finlayson, 1999), playing a passive role in human/bio logical evolution. From this traditional point of view, the presence of relict taxa has been attributed to the position of the Southern Iberian Peninsula and its isolation from the major source of Euro-Asiatic faunal/floral input (Taberlet et al., 1998, Hewitt, 2000). However, the presence of species in this area could be related to its character as a climatic refugium (Finlayson, 2006) and to the fact that it is a biodiversity hotspot (Mota et al., 2002). In the late Pleistocene, three areas have been identified as major temperate and/or Mediterranean vegetation refugia during glacial periods: the Iberian, Italian and Balkan Peninsulas, (Bennett et al., 1991; Willis, 1996; Carrión et al., 2000; Tzedakis et al., 2002; Finlayson, 2006). "Cryptic" refugia have also been described, thus explaining the presence of Neanderthals in the Belgian Ardennes during the late MIS 3 (Stewart and Lister, 2001, Stewart et al., 2003b). The populations living in these refugia re-colonised central and northern Europe several times during the Late Pleistocene. It should be kept in mind that the capacity of refugia to continue carrying an ecosystem is a function of their specific location. The main characteristics of Southern Iberian refugia are their large scale, relatively low continentality, relative climatic stability, insolation and topography. These characteristics can only be reconstructed on the basis of representative local paleoclimatic records (Finlayson, 2006). In the case of the Southern Iberian Peninsula, the Algero-Balearic and Alboran basins provide particularly reliable climatic records (e.g., Cacho et al., 1999). Research has shown that the climatic conditions in this region were subjected to significant variations, mainly as a result of Glacial-Interglacial oscillations, Heinrich Events (HE), Dansgaard-Oeschner (D/O) stadials and interstadials (Moreno et al., 2005a).

In order to understand the paleoclimatic evolution in southern Europe and its relation to the aforementioned population refugia, a multi-proxy, high-resolution analysis was carried out in a marine sediment record from the western Mediterranean sea (WMS) (ODP core 975B-1H) (Fig. VI.1). This paper attempts to use Ba and Ba/Al ratios not only as paleoproductivity proxies, but also as an indicator of climatic stability. Mineral composition and trace element ratios have been used as paleo-proxies for paleoenvironmental reconstructions. K/Al and Mg/Al ratios, as well as quartz and clay minerals (e.g., illite and chlorite), were used to characterize river supply. Aeolian input has been characterized by Zr/Al and Ti/Al ratios. Trace elements sensitive to redox conditions (e.g., Fe, U, Co and Cr) have been used as paleo-redox and ventilation proxies. The results obtained have also been compared with other marine and continental climate records on regional and global scale in order to interpret the climatic conditions that may have affected Neanderthal populations.

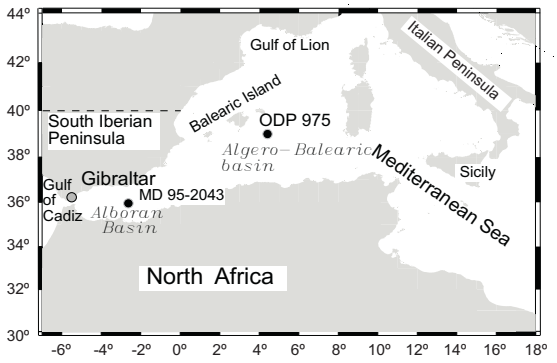


**Figure VI.1.** Figure showing the locations of ODP Site 975 and one other related core (MD 95-2043).

## VI.2. MATERIALS AND METHODS

### VI.2.1. Site description and sedimentation rate

ODP Site 975 is located in the Northern margin of the Algerian-Balearic basin (Southeast Majorca island) (38º 53.795′ N 4º 30.596′ E; 2416 m.b.s.l.). Sediments at this

site consist of nannofossils and calcareous clay, nannofossils and calcareous silty clay, and slightly bioturbated nannofossil ooze (Comas, Zahn, Klaus et al.,1996). The upper 382 cm of core 975B 1H were sampled continuously every 2 cm. Sediment samples were divided into two portions, one dried and homogenized in agate mortar for mineralogical and geochemical analyses, the other used to separate marine plancktonic foraminifers.

The age model is based on seven 14C-AMS dates (accelerator mass spectrometry) using monospecific planktonic foraminifers (Leibniz-Labor for Radiometric Dating and Isotope Research, Kiel, Germany), stable isotope stratigraphy and biostratigraphic events were also used for age determination (Jiménez-Espejo et al., submitted). In order to compare our data with other paleoclimatic records, all 14C-AMS ages were calibrated to calendar ages (cal. BP) using the Calib 5.0 software (Stuivert and Reimer, 1993). The age model was refined by graphic correlation with isotopic/geochemical data from well dated sections such as MD95-2043 (Cacho et al., 1999). This age model covers the last ~41 ky BP, whereas our study focuses on the interval of 20 to 41 ky BP. Linear sedimentation rates oscillate between 4 and 18 cm/ky. These variations in linear sedimentation rates at site 975B could be associated with gradual variations in terrigenous-detrital matter input during the time covered. Temporal resolution in the analytical series at this core is ~400 to ~100 yr, which is sufficient to distinguish millennial/centennial climatic oscillations, thereby allowing adequate millennial variance analyses.

### VI.2.2. Mineralogical and geochemical analyses

Bulk and clay mineral compositions were obtained by X-ray diffraction (XRD) following the international recommendations compiled by Kirsch (1991). X-ray diffractograms were obtained using a Philips PW 1710 diffractometer with Cu-K$\alpha$ radiation and automatic slit. The resulting diffractograms were interpreted using the Xpowder software (Martín, 2004). Estimated semiquantitative analysis error for bulk

mineralogy absolute values is 5% and error ranges from 5% to 10% for clay mineral proportions. FE-SEM analyses were performed to check barite origin.

Total organic carbon (TOC) and total Nitrogen content were measured in separate portions of air-dried sediment samples by a CHN analyser (Perkin Elmer 2400 Series 2). Each powder sample processed for TOC was treated with HCl (12N) in a silver cup, until mineral carbon was completely removed. Samples were wrapped after dehydration on a hot plate for 12 hours. Standards and duplicate analyses were used as controls for the measurements, indicating an error of under 0.05%.

Major element measurements (Mg, Al, K, Ca, Mn and Fe) were obtained by atomic absorption spectrometry (AAS) (Perkin-Elmer 5100 spectrometer) with an analytical error of 2%. An X-Ray Fluorescence scanner (University of Bremen) was also used to obtain K, Ca, Ti, Mn, Fe, Cu and Sr count fluctuations. The XRF-core scanner was set to determine bulk intensities of major elements on split sediment sections (Jansen et al., 1998; Rölh and Abrams, 2000) at intervals of 1 cm with an accuracy in standard powder samples of more than 0.20 % (wt). The AAS and XRF-scanner data were compared and results indicating a high correlation between techniques. An average concentration of Ti in the core was obtained from XRF-core scanner data in order to normalize Ti to Al contents. This normalized average will be referred to as Timean /Al. Analyses of trace elements including Ba were carried out using inductively coupled plasma-mass spectrometry (ICP-MS, Perkin Elmer Sciex Elan 5000) after HNO3 + HF digestion. Measurements were performed in triplicates using Re and Rh as internal standards. Variation coefficients determined by dissolution of 10 replicates of powdered samples were 3% and 8% for analyte concentrations of 50 and 5 ppm, respectively (Bea et al., 1996).

Stable carbon and oxygen isotope ratios of calcareous foraminifers were analysed to establish the stratigraphic framework of the samples from core 975B 1-1H. Approximately 25 specimens of Globigerina bulloides were picked from the >125 μm fraction and senescent forms were avoided. Foraminifers were cleaned in an ultrasonic

bath to remove fine-fraction contamination, rinsed with distilled water and thoroughly washed in alcohol. Stable isotopes were measured using a GV Instruments Isoprime mass spectrometer. Analytical reproducibility of the method is +0.10‰ for both δ18O and δ13C 122 based on repeated standards.

## VI.3. RESULTS

### VI.3.1. Paleoproductivity proxies

TOC and Ba content have been used to determine productivity fluctuations. TOC content oscillates between 0.2 and 0.35. Corg/N ratio values oscillate between 2 and 6, which suggests a marine provenance (Meyers, 1994). However, TOC content displays a low correlation with Ba content, probably indicating poor preservation of the TOC record, as has also been shown for Holocene sediments from this same site (Jiménez-Espejo et al., submitted). In contrast, the Ba record seems to be well preserved. The FE-SEM analyses corroborated the presence of barite crystals with morphologies corresponding to typical marine barite (1-7 μm in size with round and elliptical crystals). Despite discussion regarding paleoproductivity estimates based on Ba excess (Eagle et al., 2003; Eagle Gonneea and Paytan, 2006), at this site the Ba content can still be considered a good indication of productivity fluctuations, specifically since we established the presence of authigenic marine barite in the samples. Within the analyzed time interval no substantial changes in sediment composition are detected suggesting that changes in Ba bearing phases are negligible and therefore the fluctuations obtained derive from productivity variations. Although uncertainties regarding the correction for silicate-associated Ba do not allow one to obtain quantitative export production values, information on productivity variations is still valid. The latter has been obtained by subtracting the amount of terrigenous Ba from total Ba content (e.g., Eagle et al., 2003).

$$(\text{Ba excess}) = (\text{total-Ba}) - \text{Al}(\text{Ba/Al})\text{c}$$

where total-Ba and Al are concentrations and (Ba/Al)c is the crustal ratio for these elements. For this site we have used (Ba/Al)c= 0.002, as estimated by Weldeab et al. (2003) for the Balearic Sea on the basis of surface sediments and current o ligotrophic conditions. It is assumed that the (Ba/Al)c ratio of the terrigenous matter remains constant over the period considered. Changes in catchment areas could affect the (Ba/Al)c ratio of the terrigenous matter, but the (Ba/Al)c ratio shows no significant changes during the last glacial period. The lack of correlation between Ba peaks and detrital elements also suggests a mainly authigenic origin for Ba enrichments. Maximum $Ba_{excess}$ content is observed at ~23.3 ky BP (Fig. VI.2) along with other peaks (e.g., ~34, ~29.2, ~24.7 and ~20.5 ky cal BP). $Ba_{excess}$ and TOC do not follow similar trends. Maximum TOC content during the last glacial period was reached at ~25.8 and ~20.3 ky cal BP with occasional, sharp low/high TOC values.

### VI.3.2. Sea surface conditions obtained through stable isotopes

The oxygen stratigraphic framework for the time interval analyzed at site 975 can be correlated with episodes of changing temperature, resembling the global variation of the SPECMAC isotope curve (Martinson et al., 1987). The maximum amplitude between 20 to 41 ky cal BP of $\delta^{18}O$ G. bulloides in core 975B-1H lies between 2.67 ‰ and 3.76‰, with a total oscillation of 1.09 ‰. The $\delta^{18}O$ G. bulloides develops a cyclical pattern with sudden oscillations that could be associated with abrupt warmings (~21.3, ~28.8 and ~33.6 ky cal BP) or coolings (~21.8, ~22.8, ~25.5 and ~27.4 ky cal BP) (Fig. VI.2). Such variations could be related to the climate cycles defined by Moreno et al. (2005a) in the Western Mediterranean Sea (WMS). Values of $\delta^{13}C$ G. bulloides were found to be highly variable. Maximum amplitude of $\delta^{13}C$ G. bulloides is between –0.24 ‰ and –1.32 ‰, with a total oscillation of 1.08‰. $\delta^{13}C$ G. bulloides undergoes sudden increase/decrease shifts which may be correlated with variations in Atlantic inflow fertilisation and/or gyre activities (Bárcena et al., 2001; Rogerson et al., 2004; Voelker et al., 2006).

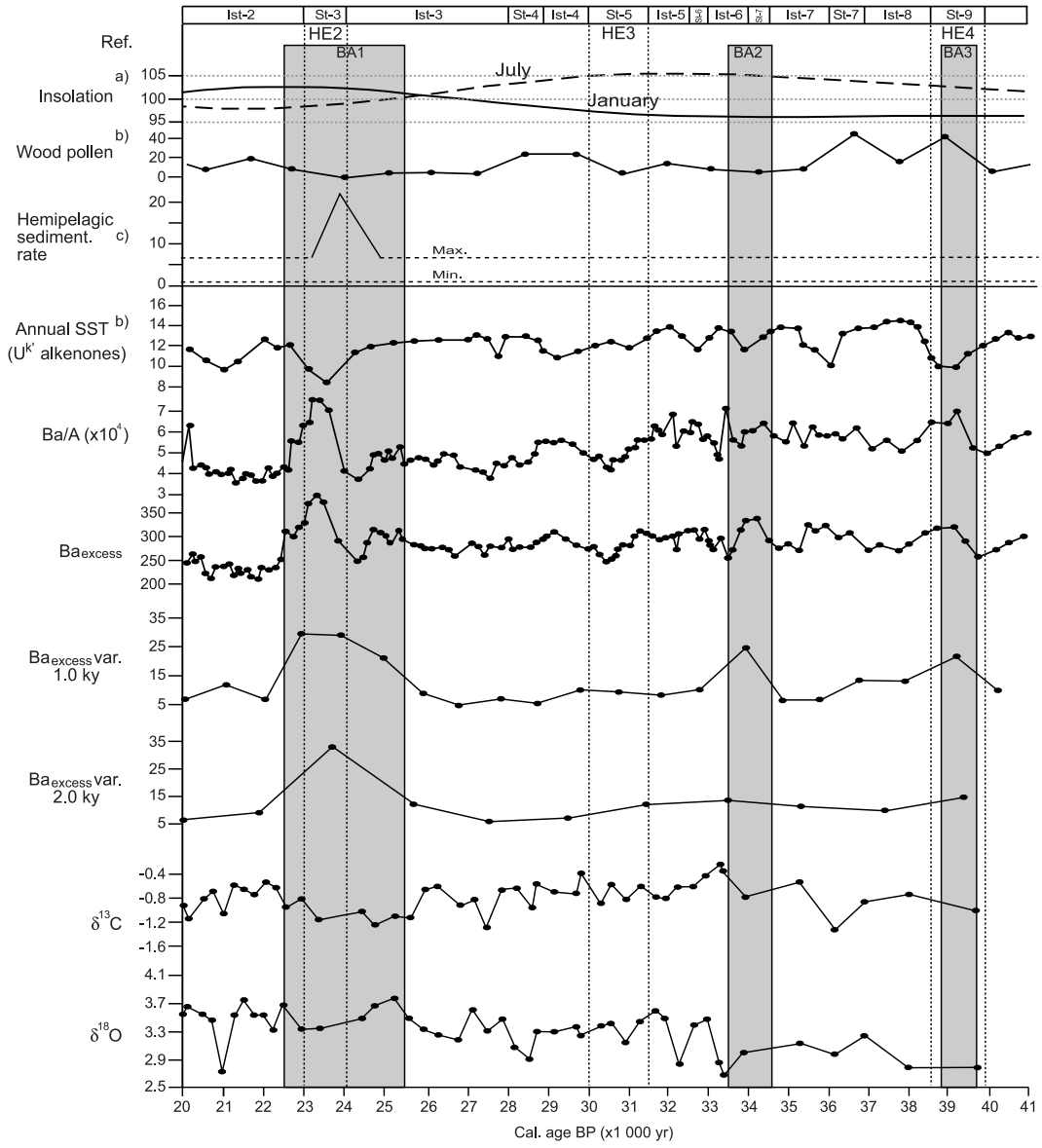


**Figure VI.2.** Insolation curve, wood pollen, hemipelagic sedimentation rates on the Balearic abyssal plain, mean annual SST ($U^{k'}$alkenones), Ba/Al (x$10^4$), $Ba_{excess}$, Ba $_{excess}$ variability per 1.0 ky, Ba $_{excess}$ variability per 2.0 ky and *G. bulloides* isotopic stratigraphy ($\delta^{18}O$ and $\delta^{13}C$, in ‰) according to age. $\delta^{18}O$ values are plotted with reversal *Y* axis. References: a)_Berger, 1978 b)_Martrat et al., 2004 c)_Hoogakker et al., 2004.

### VI.3.3 Detrital and redox proxies

The terrigenous sediment fraction includes clay minerals (20% to 50%), quartz (15% to 30%), and minor amounts of feldspar (<5%), dolomite (<5%), and accessory minerals. Clay mineral assemblages consist of illite (55% to 80%), smectite (<5% to 15%) and kaolinite + chlorite (20% to 40%). These terrigenous sediments also included accessory minerals, such as zircon, rutile, apatite and biotite, while the authigenic minerals identified were anhydrite-gypsum, pyrite, Mn and Fe oxi-hydroxides. Figure VI.3 shows the distribution of selected profiles of major and trace element ratios related with terrigenous input. Elemental concentrations have been normalized to Al. This normalization assumes that Al in these sediments is contributed only by terrigenous alumino-silicates (Calvert, 1990).

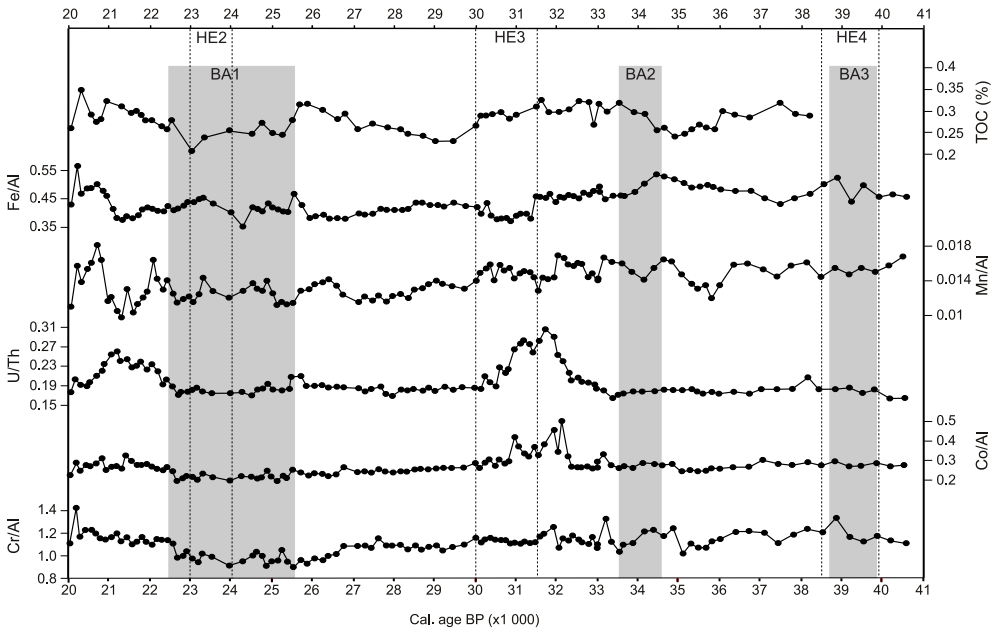


**Figure VI.3.** TOC content (%), U/Th and other redox-sensitive trace elements/Al ($x10^4$) according to age. Vertical dotted lines indicate the time intervals of Heinrich events. Grey areas indicate BA events (for definitions of such events, see section 4.3).

Ti and Zr are related with heavy minerals (e.g., zircon, rutile, anatase, titanite, ilmenite) and have been used by different authors as aeolian input proxies (e.g., Calvert et al., 1996; Haug et al., 2003). Both elements are well correlated over almost the entire period studied. In contrast, they have a low correlation with other detrital elements (Al, K and Mg), suggesting a different origin and ruling out the presence of turbidites, which usually produce quartz and heavy mineral enrichment (Wehausen and Brumsack, 1999).

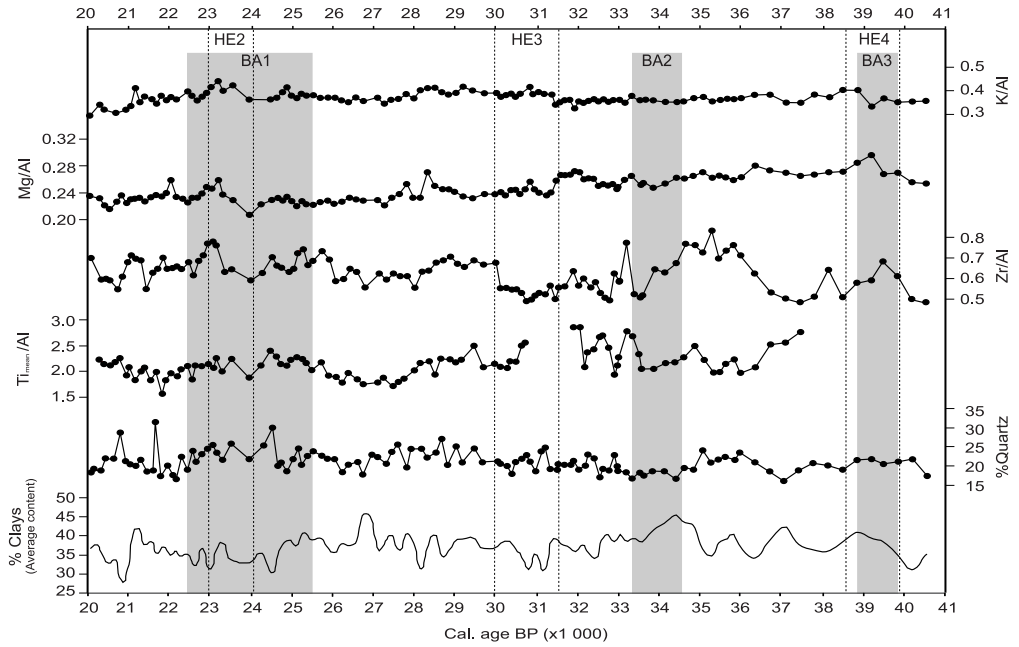


**Figure VI.4.** Relative quartz and clay mineral average concentrations (%), and elemental/Al ($x10^4$) ratios according to age, plotted as lithogenic proxies. $Ti_{mean}$ is an average value obtained by using an XRF-scanner. Vertical dotted lines indicate the time intervals of Heinrich events. Grey areas indicate BA events (for definitions of such events, see section 4.3).

The ratios of specific elements to Al have been considered as redox sensitive proxies (e.g., Fe/Al, Mn/Al, U/Th, Co/Al, Cr/Al) (e.g., Mangini et al., 2001; Marin and Giresse, 2001) for oxygen conditions and digenetic remobilisation. Regarding oxygenation, two major enrichment periods in redox sensitive elements have been

detected from 33.2 to 30 ky cal BP and from 22.7 to 20.4 ky cal BP (see U/Th ratio on Fig. VI.4). Postdepositional alteration resulted in re-oxidation fronts promoting element mobilisation along the sediment column (Fe and Mn), which provides information on reventilation processes.

## VI.4. DISCUSSION

### VI.4.1. Continental and marine environments in the WMS during MIS 3

Different proxies have shown that MIS 3, like other interglacials, is characterized by a saw-tooth temporal temperature pattern. However some features unique to this period exist, specifically, the main difference between this period and the other MIS stages (1 to 7) is that it represents a time for which "non analogue" conditions exist. This is evident in the mammalian fauna record (Stewart et al., 2003a; Stewart, 2005) and have also been observed in wind dust from marine sediment in the Algero-Balearic basin (Weldeab et al., 2003) and for the vegetation and fauna of Gibraltar (Finlayson, 2006). For example, $^{87}Sr/^{86}Sr$ and $^{143}Nd/^{144}Nd$ ratios indicate that during MIS 3 the main dust source for the WMS was probably located between the Northwestern Sahara (Morocco/NW Algeria) and the Sahara and Sahelian regions; another unknown source could also be involved (Weldeab et al., 2003). These source areas are substantially different from those of other MIS stages (1 to 7). The response to this even in terrestrial flora is however not clear. Marine pollen records have been established in WMS cores corresponding to MIS 3. However, interpretations of pollen sources have not led to unequivocal conclusions. For example, D'Errico and Sánchez-Goñi (2003) have considered them to be Iberian, whereas Magri and Parra (2002) and Carrión (2004) disagree. On land, a rapid vegetational response to climatic changes has been observed (Sánchez-Goñi et al., 2005; González-Sampériz et al., 2006). At present, however, the resolution of age models does not allow for the identification of abrupt variations, such as those which took place during the D/O cycles as recorded in the marine record.

Marine records from the Iberian margin are especially suitable for paleoclimate research (Bard et al., 2004). Various multiproxy studies have been carried out (e.g., isotopic ratios, alkenones, pollen and geochemistry), which revealed significant climatic oscillations (e.g., Martrat et al. 2004). However, when looking into the effect of these changes on the terrestrial ecosystem, it should be noted that some of these variations can be assimilated by an ecosystem without major disturbances. Indeed, vegetal distribution is affected mainly by minimum temperatures, growth season and precipitation (Woodward, 1987), rather than mean sea surface temperatures, sea level, or water chemistry. Thus, the use of marine records to measure variance in a continental ecosystem may be some times difficult (Robinson et al., 2006). However, several chemical elements in marine records are of mainly continental origin, for example, Mg/Al and K/Al ratios have been associated with fluvial input (precipitation), and Ti/Al and Zr/Al with aeolian input (wind). Thus, these ratios provide information on continental areas, although they are highly influenced by multip le physical/chemical phenomena (e.g., wind intensity/direction, erosion rate, soil alteration, pluvial regime, marine currents and catchment areas, etc.) which complicate their use for variance analyses.

**VI.4.2. Ba excess as a climatic stability proxy**

The use of Ba enrichments as a proxy for productivity has been intensely discussed since the early eighties. This proxy is based on the strong correlation between the fluxes of excess Ba and organic matter in sinking particulates. It is also supported by the observations that Ba-rich sediments usually underlie high biologically productive (e.g., Dehairs et al., 1987; Dymond et al., 1992) areas and surface sediment barite accumulation rates correlate with upper water column productivity (Paytan et al., 1993, 1996). The use of this proxy assumes that the excess of Ba is related to barite crystals that originate in the water column. Only in such cases can $Ba_{excess}$ thus be used as a reliable proxy, assuming that $Ba_{excess}$ (total Ba normalized to Al) correspond to the Ba fraction that is not associated with terrigenous components. Data from different settings has shown that this proxy should be used with caution in

diagenetic environments where reducing conditions may have compromised barite preservation (McManus et al., 1998). In addition, recent research (Eagle Gonneea and Paytan, 2006) has shown that Ba content in different phases depends not only on primary productivity, but also on sediment provenance, sedimentation rates and Ba cycling within sediments. Corrections for detrital Ba may be highly variable and $Ba_{excess}$ algorithms should therefore be used with extreme care when calculating export production (Eagle Gonneea and Paytan, 2006).

However, many studies have shown that Ba is an accurate indicator of past productivity in the Mediterranean Sea (e.g., Emeis et al., 2000; De Lange et al., 1999; Martínez-Ruiz et al., 2000). Paleoproductivity reconstructions using this proxy in marine Pliocene and Pleistocene sediments have confirmed that widespread deposition of sapropels resulted from enhanced export production fluxes. Increasing productivity was a consequence of changes in climatic conditions leading to higher nutrient supply. Sulfur isotope composition of marine barite from Mediterranean sapropels revealed that barite is an authigenic phase originating in the upper water column and is thus a reliable proxy for productivity at the time of sapropel deposition (Paytan et al., 2004). The high accumulation and good preservation of biogenic barite also indicate that bottom-water and pore water sulfate concentrations in Mediterranean basins were plentiful. The $Ba_{excess}$ proxy is also of exceptional importance in Mediterranean basins because at some locations the organic matter in the original sapropels has been oxidized and erased from the sediment record. Although estimates of past productivity using $Ba_{excess}$ may be inaccurate due to detrital Ba corrections or variable preservation, it is clear that Ba enrichments in Mediterranean sapropels indicate enhanced export productivity. In the deep areas of the Alboran and Algero-Balearic basins, productivity has been related to: i) surface water fertilization, provoked by different water mass mixing and/or gyre activity (Bárcena et al., 2001); ii) increases in nutrient supply due to high river runoff associated with wetter climates and/or melt water (Martínez-Ruiz et al., 2003; Moreno et al., 2004); iii) pycnocline depth changes (Rohling et al., 1995; Flores et al.,1997) and, finally, iv) highly fertilized Atlantic jet inflow (Rogerson et al., 2004). A change in productivity caused by pycnocline deepening has most likely only occurred

once in the last 50 ky (at ~8 ky BP) (Flores et al., 1997). All other productivity fluctuations in this region are associated directly or indirectly with atmospheric conditions. Thus, abrupt variations in marine productivity mostly reflected major variations in atmospheric/oceanographic (climatic) conditions. Continental environments should therefore also be affected by such climatic variations. When statistical analyses are considered, the variance may indicate the disruptive potential of climate fluctuations. Especially within the time interval studied, statistical analyses have provided valuable information regarding climate stability. Figure VI.2 represents the millennial and bi-millennial $Ba_{excess}$ coefficient of variation ($Ba_{excess}$ var.). High $Ba_{excess}$ var. values may indicate periods characterised by highly unstable conditions in marine ecosystems. High values in $Ba_{excess}$ var. coincide with major changes in planktonic foraminifera bioevents (see Table VI.1), (Perez-Folgado et al., 2003). This further supports the validity of $Ba_{excess}$ var. as a tool for understanding the climatic/biological variability in the WMS area.

**Table VI.1.** BA events (see section 4.3) and their relationship with plancktonic foraminifera events defined in Pérez-Folgado et al., 2003.

| High $Ba_{excess}$ var. Events | Bioevents | | | | | |
|---|---|---|---|---|---|---|
| | *N. pachyderma* (r.c.) | *N. pachyderma* (l.c.) | *T. quinqueloba* | *G. scitula* | *G. inflata* | *G. bulloides* |
| BA1 | Pm2 | Ps2 | Q3 | Sc2 | | B2 |
| BA2 | | | Q5 Bot. | Sc4 Bot. | I4 Max. | |
| BA3 | | Ps4 Bot. | | | I5 Top | B4 Bot. |

### VI.4.3. Conditions during intervals of high $Ba_{excess}$ variability

As is the case for sea surface temperature (SST) in the WMS (Cacho et al., 1999), the Ba signal is affected by D/O cycles (Moreno et al., 2005a). Three high $Ba_{excess}$ variability periods can be recognized between 41 and 20 ky BP (we have established

them as BA3, BA2 and BA1 events). Correlations of significant interest are obtained when such periods are compared with other paleoclimatic records:

a) The BA3 event (aprox. 39-40 ky BP) can be correlated with the HE 4, which took place aprox. 38 to 39.5 ky BP (Bond et al., 1999; Hemming, 2004; Llave et al., 2006). Rapid changes in Atlantic deepwater currents and heat piracy between the Northern and Southern Hemispheres have been described for this period (Maslin et al., 2001; Seidov et al., 2001). HE 4 seems to be distinct from other HEs (Cortijo et al. 1997; Elliot et al., 2002; Cortijo et al., 2005). There was probably a cold current flowing from the Norwegian Sea along the European coast (Cortijo et al., 1997), with polar water reaching the WMS (Voelker et al., 2006). Recent studies indicate that ice-rafted debris were deposited in the Gulf of Cadiz (Llave et al., 2006), but apparently most of the melting took place in northern areas between 45ºN and 55ºN (Roche and Paillard, 2005). An increase in N. pachyderma recorded at core MD95-2043 (approx. 25 %) confirms that cold waters arrived at the WMS. Temperature estimates from Uk' alkenones indicate a mean annual SST of around 10ºC (Martrat et al., 2004). On the continent, a high degree of seasonality has been reported with large temperature fluctuations (Summer approx. 15ºC to 20ºC, Winter approx. –5ºC to 0ºC) (The Stage Three Project database). A major decline in Pinus and Quercus, and an increase in Ericaceae are observed (Roucoux et al., 2005). For this period results from ODP 975B indicate a relative increase in Zr/Al and a major decrease in K/Al (F ig. 3). This suggests that conditions were more arid and that wind velocities were stronger. Our results would seem to indicate a scenario in which the Iberian Peninsula was subjected to abrupt changes includ ing an extreme, continental climate. Insolation variation was, however, very limited during this event despite the large climatic changes suggesting the influence of other causes and feedbacks (Cortijo et al., 1997).

b) The BA2 event (aprox 33.5-34.5 ky BP) could be the culmination of progressive climate deterioration, which is characterized by short D/O (6 and 7 stadials-interstadials). D/O cycles in the WMS were apparently less severe than in the Atlantic (Hoogakker et al., 2004). Nevertheless, they imply major changes in high-latitude

circulation and monsoonal weakness (D/O stadial) (Moreno et al., 2002) (Rohling et al., 2003). No ice-rafted debris have been observed in cores from the Atlantic Iberian margins during that time (Llave et al., 2006). However, cold waters penetrated the WMS during D/O stadial. SST ranged from aprox. 15ºC D/O interstadial to 11ºC D/O stadial for this period (The Stage Three Project database), which indicates more hospitable conditions than during HE 4. The afore-mentioned observations would together suggest a sudden change in temperature, and especially in humidity/rainfall in the Mediterranean area (Voelker and workshop participants, 2002). An input of cold water into the WMS could have promoted a reduction in evaporation and less precipitation throughout the Mediterranean area, with more significant effects in the Levant (Bartov et al., 2003; Begin et al., 2004). Fluctuations in the abundance of certain foraminifers species (e.g., Turborotalia quinqueloba) (Perez- Folgado et al., 2003) could reveal an unstable cold water input. This could have led to highly erratic rainfall in the Mediterranean area. In fact, the formation of talus flatiron, which requires alternation of aggradation and incis ion periods, has been detected on the Iberian Peninsula (Gutierrez et al., 2006). Pollen records indicate that Quercus almost disappeared in the Monticchio record (Allen et al., 2000a) and that Ericaceae and Pinus shrunk in the Northwestern Iberian regions (Roucoux et al., 2005). The latter are less affected, which could be associated with the passing of tolerance limits for deciduous Quercus. However, Mediterranean forest continued to exist in coastal areas of SW, SE Spain and North Africa throughout MIS 3 (Carrión et al., 1995; Carrión, 2004; F inlayson, 2006). Results from Site ODP 975 indicate major changes in Zr/Al and Timean/Al that could be related to high variations in aeolian input into the basin. Moreover, K/Al and Mg/Al, which are related to fluvial sediment input, did not undergo significant changes. Redox sensitive ratios present an inflexion point fo llowing the end of the BA2 event, with increases in U/Th, Cr/Al and Co/Al that point to less ventilated bottom waters. In the Gulf of Cadiz a more intense Mediterranean outflow water has been described during cold phases (Llave et al., 2006).

This intensification resulted from colder, drier Mediterranean conditions. The expansion of the polar vortex generated masses of cold air, responsible for Western

Med iterranean Deep Water (WMDW), which, in turn, ventilated the Balearic basin (Cacho et al., 2000; Rohling et al., 2003; Jiménez-Espejo et al., submitted). These low ventilation conditions came to an end around 30 ky BP, with the onset of the HE 3 (30.5 ky BP). Cold conditions have been described in Iberian lacustrine records (e.g., El Portalet, González-Sampériz et al., 2006). No significant changes appear in $Ba_{excees}$ var.during HE 3. This could be related to the gradual, rather than abrupt HE 3 pattern (Gwiazda et al., 1996) and to its particular features(Elliot et al., 2002), which differ from other HE's. No evidence of ice-rafted debris has been found in Southern Iberian latitudes (Llave et al., 2006).

c) The BA1 event (aprox. 22.5-25.5 ky cal BP) can be related to the transition from MIS 3 to MIS 2 and to the HE 2. A bi-phase signal has been described for HE 2 in the Iberian region, one centred at 25 ky (HE 2b) and the other at 23.5 (HE 2a) (Sánchez-Goñi et al., 2000; Turon et al., 2003). Within this period, the most inhospitable conditions of the previous 250 ky were reached in the WMS (Martrat et al., 2004). During HE 2, an armada icebergs reached the Portugal margin (Abreu et al., 2003). No ice-rafted debris have been detected in the Gulf of Cadiz, although a high percentage of coarser fraction (>63μ) suggests a very strong Mediterranean outflow water current (Llave et al., 2006). Despite a reduced supply of icebergs, the lowest temperatures of the last 250 ky were reached, with an annual mean SST of around 8ºC (Uk' index) (Martrat et al., 2004). These low temperatures can be associated with strong thermohaline circulation and/or with the minimum daily total solar radiation, the latter resulting from orbital geometry (Berger, 1978). A minimum in seasonality was reached at 24 ky BP, (Berger, 1978) and probably affected marine currents. Indeed, previous summer insolation minima (40 to 45 ky BP) have been linked with high variations in sedimentation rates in nearby areas (Voelker et al., 2006). On land, pollen analysis results indicate extreme conditions in Iberia during HE 2. A minimum of arboreal pollen correlates with a maximum in Artemisia and Chenopodiaceae (e.g., Turon et al., 2003; Roucoux et al., 2005), thus indicating a dominance of steppic group taxa that was not reached during the previous 65 ky. Low seasonality can be expected for this period, with cooler summers and warmer winters than during previous BA events. Indeed, relatively warm winters are

necessary to explain the presence of traces of Quercus (deciduous) pollen in Padul (SE Spain) (Allen and Huntley, 2000b). Detrital proxies at Site 975 indicate a minimum Mg/Al ratio at 24 ky BP, which could points to a pronounced decrease in riverine input. K/Al ratio oscillations could be related to a highly unstable river discharge from the Rhône, or with mineralogical changes. Rapid oscillations have also been detected in other global records (e.g., 4ºC-6ºC warming in less than 50 years at ~22 ky cal BP (Taylor et al., 2004). Aeolian input, as indicated by the Zr/Al ratio, shows low values at 24 ky and reaches a relative maximum at 23 ky. These variations could be linked with abrupt changes in atmospheric conditions. An inflexion point in our age model also reveals a change in the linear sedimentation rates during this period. Other cores from the Algero-Balearic basin also reveal abnormal accumulation rates at 24 ky, up to three times higher than any other value during at least the last 130 ky (Hoogakker et al., 2004). These oscillations have been interpreted as being due to higher aeolian input, the latter being a consequence of increasing arid ity and/or higher wind speeds (Hoogakker et al., 2004). Furthermore, an unusually high thermohaline circulation, transporting material from an unknown source to the Algero-Balearic basin, cannot be ruled out. In any case, major changes can be observed in the WMS borderlands, which may not have undergone such extreme conditions in previous periods. Redox sensitive ratios indicate well oxygenated conditions between 25.5 and 22.5 ky BP, an interval during which a few of the ratios reach their lowest values (e.g., Cr/Al). Afterwards, a period of less ventilated conditions began, promoting an increase in redox sensitive ratios (e.g., U/Th and Co/Al). These ventilation conditions are once again correlated with Mediterranean outflow water activity in the Gulf of Cadiz (Llave et al., 2006).

### VI.4.4. The role of climatic variability for archaic populations

Figure VI.5 indicates frequency distribution of Solutrean, Gravettian, Aurignacian and Mousterian dated sites per millennium in the Southern Iberia Peninsula (modified from Finlayson et al., 2006 and unpublished database) (CalPal 2005 SFCP). Cross calibration is fundamental for the comparison of marine and continental data. Moreover, uncertainties associated with

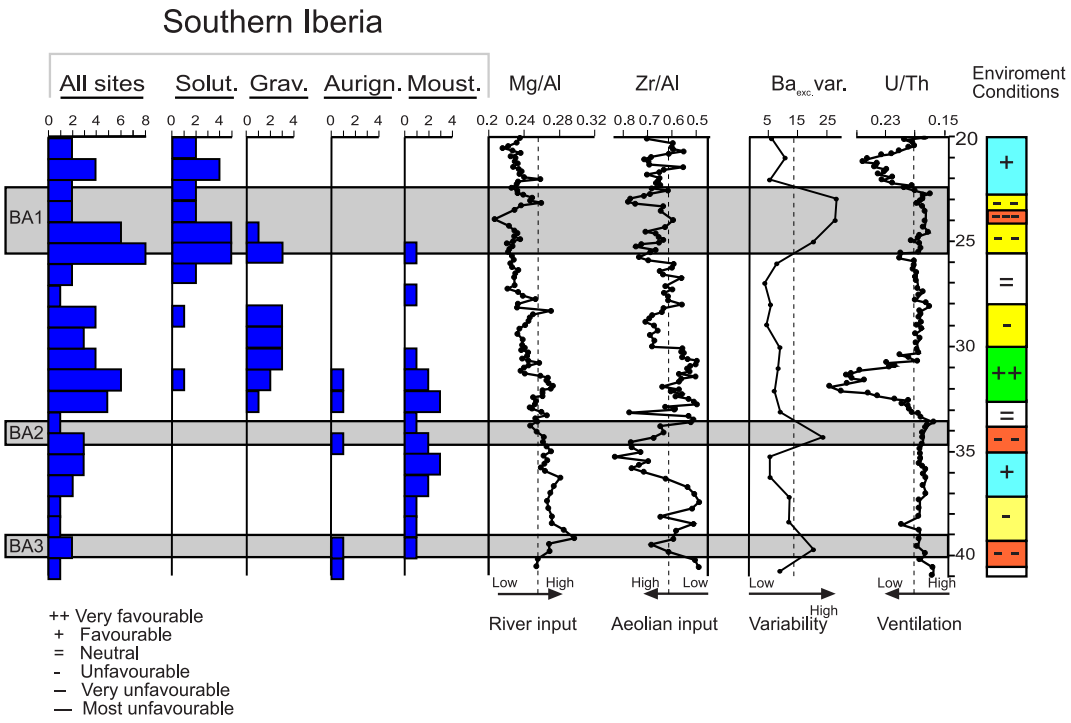


**Figure VI.5.** Frequency distributions of Solutrean, Gravettian, Aurignacian and Mousterian calibrated dated sites per millennium in South Iberia. These distributions are compared with $Ba_{excess}$ var., U/Th, Zr/Al and Mg/Al according to age. Such proxies are interpreted as climatic stability, deep water ventilation, aeolian input and fluvial input, respectively. Environmental conditions have been interpreted on the basis of combinations of these factors. Uncalibrated data base distribution follows a similar "peak and valleys" pattern, and relationship between industrial replacements do not change.

calibration methods, continuous updates and different calibration curves/programs, lead to a certain degree of confusion among researchers (Housley et al., 2001; Turner et al., 2006). In the case of Calpal, regularly updated internationally standardised calibration curves are available (Reimer et al., 2006). The use of millennial scale and average values attempt to avoid such uncertainties. This information can be considered highly representative, although it is incomplete, as is otherwise to be expected from the nature of the fossil record itself, as well as the fact that the Southern Iberian Peninsula has yet

to be studied more exhaustively. The database has been compared with $Ba_{excess}$ var., deep water ventilation, and aeolian and fluvial input characterized by the U/Th, Zr/Al and Mg/Al, respectively. Two main observations can be made: i) archaeological outcrops are more abundant during conditions of low $Ba_{excess}$ var. and low ventilation; and ii) the number of outcrops is clearly affected by BA3, BA2 and BA1 events. During BA3 a low number of Mousterian sites has been registered. This appears to coincide with a weak early presence of the Aurignacian in the Iberian Peninsula associated with the most extreme climatic conditions (cold and dry). Between BA3 and BA2, a progressive increase in Mousterian sites occurred with the disappearance of Aurignacian sites. During this period (40-35 ky) the number of Mousterian sites reached a maximum and probably dominated southern Iberia. During BA2 there was a dramatic decrease in Mousterian sites, with a reappearance of Aurignacian ones. The most hospitable conditions occurred between 30.5 and 34 ky cal BP and Mousterian population reached a new maximum. Moreover, a progressive increase in Gravettian sites is synchronous with decrease in Mousterian sites. Therefore, relict Mousterian sites prevailed during the relatively hostile 30 to 25 ky period (Fig. VI.5). During the prolegomena of the BA1 event, Solutrean industries were dominant and Gravettian and Mousterian industries probably disappeared. During the latter part of the BA1 event, Solutrean sites also underwent a decrease in number. Apparently major technological replacements took place during unstable periods. This could indicate that the proliferation of these industries was impacted by climate and a selection of cultural styles occurred. Indeed, in the second half of MIS 3 a number of "transitional industries" (e.g., Uluzzian, Bohunician and Szeletian) could represent cultural diversification as a response to new challenges (Finlayson and Giles-Pacheco, 2000; Finlayson, 2004).

The present study does not attempt to address the issue of whether the main Modern expansion in Europe took place during the H4 event or whether it occurred during improved conditions associated with the Hengelo interstadial (mainly 41-42 ky cal BP) (Mellars, 2006). The idea of a new species displacing an earlier (more primitive) one to a peripheral area has been shown repeatedly to be inadequate (e.g., Coope, 1979). It is almost impossible to demonstrate inter- or intra-specific competition on the basis of the fossil record (Finlayson, 2004). Neanderthals and Moderns probably coexisted for a prolonged period of time. Such coexistence started at least during MIS 5 in western Asia (Bar-Yosef, 1998) and could be the origin of a gradient in the "Neanderthalisation" of industries (Moncel and Voisin, 2006). Nevertheless, it is unlikely that climatic changes and synchronous human events were a fortuitous coincidence.

### VI.4.5. The Southern Iberian Neanderthal habitat

During the MIS 3 Neanderthals successfully occupied transitional areas, such as the edges of limestone massifs adjacent to lowland plains (Davies et al., 2003) in the Overlap Province defined by Stewart et al., (2003a). However, persistent Neanderthal populations inhabited the Southern part of Iberia (Finlayson 2004, 2005). Thus, the characteristics that distinguish the Southern Iberian from the Northern European Neanderthal habitats must be adequately taken into account. Neanderthal populations living in Southern Iberian probably took advantage of the following factors: i) Mediterranean forest, rich in fatty fruits, and mainly controlled by climatic change and a heterogeneous topography (Cowling et al., 1996); ii) a rich biotope area promoted by a complex topographical pattern which produced many environments and microclimatic conditions (e.g., Finlayson et al., 2001; Mota et al., 2002); iii) a more diversified nutritional pattern, partially composed of Pine nuts, bivalves, shellfish (Finlayson et al., 2001) and marine mammals (Antunes, 2000); this diet may have generated a lower maternal foetus-infant mortality rate and higher life expectancy (Hockett and Haws, 2005); a highly diversified geological bedrock (e.g., ultramafic, volcanic acid and sedimentary rocks) may also have helped to provide essential

nutrients via plants and/or herbivores; iv) a "buffered climate" promoted by the WMS, which has its own thermohaline circulation system (Brankart and Brasseur, 1998); climate changes are slower and more moderate in the Alboran Sea, as compared to the Gulf of Cadiz or the Tyrrhenian Sea (Cacho et al., 2002); and finally, v) one of the highest insolation coefficients in Europe, which must have guarantied hospitable diurnal temperatures, even during cold periods.

The complexity of such factors makes it necessary to analyse local climate records in order to reconstruct the paleoclimatic conditions. To date, paleoclimatic models have not taken topography into account and are based mainly on the Padul record (Huntley et al., 2003; Ortiz et al., 2004). However, since the latter is an intramountain basin, the temperatures for Southern Iberian may seem cooler in climatic reconstructions based on this location than they actually were.

**VI.4.6 The end of the southern Iberian Neanderthals**

Glacial Maxima were critical periods during which extinction rates were exceptionally high. For example, tens of megafaunal species disappeared during the Last Penultimal Glacial Maxima (e.g., Wroe et al., 2006). Southern European refugia were also affected by such crises (O'Regan et al., 2002). For this reason, the number of warm species in present-day Iberian fauna is comparatively low (Blondel and Aroson, 1999). It is thought by some workers that Neanderthals were highly skilled in adapting to climatic changes and that their adaptive capacities were similar to those of Moderns (Boëda et al., 1996; d'Errico et al., 2001). Neanderthals may even have been able to survive during stable conditions of extreme cold. However, high climatic variability provokes generalised effects in ecosystems. Continuous variations in seasonal moisture or temperature tend to produce stressed environments. It has been shown that in current environments, which display a slight warming trend, imbalances can be observed in insect populations (Harrison et al., 2006), certain illnesses have widened their spread (e.g., Flahault et al., 2004), and there have been synchronous multi-biotope crises (Moreno et al., 2005b), as well as alterations in migrational-altitudinal patterns

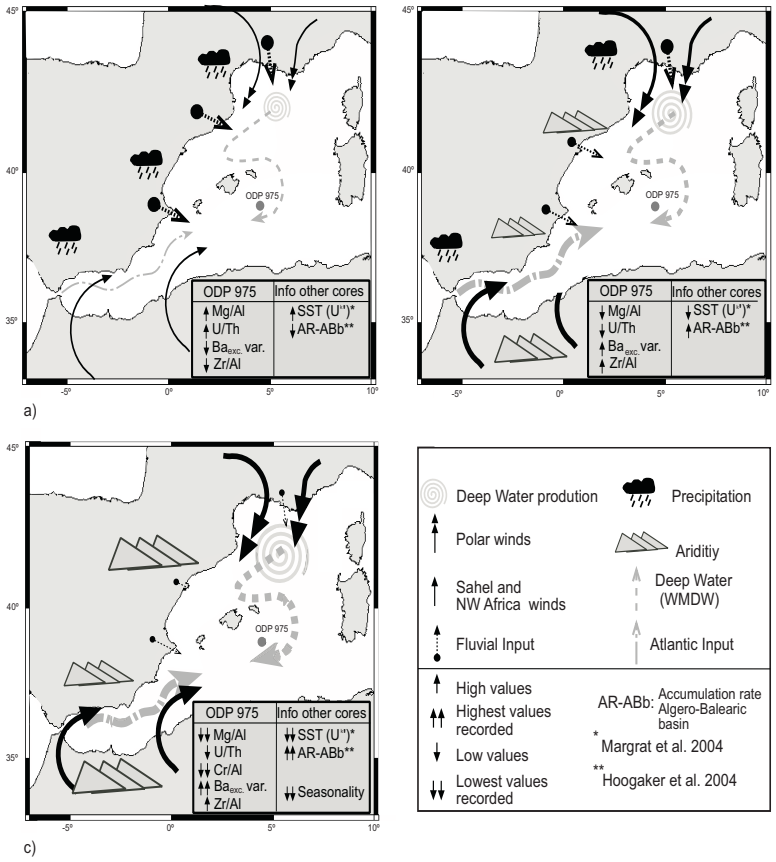


**Figure VI.6.** Hypothetical climatic conditions constructed on the of basis of models (Finlayson, 2006), our data and marine records (e.g., Sánchez-Goñi et al. 2000 and Moreno et al., 2002) between 40 to 20 ky BP. (a) Favourable periods: D/O interstadials. (b) Non favourable periods: D/O stadials and Heinrich events. (c) Extreme conditions during the BA3 event probably between 25-24 ky cal BP.

(e.g., Peñuelas and Boada, 2001; Peñuelas and Filella, 2003). Variations in vegetation type, plant digestibility, consumption rates and growth/mortality in herbivores, can be expected under such conditions (e.g., Lawler et al., 1997). Deficiencies in soil moisture caused by cold marine waters could lead to shorter growth seasons and an increase in days of snow cover, thus affecting herbivorous mammals and their occurrence ratios (Markova, 1992; Musil, 2003, Hernández-Fernández and Vrba 2005). Any one of these factors could have provoked periods of poor nutritional quality or famine, leading to

the extinction of highly regional populations. The last Neanderthals in southern Iberia were probably subjected to such isolated conditions from the BA2 event onwards. The disappearance of other reduced European populations around 30 ky BP may have been due to the afore-mentioned or other causes, such as genetic swamp and increasing continentality (Finlayson, 2004). It is also possible, however, that the extinction of the last southern Iberian Neanderthal populations occurred during the BA1 event, especially during a hypothetical extreme thermohaline activity event. Figure VI.6 c) represents this event mainly on the basis of our and other marine data (e.g., Sanchez-Goñi et al., 2000; Moreno et al., 2002) and models (Finlayson, 2006). The Neanderthal archaeological proxies found in southern Iberia and dated at between 25-30 ky BP could be accounted for by situating Neanderthal extinction during BA1. On the other hand, it is thought that the last Neanderthals were located in various European climatic refugia, such as the Iberian, Italian and Balkan peninsulas. However, the more favourable conditions characterising the Iberian refugia (see section 4.5) may have allowed them to survive longer (Finlayson and Giles-Pacheco, 2000; Stewart et al., 2003b; Finlayson, 2004). In any case, recent studies appear to indicate that, despite their greater adaptability to open environments (e.g., the North Plains) (Finlayson, 2004), Moderns were also subjected to conditions of isolation during the subsequent Last Glacial Maximum in southern European refugia (Hewitt and Ibrahim, 2001; Jobling et al., 2004).

### VI.4.7. To what extent were climatic conditions really influential?

Because it is only in archaeological outcrops that direct interaction between humans and environment can be recorded, it is highly probable that the underlying causes of Neanderthal extinction will be found in such sites (Vega Toscano, 2005). However, due to the extremely complex sedimentation of archaeological deposits, their use in the reconstruction of climatic conditions is cumbersome. These complexities may be better handled by multidisciplinary studies which closely examine depositional systems and taphonomical features, thus enabling more coherent interpretations. Indeed, climatic factors could be linked to occupational patterns in coastal outcrops by

geochemical research using non- destructive techniques, such as XRF core scanner (Jiménez-Espejo et al., in preparation) and stable isotope analysis (Delgado-Huertas, pers. com.), in combination with other disciplines, (e.g., Yll et al., 2006).

If climate did play an important role in the extinction of the Neanderthals and the expansion of the Moderns, some of the hypotheses regarding this process are likely to be corroborated. Climatic variability during cold periods probably acted as a "territory cleanser", thus favouring a subsequent colonisation by Moderns. Stable "frontiers" could be expected when hospitable conditions prevailed. It is likely that the most important episodes of replacement took place over relatively short periods, coinciding with adverse climatic conditions. For as yet unknown reasons, these areas were apparently more successfully recolonised by Moderns during subsequent periods of hospitable conditions. Therefore, the temporal- spatial location of the outcrops may play a major role in confirming climatic influence. North Africa also deserves particular attention, since chronological patterns could have been similar and disappearances may have been simultaneous.

## VI.5. CONCLUSIONS

Geochemical and mineralogical proxies show evidence of significant paleoenviromental changes in the WMS at time of Neanderthal extinction. Comparisons of different records suggest that from 250 ky down to 24 ky BP, the most extreme conditions in WMS were reached between 24-25 ky cal BP. Climatic changes apparently affected the number and distribution of Modern and Neanderthal sites in southern Iberia. Especially high values in millennial Ba excess var. (BA events) are well correlated with some of the changes in the number of sites and in replacements of industries. Cold, arid and highly variable conditions could be associated with the penetration and presence of Modern industries. This suggests that climatic variability during cold periods in the non-analogue MIS 3 could have affected Neanderthal populations, thus promoting weakness, isolation or extinction. Indeed, the definitive disappearance of Neanderthals could be linked with the unfavourable conditions

during BA1 (22.5-25.5 ky cal BP). However, in order to further clarify the causes of this disappearance, more in-depth studies should be carried out on outcrops in southern Iberia and North Africa.

# VII. Thesis conclusions

## VII. THESIS CONCLUSIONS

Both geochemical and mineralogical proxies evidence significant climate and oceanographic changes in the western Mediterranean during the last glacial cycle:

- Productivity, characterized by $Ba_{excess}$, strongly fluctuated, mainly due to the Atlantic inflow and the freshwater input. Productivity was higher during glacial periods reaching highest values during the YD and studied Heinrich events. High riverine influence on marine productivity in the Alboran basin is suggested by the Mg/Al ratio during wet periods such as the Bølling-Allerød, Early Holocene and also during the first half of YD. A significant productivity decrease started between 8.5 and 8.0 cal. ky BP, roughly coincident with the 8.2 cal. ky BP cold event. Additionally, Ba profiles also support significant productivity differences between the western and eastern Mediterranean basins at time of S1 sapropel deposition.

- A persistent isotopic and geochemical offset indicates the presence of gradients between the Alboran and the Algero-Balearic basins. Variations in the Atlantic input and different climate responses between both the Alboran and the Algero-Balearic basins are recognized.

- In the Algero-Balearic basin, a redox event (LRE) occurred between 7.5 and 7.0 cal. ky BP. This event strongly influenced both TOC preservation and redox element distribution in this basin, and has been related to the beginning of recent frontal circulation in the WMS during late Quaternary.

- Changes in sea level, Atlantic input features as well as atmospheric and oceanographic conditions, such as river/runoff input, wind intensity and sea surface temperature, in the Mediterranean sub-basins have modulated Mediterranean

thermohaline circulation. Thus, comparison of the Alboran and Algero–Balearic with other Mediterranean basins supports the hypothesis that the Mediterranean Sea responded differently to climate forcing during the studied time interval. Consequently, this region represents a key location for further understanding of the relationships between the North Atlantic and the eastern Mediterranean basins.

- Our data suggest that the South Alboran area was especially sensitive to LIW oscillations, and comparisons with studies in the Gulf of Cadiz indicate that enhanced MOW flow was principally driven by LIW input. In fact, a north-south gradient in the eastern Alboran is recognized, promoted mainly by intense LIW flow, river/coastal influence and sea level.

- Geochemical and mineralogical proxies also show evidence of significant paleoenviromental changes in the WMS at time of *Neanderthal* extinction. Comparisons of different records suggest that from 250 ky throughout to 24 ky BP, the most extreme conditions in WMS were reached between 24-25 ky cal BP. Climatic changes apparently affected the number and distribution of Modern and Neanderthal sites in southern Iberia. Especially high values in millennial $Ba_{excess}$ variability coefficients (BA events) are well correlated with some of the changes in the number of sites and in replacements of prehistoric industries. Cold, arid and highly variable conditions could be associated with the penetration and presence of Modern industries. This suggests that climatic variability during cold periods in the non-analogue MIS 3 could have affected *Neanderthal* populations, thus promoting weakness, isolation or extinction. Indeed, the definitive disappearance of *Neanderthals* could be linked with the unfavourable climate conditions during BA1 (22.5-25.5 ky cal BP).

# VIII. Agradecimientos

## VIII. AGRADECIMIENTOS

Mi más sincera gratitud a todas las personas que han contribuido a la elaboración de esta memoria de Tesis.

En primer lugar quiero agradecer a mi directora de tesis, Francisca Martínez Ruiz, todo su apoyo, su indescriptible comprensión y las numerosas ideas que se plasman en esta tesis. Su fe en mi trabajo, su capacidad, esfuerzo y disponibilidad han permitido que esta memoria haya podido realizarse. Paqui, me siento muy afortunado y orgulloso de haber trabajado todos esto años contigo, tu profesionalidad solo es superada por tu bondad.

A Miguel Ortega Huertas, director del Departamento de Mineralogía y Petrología de la Universidad de Granada, por su apoyo a esta investigación, cordialidad y amabilidad, y por su cálida acogida en el Departamento, así como a Inmaculada Palomo, amiga y tutora durante los cursos de doctorado. A Menchu Comas, amiga y compañera que tanto cariño y buenos consejos me ha dado. A Oscar Romero por su ayuda, total disponibilidad y simpatía.

Al Instituto Andaluz de Ciencias de la Tierra, por poner a mi disposición su infraestructura, y a todos sus miembros, con especial cariño a Concha, Mª Teresa e Isabel, Alberto, Carlota, Hans y Paco, así como a todo el personal investigador. A cada uno de los compañeros del Departamento de Mineralogía y Petrología de la Universidad de Granada les agradezco que hayan hecho sentir como en casa durante estos años. Tampoco puedo olvidar a los miembros del Departamento de Paleontología, Estratigrafía y Sedimentología que siempre me han tratado como a uno de ellos...

Quiero agradecer muy especialmente a Clive y Geraldine Finlayson, Darren Fa, a Francisco Giles Pacheco, a Joaquin Rodríguez Vidal, a José Carrión y a todo el equipo

de excavación de Gorham's Cave, su confianza y amistad, gracias a los cuales se han multiplicado las aplicaciones de este trabajo.

A Mª Dolores Asquerino del departamento de Prehistoria de la Universidad de Córdoba por su orientación, tutela y paciencia que han sido fundamentales desde mi más temprana formación. Mi agradecimiento más afectuoso a Luis, Manolo, Federico y Raimundo del Museo Histórico de Montilla que tanto me han enseñado. También dedicar mi gratitud a Mimi, que fue capaz de todo por mí.

Hubiera sido imposible obtener los resultados que se exponen en esta tesis sin el trabajo profesional y dedicado de grandes técnicos y mejores personas, como: Elisa, Jesús, Diana, Carmen, Rubén, Elena, Miguel, Manolo, Isabel y Emi, con los que ha sido fantástico trabajar (y más cosas...). También agradecer su dedicación y profesionalidad a todos los miembros del Centro de Instrumentación Científica que han colaborado en esta tesis, especialmente a Olga, Mª del Mar, Alicia, Isabel, Bendi, Marisa y Juande.

Por supuesto, no puedo olvidar a todos mis compañeros becarios: Ismael, Anita, Vincenzo, Concha, Julia, Luisa, Vicente, Fermín, Raquel, Idael, Pedrera, Isabel Abad, Matías, Chinche, Patro, Silvia, Alexander, Sandra, Vanesa, Pili, Patricia, Angel, Sila, Fernando, Gonzalo, Pedro, Pedrito, Cristina Mercedes, Jose Alberto, Jose María, Guillermo, Marga y Maja. Por supuesto a mis compañeros de despacho, que han tenido que padecerme: Jose Marí, Iñaki, David y la encantadora Encarni.

Especial agradecimientos a Nono, Alicia, Raef, Miguel, Javi, Lucia, Claudio, Asrat, Ana y Elena que han cuidado de mi salud mental y me han dado tanto que sería imposible devolver tales cuidados... declararles mi eterno y profundo agradecimiento... gracias, gracias y gracias... y mil gracias más...

Otro factor muy importante para la elaboración de esta tesis han sido las personas que he encontrado en los distintos centros en los que he trabajado, Marko, Maria, Emilia y Walter de la Universidad de Bremen y del ODP repository; Joseph,

Kristen, Karen y Nick de la Universidad de Stanford; Koichi, Sugisaki y Toyofuku del IFREE Institute en Yokosuka; Noel, Raquel, Mónica y Eduardo del ETH-Zurich. Por supuesto a todos los investigadores que me han tutelado durante mi estancia en estos centros: Judith Mckenzie, Chris Vasconcelos, Stephano Bernasconi, Adina Payta, T. Sakamoto y Oscar Romero, que en todos los casos me acogieron con el mayor afecto y atención. También expresar mi gratitud a toda la tripulación del R/V Prof. Logachev, que también me trataron, en especial a Eugene, Valentina, Alexandra, Elena y al Dr. Ivanov.

También agradecer las correcciones y sugerencias de distintos revisores e investigadores que han mejorado la calidad de mi trabajo, en concreto a los doctores Emeis, Fagel, Correge, Moreno, González-Samperiz, Valero-Garces, Romero, Carrión y Rose, así como a revisores anónimos.

El desarrollo de esta tesis hubiera sido inviable sin la financiación los siguientes proyectos: REN2003-09130-CO2-01, CGL2006-13327-C04-04/CLI del Ministerio de Educación y Ciencia y del Grupo de Investigación RNM0179 de la Junta de Andalucía. Así como la beca F.P.I. otorgada por el Ministerio Educación y Ciencia y al contrato otorgado por el proyecto de excelencia RNM 432 de la Junta de Andalucía. En este sentido, debo agradecer expresamente al Dr. Miguel Ortega su decidido apoyo.

Gracias a Tamae, con todo mi cariño, capaz de dar la vuelta al mundo solo para ayudarme y darme lo mejor de ella.

Quiero expresar el mayor cariño a mi familia. A mis padres Aurora y Solano, que me han dado todas las facilidades, apoyo y amor para emprender esta carrera. A mi hermana Aurora, por esta siempre dispuesta a sacarme de un apuro. Y a todos mis familiares, en especial a mis primos Rubén y Sandra, a mis tíos Joaquina, Juan, José y Antonio, a mis abuelos Pilar y Rafael, con los que no he podido pasar todo el tiempo que a ellos y mi nos hubiera gustado.

Finalmente, como estoy seguro de olvidarme algún nombre, que estás ultimas palabras sirvan para agradecer la ayuda de todos los que de cualquier manera han contribuido a la elaboración de esta tesis. Gracias.

# IX. References

## IX. REFERENCES

Abreu, L., Shackleton, N.J., Schönfeld, J., Hall, M., Chapman, M.R., 2003. Millennial-scale oceanic climate variability off the Western Iberian margin during the last two glacial periods. Marine Geology 196, 1–20.

Allen, J.R., Huntley, B., Watts, W.A., 1996. The vegetation and climate of north-west Iberia over the last 14,000 yr. Journal of Quaternary Science 11, 125-147.

Allen, J.R.M., Huntley, B., 2000b. Weichselian palynological records from southern Europe: correlation and chronology. Quaternary International 73-74, 111-125.

Allen, J.R.M., Watts, W.A., Huntley, B., 2000a. Weichselian palynostratigraphy, palaeovegetation and palaeoenvironment; the record from Lago Grande di Monticchio, southern Italy. Quaternary International 73-74, 91-110.

Allen, J.R.M., Watts, W.A., McGee, E., Huntley, B., 2002. Holocene environmental variability-the record from Lago Grande di Monticchio, Italy, Quaternary International 88, 69-80.

Alley, R.B., Agustsdottir, A.M., 2005. The 8k event: cause and consequences of a major Holocene abrupt climate change. Quaternary Science Review 24, 1123-1149.

Alves, M., Gaillard, F., Sparrow, M., Knoll, M., Giraud, S., 2002. Circulation patterns and transport of the Azores Front-Curent system. Deep Sea Res. II 49, 3983-4002.

Anderson, R.F., 1982. Concentration, vertical flux, and remineralization of particulate uranium in seawater. Geochimica et Cosmochimica Acta 46, 1293-1299.

Andersen, K.K. et al., 2004. High-resolution record of Northern hemisphere climate extending into the last interglacial period Nature 431, 147-151.

Antunes, M., 2000. The Pleistocene fauna from Gruta do Figueira Brava: a synthesis. In: Antunes, M. (Eds.), Last Neanderthals in Portugal: Odontologic and Other Evidence. Memorias da Academia das Ciencias de Lisboa, Lisbon, 259-282.

Aparicio, P., Ferrell, R.E., 2001. An application of profile fitting and CLAY++ for the quantitative representation (QR) of mixed-layer clay minerals. Clay Minerals 36, 501-514.

Ariztegui, D., Asioli, A., Lowe, J.J., Trincardi, F., Vigliotti, L., Tamburini, F., Chondrogianni, C., Accorsi, C.A., Bandini Mazzanti, M., Mercuri, A.M., 2000. Palaeoclimate and the formation of sapropel S1: inferences from Late Quaternary lacustrine and marine sequences in the central Mediterranean region. Palaeogeography, Palaeoclimatology, Palaeoecology 158, 215-240.

Asquerino, M.D., 1977. Notas sobre la periodización del neolítico español: el proceso de neolitización y el horizonte cardial. XIV Congreso Arqueológico Nacional, pp. 231-240.

Baena, J., Carrión, E., Ruiz, B., Sesé, C., Yravedra, J., Jordá, J., Uzquiano, P., Velázquez, R., Manzano, I., Sánchez-Marco, A., Hernández, F., 2005. Paleoecología y comportamiento humano durante el Pleistoceno Superior en la comarca de Liébana: la secuencia de la Cueva de El Esquilleu (Occidente de Cantabria, España). In: Barquín, R. M., Lasheras, J.A. (Coord.), Museo de Altamira. Monogr. nº 20, Santander 461-487.

Balistrieri, L.S., Murray, J.W., 1986. The surface chemistry of sediments from the Panama Basin: The influence of Mn oxides on metal adsorption. Geochimica et Cosmochimica Acta 50, 2235-2243.

Barcena, M.A., Cacho, I., Abrantes, F., Sierro, F.J., Grimalt, J.O., Flores, J.A., 2001. Paleoproductivity variations related to climatic conditions in the Alboran Sea (western Mediterranean) during the last glacial-interglacial transition: the diatom record. Palaeogeography, Palaeoclimatology, Palaeoecology 167, 337-357.

Bard, E., Arnold, M., Maurice, P., Moyes, J., Duplessy, J.C., 1987. Retreat velocity of the North Atlantic polar front during the last deglaciation determined by $^{14}C$ accelerator mass spectrometry. Nature 328, 791-794.

Bard, E., Rostek, F., Menot-Combes, G., 2004. Radiocarbon calibration beyond 20,000 $^{14}C$ yr B.P. by means of planktonic foraminifera of the Iberian Margin. Quaternary Research 61, 204-214.

Bar-Matthews, M. Ayalon, A., Kaufman, A., Wasserburg, G.J. 1999. The Eastern Mediterranean paleoclimate as a reflection of regional events: Soreq cave, Israel. Earth and Planetary Science Letters, 166, 85-95.

Bar-Matthews, M., Ayalon, A., Gilmour, M., Matthews, A., Hawkesworth, C.J., 2003. Sea-land oxygen isotopic relationships from planktonic foraminifera and speleothems in the Eastern Mediterranean region and their implication for paleorainfall during interglacial intervals. Geochim. et Cosmochim. Acta 67, 3181-3199.

Barnes, C.E., Cochran, J.K., 1990. Uranium removal in oceanic sediments and the oceanic U balance. Earth and Planetary Science Letters 97, 94-101.

Bartov, Y., Goldstein, S.L., Stein, M., Enzel, Y., 2003. Catastrophic arid episodes in the Eastern Mediterranean linked with the North Atlantic Heinrich events. Geology 31, 439-442.

Bar-Yosef, O., 1998. The Chronology of the Middle Paleolithic of the Levant. In: Akazawa ,T, Aochi, K., Bar-Yosef, O. (Eds.), Neanderthals and Modern Humans in Western Asia. Plenum Press, New York, 39-56.

Bea, F., 1996. Residence of REE, Y, Th and U in granites and crustal protoliths: implications for the chemistry of crustal melts. Journal of Petrology 37, 521-532.

Bea, F., Montero, P., Stroh, A., Baasner, J., 1996. Microanalysis of minerals by an Excimer UV-LA-ICP-MS system. Chemical Geology 133, 145-156.

Begin, Z.B., Stein, M., Katz, A., Machlus, M., Rosenfeld, A., Buchbinder, B., Bartov, Y., 2004. Southward migration of rain tracks during the last glacial, revealed by salinity gradient in Lake Lisan (Dead Sea rift). Quaternary Science Reviews 23, 1627-1636.

Bennett, K.D., Tzedakis, P.C., Willis, K.J., 1991. Quaternary Refugia of north European trees. Journal of Biogeography 18, 103-115.

Benzohra, M., Millot, C., 1995. Characteristics and circulation of the surface and intermediate water masses off Algeria. Deep-Sea Research Part I: Oceanographic Research Papers 42, 1803-1830.

Berger, A.L., 1978. Long term variations of daily insolation and Quaternary climatic changes. Journal of the Atmospheric Sciences 35, 2362-2367.

Bethoux, J.P., Gentili, B., Tailliez, D., 1998. Warming and freshwater budget change in the Mediterranean since the 1940s, their possible relation to the greenhouse effect. Geophysical Research Letters 25, 1023-1026.

Bethoux, J.P., Pierre, C., 1999. Mediterranean functioning and sapropel formation: Respective influences of climate and hydrological changes in the Atlantic and the Mediterranean. Marine Geology 153, 29-39.

Bianchi, G.G., McCave, I.N., 1999. Holocene periodicity in North Atlantic climate and deep-ocean flow south of Iceland, Nature 397, 515-517.

Blondel, J., Aronson, J., 1999. Biology and Wildlife of the Mediterranean Region. Oxford University Press, Oxford, 328 pp.

Boëda, E., Connan, J., Dessort, D., Muhesen, S., Mercier, N., Valladas, H., Tisnérat, N., 1996. Bitumen as a Hafting Material on Middle Palaeolithic Artefacts. Nature 380, 336-337.

Bond, G., Showers, W., Cheseby, M., Lotti, R., Almasi, P., de Menocal, P., Priore, P., Cullen, H., Hajdas, I., Bonani, G., 1997. A pervasive millenial-scale cycle in North Atlantic Holocen and glacial climates. Science 278, 1257-1266.

Bond, G.C., Broecker, W.S., Johnsen, S., McManus, J.F., Labeyrie, L.D., Jouzel, J., Bonani, G., 1993. Correlations between climate records from North Atlantic sediments and Greenland ice. Nature 365, 143-147.

Bond, G.C., Showers, W., Elliot, M., Evans, M., Lotti, R., Hajdas, I., Bonani, G., Johnson, S., 1999. The North Atlantic's 1-2 kyr climate rhythm: relation to Heinrich events, Dansgaard/Oescher cycles and the Little Ice Age. In: Clark, P.U., Webb, R.S., Keigwin, L.D. (Eds.), Mechanisms of Global Climate Change at Millennial Time Scales. Geophysical Monographs 112, 35-58.

Brankart, J.M., Brasseur, P., 1998. The general circulation in the Mediterranean Sea: a climatic approach. Journal of Marine Systems 18, 41-70.

Brauer, A., Mingram, J., Frank, U., Gunter, C., Georg Schettler, Wulf, S., Zolitschka, B., Negendank, J. F.W., 2000. Abrupt environmental oscillations during the Early Weichselian recorded at Lago Grande di Monticchio, southern Italy. Quaternary International 73-74, 79-90.

Brauer, G., 1992. Africa's place in the evolution of modern humans. In: Brauer, G., Smith, F.H. (Eds.), Continuity or Replacement. Controversies in Homo sapiens Evolution. A A Balkema, Rotterdam, 63-98.

Broecker, W.S., 1994. Massive iceberg discharges as triggers for global climate change Massive iceberg discharges as triggers for global climate change. Nature 372, 421-424.

Broecker, W.S., 1992. The Glacial World according to Wally. A "proto" book. Lamont-Doherty Geological Observatory, Columbia University, Palisades, NY.

Broecker, W.S., Maier-Reimer, E., 1992. The influence of air and sea exchange on the carbon isotope distribution in the sea. Global Biogeochemical Cycles 6, 315-320.

Brumsack, H.J., 1986. The inorganic geochemistry of Cretaceos black shales (DSDP Leg 41) in comparison to modern upwelling sediments from the Gulf of California. In: Shackelton, N.J. Summerhayes, C.P., (Eds), North Atlantic paleoceanography, London, Geological Society Special Publication 21, 447-462.

Brunet, M., Aguilar, E., Saladíe, O., Sigró J., López, D., 2001b. A Differential Response of Northeastern Spain to Asymmetric Trends in Diurnal Warming Detected on a Global Scale. In Detecting and Modelling Regional Climate Change, Brunet and López (Eds.), Springer-Verlag, Berlin, 95-107.

Brunet, M., López, D., 2001a. Detecting and Modelling Regional Climate Change. Springer-Verlag, Berlin, 651pp.

Budillon, F., Violante, C., Conforti, A., Esposito, E., Insinga, D., Ioro, M., Porfico, S., 2005. Event beds in the recent prodelta stratigraphic record of the small flood-prone Bonea Stream (Amalfi Coast, Southern Italy). Marine Geology 222-223, 419-441.

Burroughs, W.J., 2005. Climate change in Prehistory: the End of the reign of chaos. Cambridge University Press, Cambridge, 368 pp.

Cacho, I., Grimalt, J.O., Canals, M., 2002a. Response of the western Mediterranean Sea to rapid climatic variability during the last 50,000 years: a molecular biomarker approach. Journal of Marine Systems 33-34, 253-272.

Cacho, I., Grimalt, J.O., Canals, M., Sbaffi, L., Shackleton, N.J., Schonfeld, J., Zahn, R., 2001. Variability of the Western Mediterranean Sea-Surface Temperature during the last 25,000 years and its connection with the Northern-Hemisphere Climatic Changes. Paleoceanography 16, 40-52.

Cacho, I., Grimalt, J.O., Pelejero, C., Canals, M., Sierro, F.J., Flores, J.A., Shacklenton, N.J., 1999. Dansgaard-Oeschger and Heinrich event imprints in Alboran Sea temperatures. Paleoceanography 14, 698-705.

Cacho, I., Grimalt, J.O., Sierro, F.J., Shackleton, N., Canals, M., 2000. Evidence for enhanced Mediterranean thermohaline circulation during rapid climatic coolings. Earth and Planetary Science Letters 183, 417-429.

Cacho, I., Shackleton, N., Elderfield, H., Sierro, F.J., Grimalt, J.O., 2006. Glacial rapid variability in deep-water temperature and $\delta^{18}O$ from the Western Mediterranean Sea. Quaternary Science Review, doi:10.1016/j.quascirev.2006.10.004

Cacho, I., Sierro, F., Shackleton, N.J., Elderfield, H., Grimalt, J., 2002b. Reconstructing Alboran Sea hydrography during the last organic rich layer formation. Geochimica et Cosmochimica Acta 66, A115.

Calvert, S.E., 1990. Geochemistry and origin of the Holocene sapropel in the Black Sea. In: Ittekkot, V., Kempe, S., Michaelis, W., Spitzy, A. (Eds.), Facets of Modern Biogeochemistry. Springer-Verlag, Berlin, 326-352.

Calvert, S.E., Bustin, R.M., Ingall, E.D., 1996. Influence of water column anoxia and sediment supply on the burial and preservation of organic carbon in marine shales. Geochimica et Cosmochimica Acta 60, 1577-1593.

Calvert, S.E., Pedersen, T.F., 1992. Organic carbon accumulation and preservation in marine sediments : How important is anoxia? In: Whelan,J.K., Farrington,J.W. (Eds.), Productivity, Accumulation and Preservation of Organic Matter in Recent and Ancient Sediments. Columbia University Press, New York, 231-263.

Capotondi, L., Vigliotti, L., 1999. Magnetic and microfaunal characterization of Late Quaternary sediments from the Western Mediterranean: influences about sapropel formation and paleoceanographic implication. In: Zahn, R., Comas, M.C., Klaus, A. (Eds.), Proceedings of the Ocean Drilling Program, Scientific Results. Ocean Drilling Project, College station, TX, 505-517.

Carboni, M.G., Bergamin, L., Di Bella, L., Landini, B., Manfra, L., Vesica, P., 2005. Late Quaternary paleoclimatic and paleoenviromental changes in the Tyrrhenian Sea. Quaternary Science Review 24, 2069-2082.

Carrion, J.S., 2002. Patterns and processes of Late Quaternary environmental change in a montane region of southwestern Europe. uaternary Science Review 21, 2047-2066.

Carrión, J.S., 2004. The use of two pollen records from deep sea cores to frame adaptive evolutionary change for humans: a comment on "Neanderthal extinction and the millennial scale climate variability of OIS 3" by F. d'Errico and M.F. Sánchez-Goñi. Quaternary Science Reviews 23, 1217-1219.

Carrión, J.S., Dupre, M., Fumanal, M.P., Montes, R.A., 1995. Paleoenvironmental study in the semi-arid southeastern Spain: the palynological and sedimentological sequence at Perneras Cave (Lorca, Murcia). Journal of Archaeological Science 22, 355-367.

Carrión, J.S., Munuera, M., Navarro, C., Sáez, F., 2000. Paleoclimas e historia de la vegetación cuaternaria en España a través del análisis polínico: viejas falacias y nuevos paradigmas. Complutum 11, 115-142.

Carter, J.M.L., 1984. An application of scanning electron microscopy of quartz sand surface textures to the environmental diagnosis of Neogene carbonate sediments, Finestrat Basin, south-east Spain. Sedimentology 31, 717-731.

Casford, J.S.L., Rohling, E.J., Abu-Zied, R.H., Fontanier, C., Jorissen, F.J., Leng, M.J., Schmiedl, G., Thomson, J., 2003. A dynamic concept for eastern Mediterranean circulation and oxygenation during sapropel formation. Palaeogeography, Palaeoclimatology, Palaeoecology 190, 103-119.

Cliff, G., Lorimer, G.W., 1975. The quantitative analysis of thin specimens. Journal of Microscopy 103, 203-207.

Colmenero-Hidalgo, E., Flores, J.A., Sierro, F.J., Bárcena, M.A., Löwermark, L., Schönfeld, J., Grimalt, J.O., 2004. Ocean surface water response to short-term climate changes revealed by coccolithophores from the Gulf of Cadiz (NE Atlantic) and Alboran Sea (W Mediterranean). Palaeogeography, Palaeoclimatology, Palaeoecology 205, 317-336.

Comas M.C., Ivanov, 2006. Eastern Alboran margin: the transition between the Alboran and the Balearic-Algerian basins. In: Kenyon, N.H., Ivanov, M.K., Akhmetzhanov, A.M., Kozlova E.V., (Eds), Interdisciplinary geoscience studies of the Gulf of Cadiz and Western Mediterranean basins. IOC Technical Series No. 70, UNESCO.

Comas, M.C., Zahn, R., Klaus, A., et al., 1996. Proc. ODP Init. Reports 161. Ocean Drilling Program, College Station, TX.

Combourieu-Nebout, N., Paterne, M., Turon, J.L., Siani, G., 1998. A high-resolution record of the last deglaciation in the Central Mediterranean Sea: Palaeovegetation and Palaeohydrological Evolution. Quaternary Science Review 17, 303-317.

Coope, G.R., 1979. Late Cenozoic fossil coleoptera: evolution, biogeography and ecology. Annual Review of Ecology and Sistematics 10, 247-267.

Cortijo, E., Duplessy, J.-C., Labeyrie, L., Duprat, J., Paillard, D., 2005. Heinrich events: hydrological impact. Comptes Rendus Geosciences 337, 897-907.

Cortijo, E., Labeyrie, L., Vidal, L., Vautravers, M., Chapman, M., Duplessy, J.C., Elliot, M., Arnold, M., Turon, J.L., Auffret, G., 1997. Changes in sea surface hydrology associated with Heinrich event 4 in the North Atlantic Ocean between 40º and 60º N. Earth and Planetary Science Letters 146, 29-45.

Cowling, R.M., Rundel, P.W., Lamont, B.B., Arroyo, M.K., Arianoutsou, M., 1996. Plant diversity in mediterranean-climate regions. Trends in Ecology and Evolution 11, 362-366.

Cramp, A., O'Sullivan, G., 1999. Neogene sapropels in the Mediterranean: a review. Marine Geology 153, 11-28.

Cruzado, A., 1985. Chemistry of Mediterranean Waters. In: Margalef, R. (Ed.), Western Mediterranean. Pergamon Press, Oxford, 126-147.

Cullen, H.M., de Menocal, P.B., Hemming, S., Hemming, G., Brown, F.H., Guilderson, T., Siroco, F., 2000. Climate change and the collapse of the Akkadian Empire: Evidence from the deep sea. Geology 28, 379-382.

Curry, W.B., Oppo, D.W., 1997. Synchronous, high-frequency oscillations in tropical sea surface temperatures and North Atlantic Deep Water production during the last glacial cycle. Paleoceanography 12, 1-14.

Dafner, E.V., Sempere, R., Bryden, H.L., 2001. Total organic carbon distribution and budget through the Strait of Gibraltar in April 1998. Marine Chemistry 73, 233-252.

Dansgaard, W., Johnsen, S.J., Clausen, H.B., Dahl-Jensen, D., Gundestrup, N.S., Hammer, C.U., Hvidberg, C.S., Steffensen, J.P., Sveinbjornsdottir, A.E., Jouzel, J., Bond, G., 1993. Evidence for general instability of past climate from a 250-kyr ice-core record. Nature 364, 218–220.

Davies, W., Valdes, P., Ross, C., Van Andel, T., 2003. The human presence in Europe during the last glacial period III: site clusters, regional climates and resource attractions. In: Vvan Andel, T.H., Davies, W. (Eds.), Neanderthals and Modern Humans in the European Landscape during the Last Glaciation, 60,000 to 20,000 years ago: Archaeological Results of the Stage 3

Project. McDonald Institute Monograph Series, 167-190.

De Lange, G.J., Van Santvoort, P.J.M., Langereis, C., Thomson, J., Corselli, C., Michard, A., Rossignol-Strick, M., Paterne, M., Anastasakis, G., 1999. Palaeo-environmental variations in eastern Mediterranean sediments: a multidisciplinary approach in a prehistoric setting. Progress in Oceanography 44, 369-386.

de Menocal, P.D., 2001. Cultural responses to climate change during the late Holocene. Science 292, 667-673.

de Menocal, P.D., Ortiz, J., Guilderson, T., Sarnthein, M., 2000. Coherent high-and low-latitude climate variability during the Holocene warm period. Science 288, 2198-2202.

De Rijk, S., Hayes, A., Rohling, E.J., 1999. Eastern Mediterranean sapropel S1 interruption: an expression of the onset of climatic deterioration around 7 ka BP. Marine Geology 153, 337-343.

Dearing, J.A., 2006. Climate-human-environment interactions: resolving our past. Climate of the Past 2, 187-203.

Dehairs, F., Lambert, C.E., Chesselet, R., Risler, N., 1987. The biological production of marine suspended barite and the barium cycle in the western Mediterranean sea. Biogeochemistry 4, 119-139.

DeMaster, D.J., 1981. The supply and accumulation of silica in the marine environment. Geochimica et Cosmochimica Acta 45, 1715-1732.

d'Errico, F., Sánchez-Goñi, M.F., 2003. Neanderthal extinction and the millennial scale climatic variability of OIS 3. Quaternary Science Reviews 22, 769-788.

d'Errico, F., Henshilwood, C., Nilssen, P., 2001. An engraved bone fragment from c. 70,000-year-old Middle Stone Age levels at Blombos Cave, South Africa: implications for the origin of symbolism and language . Antiquitiy 75, 309-318.

Diamond, J., 2005. Collapse: how societies choose to fail or survive. Allen Lane, London, 590 pp.

Dolukhanov, P.M., 1997 The Pleistocene - Holocene transition in Northern Eurasia: Environmental changes and human adaptations. Quaternary International 41/42, 181-191.

Dymond, J., Suess, E., Lyle, M., 1992. Barium in deep-sea sediment: a geochemical proxy for paleoproductivity. Paleoceanography 7, 163-181.

Eagle Gonnea, M., Paytan, A., 2006. Phase associations of barium in marine sediments. Marine Chemistry 100, 124-135.

Eagle, M., Paytan, A., Arrigo, K., Van Dijken, G., Murray, R., 2003. A comparison between excess Barium and Barite as indicators or export production. Paleoceanography 18, 21.1-21.13.

Elderfield, H. ed., 2004. The ocean and marine geochemistry. In: Holland, H.D., Turekian, K.K. (Eds.), Treatise on geochemistry vol. 6. Elsevier-Pergamon, Oxford.

Elliot, M., Labeyrie, L., Duplessy, J.C., 2002. Changes in North Atlantic deep-water formation associated with the Dansgaard-Oeschger temperature oscillations (10-60 ka). Quaternary Science Reviews 21, 1153-1165.

Emeis, K.C., Robertson, A.H.F., Ritcher, C., et al., 1996. Proc. ODP Init. Reports 160. Ocean Drilling Program, College Station, TX.

Emeis, K.C., Sakamoto, T., 1998. The sapropel theme of Leg 160. Proc. ODP Sci. Res. 160. Ocean Drilling Program, College Station, TX, 29-36.

Emeis, K.C., Sakamoto, T., Wehausen, R., Brumsack, H.J., 2000a. The Sapropel record of the Eastern Mediterranean Sea- Results of Ocean Drilling Program Leg-160. Palaeogeography, Palaeoclimatology, Palaeoecology 158, 371-395.

Emeis, K.C., Schulz, H., Struck, U., Rossignol-Strick, M., Erlenkeuser, H., Howell, M.W., Kroon, D., Mackensen, H., Ishizuka, S., Oba, T., Sakamoto, T., Koizumi, I., 2003. Eastern Mediterranean surface water temperatures and $\delta^{18}O$ composition during deposition of sapropels in the late Quaternary. Paleoceanography, 18, 5-1, 5-18.

Emeis, K.C., Struck, U., Schulz, H.M., Rosenberg, R., Bernasconi, S., Erlenkeuser, H., Sakamoto, T., Martinez-Ruiz, F., 2000b. Temperature and salinity variations of Mediterranean Sea surface waters over the last 16,000 years from records of planktonic stable oxygen isotopes and alkenone unsaturation ratios. Palaeogeography, Palaeoclimatology, Palaeoecology 158, 259-280.

Fabregas Valcarce, R., Martinez Cortizas, A., Blanco Chao, R., Chesworth, W., 2003. Environmental change and social dynamics in the second-third millennium BC in NW Iberia, Journal of Archaeological Science 30, 859-871.

Fabres, J., 2002. Transferencia de material fi i registre ambietal en conques marginals: les conques d'Alboran i de Bransfield. Ph. D. Thesis.Univ. Barcelona, Spain.

Faugeres, J.C., Bonthier, E., Stow, D.A.W., 1984. Contourite drif molded by deep Mediterranean, Geology 12, 296-300.

Finlayson, C., 1999. Late Pleistocene Human Occupation of the Iberian Peninsula. Journal Iberian Archaeology 1, 59-68.

Finlayson, C., 2004. Neanderthals and Modern Humans: An Ecological and Evolutionary Perspective. Cambridge University Press.

Finlayson, C., 2005. Biogeography and evolution of the genus Homo Trends in Ecology and Evolution 20, 457-463.

Finlayson, G., 2006. Climate, vegetation and biodiversity A multiscale study of the South of the Iberian Peninsula. PhD Thesis, Anglia Ruskin University.

Finlayson, C., Barton, R., Stringer, C., 2001. The Gibraltar Neanderthals and their extinction. In: Zilhao, J., Aubry, T., Carvalho, A. (Eds.), Les Premiers Hommes Modernes de la Peninsule Iberique. Inst. Portugues de Arqueologia, Trabalhos de Arqueologia 17, Lisbon. pp. 117-122.

Finlayson, C., Fa, D., Finlayson, G., Giles-Pacheco, F., Rodríguez-Vidal, J.R., 2004. Did the moderns kill off the Neanderthals? A reply to F. d'Errico and Sánchez-Goñi. Quaternary Science Reviews 23, 1205-1209.

Finlayson, C., Giles-Pacheco, F., 2000. The southern Iberian Peninsula in the late Pleistocene: geography, ecology, and human occupation. In: Stringer, C.B., Barton, R.N.E, Finlayson, J.C. (Eds.), Neanderthals on the Edge, Oxford, Oxbow Books, 139-159.

Finlayson, C., Giles Pacheco, F., Rodríguez-Vidal, J., Fa, D. A., Gutierrez López, J.M., Santiago Perez, A., Finlayson, G., Allue, E., Baena Preysler, J., Cáceres, I., Carrión, J.S., Fernández Jalvo, Y., Gleed-Owen, C.P., Jiménez-Espejo, F.J., López, P., López Sáez, J.A., Riquelme Cantal, J.A., Sánchez Marco, A., Giles Guzman, F., Brown, K., Fuentes, N., Valarino, C.A., Villalpando, A., Stringer, C.B., Martinez-Ruiz, F., Sakamoto, T., 2006. Late survival of Neanderthals at the southernmost extreme of Europe. Nature 443, 850-853.

Fitzhugh, W.W., 1997. Biogeographical archaeology in the eastern North American arctic, Human Ecology 25, 385-418.

Flahault, A., Viboud, C., Pakdaman, K., Boëlle, P.Y., Wilson, M.L., Myers, M., Valleron, A. J., 2004. Association of influenza epidemics in France and the USA with global climate variability. International Congress Series 1263, 73-77.

Flores, J.A., Sierro, F.J., Frances, G., Vazquez, A., Zamarreno, I., 1997. The last 100,000 years in the western Mediterranean: sea surface water and frontal dynamics as revealed by coccolithophores. Marine Micropaleontology 29, 351-366.

Flores, J.C., 1998. A Mathematical Model for Neanderthal Extinction. Journal of Theoretical Biology 191, 295-298.

Foley, R.A., 1994. Speciation, extinction and climatic change in hominid evolution, Journal of Human Evolution 26, 275-289.

Foucault, A., Melieres, F., 2000. Paleoclimatic cyclicity in central Mediterranean Pliocene sediments: the mineralogical signal. Palaeogeography, Palaeoclimatology, Palaeoecology 158, 311-323.

Gamble, C., Davies, W., Pettitt, P., Richards, M., 2004. Climate change and evolving human diversity in Europe during the last glacial. Philosophical Transactions of the Royal Society of London Series B Biological Sciences 359 243-254.

Garcia, M., Alonso, B., Ercilla, G., Gracia, E., 2006. The tributary systems of the Almeria Canyon (Alboran Sea, SW Mediterranean): Sedimentary architecture. Marine Geology 226, 207-223.

Gasse, F., 2002. Diatom-inferred salinity and carbonate oxygen isotopes in Holocene waterbodies of the western Sahara and Sahel (Africa). Quaternary Science Review 21, 737-767.

Gherardi, J.M., Labeyrie, L., McManus, J.F., Francois, R., Skinner, L.C., Cortijo, E., 2005. Evidence from the northeastern Atlantic basin for variability in the rate of meridional overturning circulation through the last deglaciation. Earth and Planetary Science Letters 204, 710-723.

Gomez, F., 2003. The role of the exchanges through the Strait of Gibraltar on the budget of elements in the Western Mediterranean Sea: consequences of human-induced modifications. Marine Pollution Bulletin 46, 685-694.

Gónzalez-Donoso, J.M., Serrano, F., Linares, D., 2000. Sea surface temperature during the Quaternary at ODP Sites 976 and 975 (western Mediterranean). Palaeogeography, Palaeoclimatology, Palaeoecology 62, 17-44.

Gonzalez-Samperiz, P., Valero-Garces, B.L., Carrion, J.S., Pena-Monne, J.L., Garcia-Ruiz, J.M., Marti-Bono, C., 2005. Glacial and Lateglacial vegetation in norheastern Spain: New data and a review. Quaternary International 140-141, 4-20.

González-Sampériz, P., Valero-Garcés, B.L., Moreno, A., Jalut, G., García-Ruiz, J.M., Martí-Bono, C., Delgado-Huertas, A., Navas, A. Otto, T., Dedoubat, J.J., 2006. Climate variability in the Spanish Pyrenees during the last 30,000 yr revealed by the El Portalet sequence. Quaternary Research 66, 38-52.

Goslar, T., Kuc, T., Ralska-Jasiewiczowa, M., Rozanski, K., Arnold, M., Bard, E., Van Geel, B., Pazdur, M., Szeroczynska, K., Wicik, B., Wieckowski, K., Walanus, A., 1993. High-resolution lacustrine record of the late glacial/holocene transition in central Europe. Quaternary Science Review 12, 287-294.

Guieu, C., Chester, R., Nimmo, M., Martin, J.M., Guerzoni, S., Nicolas, E., Mateu, J., Keyse, S., 1997. Atmospheric input of dissolved and particulate metals to the northwestern Mediterranean. Deep-Sea Research Part II: Topical Studies in Oceanography 44, 655-674.

Guieu, C., Thomas, A., 1996. Saharan aerosol: from the soil to the Ocean. In: S. Guerzoni and R. Chester (Eds.), The impact of desert dust across the Mediterranean. Kluwer Academy Publishers, 207-216.

Gutierrez, M., Gutierrez, F., Desir, G., 2006. Considerations on the chronological and causal relationship between talus flatirons and palaeoclimatic changes in central and northeastern Spain. Geomorphology 73, 50-63.

Gwiazda, R.H., Hemming, S.R., Broecker, W.S., 1996. Tracking the sources of icebergs with lead isotopes: The provenance of ice-rafted debris in Heinrich layer 2. Paleoceanography 11, 77-93.

Hall, I.R., Bianchi, G.G., Evans, J.R., 2004. Centennial to millennial scale Holocene climate-deep water linkage in the North Atlantic, Quaternary Science Review 23, 1529-1536.

Harpending, H., Sherry, S.T., Rogers, A.L., Stoneking, M., 1993. The genetic structure of ancient human populations. Current Anthropology 34, 483-496.

Harrison, P.A., Berry, P.M., Butt, N., New, M., 2006. Modelling climate change impacts on species' distributions at the European scale: implications for conservation policy. Environmental Science & Policy 9, 116-128.

Hassan, F.A., 2002. Holocene environmental change and the transition to agriculture in South-weat Asia and North-east Africa. In: Yasuda, Y. (Ed.), The Origins of Pottery and Agriculture. Roli Books, New Delhi, 55-68.

Haug, G.H., Günther, D., Peterson, L.C., Sigman, D.M., Hughen, K.A., Aeschlimann, B., 2003. Climate and the Collapse of Maya Civilization. Science 299, 1731-17.

Hemming, S.R., 2004. Heinrich events: Massive late pleistocene detritus layers of the North Atlantic and their global climate imprint. Reviews of Geophysics 42, RG1005 1-43.

Hernández Fernández, M., Vrba1, E.S., 2005. Rapoport effect and biomic specialization in African mammals: revisiting the climatic variability hypothesis. Journal of Biogeography 32, 903–918.

Hewitt, G.M., 2000. The genetic legacy of the Quaternary ice ages. Nature 405, 907-913.

Hewitt, G.M., Ibrahim, K.M., 2001. Infering Glacial refugia and historical migrations with molecular phylogenies. In: Silvertown, J., Antonovics, J. (Eds.), Integrating ecology and evolution in a spatial context. British ecological society. Blackwell-Science.

Hockett, B., Haws, J.A., 2005. Nutritional ecology and the human demography of Neanderthal extinction. Quaternary International 137, 21-34.

Hong, Y.T., Hong, B., Lin, Q.H., Zhu, Y.X., Shibata, Y., Hirota., M., Uchida, M., Leng, X.T., Jiang, H.B., Xu, H., Wang, H., Yi, L., 2003. Correlation between Indian Ocean summer monsoon and North Atlantic climate during the Holocene. Earth and Planetary Science Letters 211, 371-380.

Hoogakker, B.A.A., Rothwell, R.G., Rohling, E.J., Paterne, M., Stow, D.A.V., Herrle, J.O., Clayton, T., 2004. Variations in terrigenous dilution in western Mediterranean Sea pelagic sediments in response to climate change during the last glacial cycle. Marine Geology 211, 21-43.

Horan, R.D., Bulte, E., Shogren, J.F., 2005. How trade saved humanity from biological exclusion: an economic theory of Neanderthal extinction. Journal of Economic Behavior & Organization 58, 1-29.

Housley, R.A., Gamble, C.S., Pettitt, P., 2001. Reply to Blockley, Donahue and Pollard. Antiquity 74, 119-121.

Hughen K., Baillie, M., Bard, E., Bayliss, A., Beck, J., Bertrand, C., Blackwell, P., Buck, C., Burr, G., Cutler, K., Damon, P. Edwards, R., Fairbanks, R., Friedrich, M., Guildenson, T., Kromer, B., McCormac, F., Manning, S., Bronk Ramsey, C., Reimer, P., Reimer, R., Remmele, S., Southon, J., Stuiver, M., Talamo, S., Taylor, F., Van der Plicht, J., Weyhenmeyer, C., 2004. Marine04: Marine radiocarbon age calibration, 26-0 ka BP. Radiocarbon 46, 1059-1086.

Huntley, B., Alfano, M.J., Allen, J.R.M., Pollard, D., Tzedakis, P.C., Beaulieu, J.L., Gruger, E., Watts, B., 2003. European vegetation during Marine Oxygen Isotope Stage-3. Quaternary Research 59, 195-212.

Iijima, K., Jiménez-Espejo, F.J., Sakamoto, T., 2005. "Filtration method" for semi-quantitative powder X-ray diffraction analysis of clay minerals in marine sediments. In: Japan Agency for Marine-Earth Science Technology, Frontier Research on Earth Evolution 2, 1-3.

Jalut, G., Amat, A.E., Bonnet, L., Gauquelin, T., Fontugne, M., 2000. Holocene climatic changes in the Western Mediterranean, from south-east France to south-east Spain. Palaeogeography, Palaeoclimatology, Palaeoecology 160, 255-290.

Jansen, J.H.F., Van der Gaast, S.J., Koster, B., Vaars, A.J., 1998. CORTEX, a shipboard XRF-scanner for element analyses in split

sediment cores. Marine Geology 151, 143-153.

Jiménez-Espejo, F.J., 2003. Evolución paleoclimática de la Cuenca del Mar de Alborán en los últimos 16.000 años a partir de indicadores mineralógicos y geoquímicos. Trabajo de Investigación-Diploma de estudios avanzados. Universidad de Granada.

Jimenez-Espejo, F.J., Martinez-Ruiz, F., Sakamoto, T., Iijima, K., Gallego-Torres, D., Harada, N., 2006. Paleonvironmental changes in the western Mediterranean since the last glacial maximum: High resolution multiproxy record from the Algero-Balearic basin. Palaeogeography, Palaeoclimatology, Palaeoecology (in press), doi:10.1016/j.palaeo.2006.10.005. 2006.

Jobling, M.A., Hurles, M.E., Tyler-Smith, C., 2004. Human evolutionary genetics: origins, peoples & disease. Garland Science, New York, 523 pp.

Johnson, R. G., 1997. Climate control requires a dam at the Strait of Gibraltar. EOS Trans. AGU, 78 (27), 277, 280– 281.

Jung, M., Ilmberger, J., Mangini, A., Emeis, K.C., 1997. Why some Mediterranean sapropels survived burn-down (and others did not). Marine Geology 141, 51-60.

Kageyama, M., Nebout, N.C., Sepulchre, P., Peyron, O.,Krinner, G., Ramstein, G., Cazet, J.P., 2005. The Last Glacial Maximum and Heinrich Event 1 interms of climate and vegetation around the Alboran Sea: a preliminary model-data comparison, Comptes Rendus Geosciences 337, 983-992.

Kirsch, H.J., 1991. Illite crystalinity: recommendations on sample preparation, X-ray diffraction settings, and interlaboratory samples. Journal of Metamorphic Geology 9, 665-670.

Klinkhammer, G., Heggie, D.T., Graham, D.W., 1982. Metal diagenesis in oxic marine sediments. Earth and Planetary Science Letters 61, 211-219.

Krijgsman, W., 2002. The Mediterranean: Mare Nostrum of earth sciences. Earth and Planetary Science Letters 205, 1-12.

Krom, M.D., Brenner, S., Kress, N., Gordon, L.I., 1991. Phosphorus limitation of Primary Productivity in the E. Mediterranean sea. Limnology & Oceanography 36, 424-432.

Kyoto protocol, 1997: http://unfccc.int/resource/docs/convkp/kpeng.html

Lahr, M.M., Foley, R., 1998. Towards a theory of modern human origins: geography, demography, and diversity in recent human evolution. Yearbook of Physical Anthropology 41, 137-176.

Lawler, I.R., Foley, W.J., Woodrow, I.E., Cork, S.J., 1997. The effects of elevated CO2 atmospheres on the nutritional quality of *Eucalyptus* foliage and its interaction with soil nutrient and light availability. Oecologia 109, 59-68.

Liquete, C., Arnau, P., Canals, M., Colas, S., 2005. Mediterranean river systems of Andalusia, southern Spain, and associated deltas: A source to sink approach: Mediterranean Prodelta Systems. Marine Geology 222-223, 471-495.

Llave, E., Schönfeld, J., Hernández-Molina, F.J., Mulder, T., Somoza, L., Diaz del Rio V. Sánchez-Almazo, I., 2006. High-resolution stratigraphy of the Mediterranean outflow contourite system in the Gulf of Cadiz during the late Pleistocene: The impact of Heinrich events. Marine Geology 227, 241-262.

Lobo, F.J., Fernandez-Salas, L.M., Moreno, I., Sanz, J.L., Maldonado, A., 2006. The sea-floor morphology of a Mediterranean shelf fed by small rivers, northern Alboran Sea margin. Continental Shelf Research 26, 2607-2628.

Lohrenz, S.E., Wiesenburg, D.A., DePalma, I.P., Johnson, K.S., Gustafson, Jr. D.E., 1988. Interrelationships among primary production, chlorophyll, and environmental conditions in frontal regions of the western Mediterranean Sea. Deep-Sea Research 35 A, 793-810.

Lopez-Jurado, J.L., Gonzalez-Pola, C., Velez-Belchi, P., 2005. Observation of an abrupt disruption of the long-term warming trend at the Balearic Sea, western Mediterranean Sea, in summer 2005. Geophysical Research Letters 32, 1-4.

Lyons, T.W., Werne, J.P., Hollander, D.J., Murray, R.W., 2003. Contrasting sulfur geochemistry and Fe/Al and Mo/Al ratios across the last oxic-to-anoxic transition in the Cariaco Basin, Venezuela. Chemical Geology 195, 131-157.

Magri, D., Parra, I., 2002. Late Quaternary western Mediterranean pollen records and African winds. Earth and Planetary Science Letters 200, 401-408.

Mangini, A., Jung, M., Laukenmann, S., 2001. What do we learn from peaks of uranium and of manganese in deep sea sediments? Marine Geology 177, 63-78.

Marin, B., Giresse, P., 2001. Particulate manganese and iron in recent sediments of the Gulf of Lion continental margin (north-western Mediterranean Sea): deposition and diagenetic process. Marine Geology 172, 147-165.

Markova, A.K., 1992. Influence of paleoclimatic changes in the middle and Late Pleistocene on the composition of small mammal faunas: data from eastern Europe mammalian migration and dispersal. Events in the European Quaternary. Courier Forschung-Institut Senckenberg 153, 93-100.

Martin, J.D., 2004. Qualitative and quantitative powder X-ray diffraction analysis. URL: http://www.xpowder.com ISBN: 84-609-1497-6.

Martínez-Ruiz, F., Kastner, M., Paytan, A., Ortega-Huertas, M., Bernasconi, S.M., 2000. Geochemical evidence for enhanced productivity during S1 sapropel deposition in the eastern Mediterranean. Paleoceanography 15, 200-209.

Martinez-Ruiz, F., Paytan, A., Kastner, M., Gonzalez-Donoso, J.M., Linares, D., Bernasconi, S.M., Jimenez-Espejo, F.J., 2003. A comparative study of the geochemical and mineralogical characteristics of the S1 sapropel in the western and eastern Mediterranean. Palaeogeography, Palaeoclimatology, Palaeoecology 190, 23-37.

Martinez-Ruiz. F., Gonzalez-Donoso, J.M., Linares, D., Jimenez-Espejo, F.J., Gallego-Torres, D., Romero, O., Paytan, A., 2004. Respuesta de la productividad biológica marina al cambio climático: registro de alta resolución de la cuenca del mar de Alborán. Geotemas 6, 125-128.

Martinson, D.G., Pisias, N.G., Hays, J.D., Imbrie, J., Moore, T.C., Shackleton, J., 1987. Age dating and the orbital theory of the Ice Ages: development of a high-resolution 0 to 300,000-year chronostratigraphy. Quaternary Research 27, 1-29.

Martrat, B., Grimalt, J.O., Lopez-Martinez, C., Cacho, I., Sierro, F.J., Flores, J.A., Zahn, R., Canals, M., Curtis, J.H., Hodell. D.A., 2004. Abrupt temperature changes in the Western Mediterranean over the past 250,000 years. Science 306, 1762-1765.

Maslin, M., Seidov, D., Lowe, J., 2001. Synthesis of the nature and causes of rapid climate transitions during the Quaternary. In: Seidov, D., Haupt, B.J., Maslin, M. (Eds.), The oceans and rapid climate change: past, present and future. Geophysical Monography. EGU. 126, 9-51.

Mayewski, P.A., Rohling, E.J., Stager, J.C., Karlen, W., Maasch, K.A., Meeker, L.D., Meyerson, E.A., Gasse, F., Van Kreveld, S.A., Holmgren, C.A., Lee-Thorp, J.A., Rosqvist, G., Rack, F., Staubwasser, M., Schneider, R., Steig, E.J., 2004. Holocene climate variability. Quaternary Research 62, 243-255.

McManus, J., Berelson, W. M., Klinkhammer, G.P., Johnson, K.S., Coale, K.H., Anderson, R.F., Kumar, N., Burdige, D.J., Hammond, D.E., Brumsack, H.J., 1998. Geochemistry of barium in marine sediments: implications for its use as a paleoproxy. Geochimica et Cosmochimica Acta 62, 3453-3473.

McManus, J.F., Francois, R., Gherardi, J.M., Keigwin, L.D., Brown-Leger, S., 2004. Collapse and rapid resumption of Atlantic meridional circulation linked to deglacial climate changes. Nature 428, 834-837.

Mellars, P., 2006. A new radiocarbon revolution and the dispersal of modern humans in Eurasia. Nature 439, 931-935.

Mercone, D., Thomson, J., Abu-Zied, R.H., Croudace, I.W., Rohling, E.J., 2001. High-resolution geochemical and micropalaeontological profiling of the most recent eastern Mediterranean sapropel. Marine Geology 177, 25-44.

Mercone, D., Thomson, J., Croudace, I.W., Siani, G., Paterne, M., Troelstra, S.R., 2000. Duration of S1, the most recent eastern Mediterranean sapropel as indicated by AMS radiocarbon and geochemical evidence. Paleoceanography 15, 336-347.

Meybeck, M., 1987. Global chemical weathering of surficial rocks estimated from river dissolved load. American Journal of Science 287, 401-428.

Meyers, P.A., 1994. Preservation of elemental and isotopic source identification of sedimentary organic matter. Chemical Geology 114, 289-302.

Meyers, P.A., Arnaboldi, M., 2005. Trans-Mediterranean comparison of geochemical paleoproductivity proxies in a mid-Pleistocene interrupted sapropel. Palaeogeography, Palaeoclimatology, Palaeoecology 222, 313-328.

Millot, C., 1999. Circulation in the western Mediterranean Sea. Journal of Marine Systems 20, 432-442.

Moberg, A., Sonechkin, D.M., Holmgren, K., Datsenko, N.M., Karlen, W., 2005. Highly variable Northern Hemisphere temperatures reconstructed from low- and high-resolution proxy data. Nature 453, 613-617.

Mohen, J.P., 2006. Climat et Neolithisation de I´Europe mediterraneenne. Comptes Rendus - Palevol 5, 453-462.

Molinaroli, E., 1996. Mineralogical characterization of Saharan dust with a view to its final destination. In: Mediterranean sediments. In: Guerzoni, S., Chester, R. (Eds.), The impact Desert Dust across the Mediterranean. Kluwer Academic, Dordrecht, 153-162.

Moncel, M.H., Voisin, J.L., 2006. Les <<industries de transition>> et le mode de spéciation des groupes néandertaliens en Europe entre 40 et 30 ka. Comptes Rendus Palevol 5, 183-192.

Moore, D.M., Reynolds, R.C., 1989. X-ray diffraction and the Identification and analysis of Clay Minerals, Oxford University Press, Oxford, 332 pp.

Moran, X.A.G., Taupier-Letage, I., Vazquez-Dominguez, E., Ruiz, S., Arin, L., Raimbault, P., Estrada, M., 2001. Physical-biological coupling in the Algerian Basin (SW Mediterranean): Influence of mesoscale instabilities on the biomass and production of phytoplankton and bacterioplankton. Deep-Sea Research Part I: Oceanographic Research Papers 48, 405-437.

Morel, A., 1991. Light and marine photosynthesis: a spectral model with geochemical and climatological implications. Progress in Oceanography 26, 263-306.

Moreno, A., 2002. Registro del aporte de polvo de origen sahariano y de la productividad oceánica en la Cuenca del Norte de Canarias y en el Mar de Alborán. Ph D. Thesis, Univ. Barcelona, Spain, 230 pp.

Moreno, A., Cacho, I., Canals, M., Grimalt, J.O., Sanchez-Vidal, A., 2004. Millennial-scale variability in the productivity signal from the Alboran Sea record, Western Mediterranean Sea. Palaeogeography, Palaeoclimatology, Palaeoecology 211, 205-219.

Moreno, A., Cacho, I., Canals, M., Grimalt, J.O., Sánchez-Goñi, M.F., Shackleton, N., Sierro, F.J., 2005a. Links between marine and atmospheric processes oscillating on a millennial time-scale. A multi-proxy study of the last 50,000 yr from the Alboran Sea (Western Mediterranean Sea). Quaternary land-ocean correlation. Quaternary Science Reviews 24, 1623-1636.

Moreno, A., Cacho, I., Canals, M., Prins, M.A., Sánchez-Goñi, M.F., Grimalt, J.O., Weltje, G.J., 2002. Saharan dust transport and high-latitude glacial climatic variability: the Alboran sea record. Quaternary Research 58, 318-328.

Moreno, J.M., (Coord.) et al., 2005b. Principales conclusiones de la evaluación preliminar de los impactos climáticos en España por efecto del cambio climático. Oficina Española de cambio climático. Ministerio de Medio Ambiente.

Mota, J.F., Perez-García, F.J., Jiménez, M.L., Amata, J.J., Peñas, J., 2002. Phytogeographical relationships among high mountain areas in the BAetic Ranges (South Spain). Global Ecology & Biogeography 11, 497-504.

Müller, P.J., Kirst, G., Ruhland, G., von Storch, I., Rosell-Mele, A., 1998. Calibration of the alkenone paleotemperature index Uk'37 based on core-tops form the eastern South Atlantic and the global ocean (60ºN-60º S). Geochimica et Cosmochimica Acta 62, 1757-1772.

Muller, P.J., Schneider, R., 1993. An automated leaching method for the determination of opal sediments and particulate matter. Deep-Sea Research Part I: Oceanographic Research Papers 40, 425-444.

Muller, PJ, Schneider, R, Ruhland, G., 1994. Late Quaternary PCO2 variations in the Angola Current: evidence from organic carbon $\delta^{13}C$ and alkenone temperatures. In: Carbon Cycling in the Glacial Ocean: Constraints on the Ocean´s Role in the Global Change (ed. Zahn R et al.), NATO ASI Series I, 17, Springer, Berlin, 343-366.

Musil, R., 2003. The middle and upper Palaeolithic game suite of central and southeastern Europe. In: Van Andel, T. H., Davies, W. (Eds.), Neanderthals and modern humans in the european landscape during the last glaciation, 60,000 to 20,000 years ago: archaeological results of the Stage 3 Project. McDonald Institute monograph series, 167-190.

Myers, P.G., Rohling, E.J., 2000. Modeling a 200-Yr Interruption of the Holocene Sapropel S1. Quaternary Research 53, 98-104.

Naughton, F., Sanchez Goñi, M.F., Desprat, S., Turon, J.L., Duprat, J., Malaize, B., Joli, C., Cortijo, E., Drago, T., Freitas, M.C., 2007. Present-day and past (last 25 000 years) marine pollen signal off western Iberia. Marine Micropaleontology 62, 91-114

Nederbragt, A.J., Thurow, J., 2005. Geographic coherence of millennial-scale climate cycles during the Holocene. Palaeogeography, Palaeoclimatology, Palaeoecology 221, 313-324.

Nieto, F., Ortega-Huertas, M., Peacor, R., Arostegui, J., 1996. Evolution of illites/smectite from early diagenesis through incipient metamorphims in sediments of the Basque-Cantabrian Basin. Clays and Clay Minerals 44, 304-323.

O'Regan, H.J., Turner, A., Wilkinson, D.M., 2002. European Quaternary refugia: a factor in large carnivore extinction?. Journal of Quaternary Science 17, 789-796.

Ortiz, J.E., Torres, T., Delgado, A., Julir, R., Lucini, M., Llamas, F.J., Reyes, E., Soler, V., Valle, M., 2004. The palaeoenvironmental and palaeohydrological evolution of Padul Peat Bog (Granada, Spain) over one million years, from elemental, isotopic and molecular organic geochemical proxies. Organic Geochemistry 35, 1243-1260.

Paterne, M., Kallel, N., Labeyrie, L., Vautravers, M., Duplessy, J.C., Rossignol-Strick, M., Cortijo, E., Arnold, M., Fontugne, M., 1999. Hydrological relationship between the North Atlantic Ocean and the Mediterranean Sea during the past 15-75 kyr, Paleoceanography 14, 626-638.

Paytan, A., 1997. Marine barite, a recorder of oceanic chemistry, productivity, and circulation. Ph D. Thesis, Univ. San Diego, California, USA.

Paytan, A., Kastner, M., Chavez, F.P., 1996. Glacial to Interglacial fluctuations in the Equatorial Pacific as indicated by marine barite. Science 274, 1355-1357.

Paytan, A., Kastner, M., Martin, E.E., Macdougall, J.D., Herbert, T., 1993. Marine barite as a monitor of seawater strontium isotope

composition. Nature 366, 445-449.

Paytan, A., Martínez-Ruiz, F., Ivy, A., Eagle, M., Wankel, S.D., 2004. Using sulfur isotopes in barite to elucidate the origin of high organic matter accumulation events in marine sediments. In: Amend, J.P., Edwards, K.J., Lyons, T.W. (Eds.), Sulfur biogeochemistry: Past and present. GSA Special Paper 379, Boulder CO, 151-160.

Peñuelas, J., Boada, M., 2003. A global change-induced biome shift in the Montseny mountains (NE Spain). Global Change Biology 9, 131-140.

Peñuelas, J., Filella, I., 2001. Responses to a warming world. Science 294, 793-794.

Perez-Folgado, M., Sierro, F.J., Flores, J.A., Cacho, I., Grimalt, J.O., Zahn, R., Shackleton, N., 2003. Western Mediterranean planktonic foraminifera events and millennial climatic variability during the last 70 kyr. Marine Micropaleontology 48, 49-70.

Perry, L., Sandweiss, D.H., Pipemo, D.R., Rademaker, K., Malpass, M.A., Umire, A., de la Vera, P., 2006. Earth maize agriculture and interzonal interaction in southern Peru. Nature 440, 76-79.

Pinardi, N., Masetti, E., 2000. Variability of the large scale general circulation of the Mediterranean Sea from observations and modelling: a review. Palaeogeography, Palaeoclimatology, Palaeoecology 158, 153-173.

Pinot, J.M., Lopez-Jurado, J.L., Riera, M., 2002. The Canales experiment (1996-1998). Interannual, seasonal and mesoscale variability of the circulation in the Balearic Channels. Progress in Oceanography 55, 335-370.

Potts, R., 1996. Evolution and climate variability. Science 273, 922-923

Prospero, J.M., 1985. Records of past continental climates in deep-sea sediments. Nature 315, 279-280.

Quakernaat, J., 1970. Direct diffractometric quantitative analysis of synthetic clay mineral mixtures with molibdenite as orientation-indicator. Journal of Sedimentary Petrology 40, 506-513.

Reimer, P.J. et al., 2006. Comment on ''Radiocarbon calibration curve spanning 0 to 50,000 years BP based on paired $^{230}Th/^{234}U/^{238}U$ and $^{14}C$ dates on pristine corals'' by R.G. Fairbanks et al.(Quaternary Science Reviews 24 (2005) 1781–1796) and ''Extending the radiocarbon calibration beyond 26,000 years before present using fossil corals'' by T.-C. Chiu et al. (Quaternary Science Reviews 24 (2005) 1797–1808). Quaternary Science Reviews 25, 855–862.

Reitz, A., Thomson, J., de Lange, G.J., Hensen, C., 2006. Source and development of large manganese enrichments above eastern Mediterranean sapropel S1. Paleoceanography 21, PA3007

Renssen, H., Isarin, R.F.B., Jacob, D., Podzum, R., Vandenberghe, J., 2001. Simulation of the Younger Dryas climate in Europe using a regional climate model nested in an AGCM: preliminary results. Global and Planetary Change 30, 41-57.

Reul, A., Rodriguez, V., Jimenez-Gomez, F., Blanco, J.M., Bautista, B., Sarhan, T., Guerrero, F., Ruiz, J., Garcia-Lafuente, J., 2005. Varibility in the spatio-temporal distribution and size-structure of phytoplankton across and upwelling area in the NW-Alboran Sea, (W-Mediterranean). Continental Shelf Research 25, 589-608.

Rio, M.H., Poulain, P.M., Pascual, A., Mauri, E., Larnicol, G., Santoleri, R., 2006. A Mean Dynamic Topography of the Mediterranean Sea computed from altimetric data, in-situ measurements and a general circulation model. Journal of Marine Systems doi:10.1016/j.jmarsys.2005.02.006

Rixen, M., Beckers, J.M., 2002. A synopticity test of a sampling pattern in the Alboran Sea. Journal of Marine Systems 35, 111-130.

Rixen, T., Guptha, M.V.S., Ittekkot, V., 2005. Deep ocean fluxes and their link to surface ocean processes and the biological pump. Progress in Oceanography 65, 240-259.

Roberts, N., 1998. The Holocene. An environmental history. Blackwell Publishing, 316 pp.

Robinson.A., Black, S., Sellwood, B.W., Valdes, P.J., 2006. A review of palaeoclimates and palaeoenvironments in the Levant and Eastarn Mediterranean from 25,000 to 5000 years BP: setting the environmental background for the evolution of human civilisation. Quaternary Science Review25, 1517-1541.

Roche, D.M., Paillard, D., 2005. Modelling the oxygen-18 and rapid glacial climatic events: a data–model comparison. Comptes Rendus Geosciences 337, 928-934.

Rogerson, M., Rohling, E.J., Weaver, P.P.E., 2006. Promotion of meridional overturning by Mediterranean-derived salt during the last deglaciation. Paleoceanography 21, PA4101 doi:10.1029/2006PA001306.

Rogerson, M., Rohling, E.J., Weaver, P.P.E., Murray J.W., 2004. The Azores Front since the Last Glacial Maximum. Earth and Planetary Science Letters 222, 779-789.

Rogerson, M., Rohling, E.J., Weaver, P.P.E.J., Murray, W., 2005. Glacial to interglacial changes in the settling depth of the Mediterranean Outflow plume. Paleoceanography 20, PA3007, 1-12.

Röhl, U., Abrams, L.J., 2000. High-resolution, downhole and non-destructive core measurements from Sites 999 and 1001 in the Caribbean Sea: application to the Late Paleocene Thermal Maximum. Proceedings of the Ocean Drilling Program, Scientific Results 165, 191-203.

Rohling, E.J., Bryden, H.L., 1992. Man-induced salinity and temperature increases in western Mediterranean deep water. Journal of Geophysical Research 97, 11191-11198.

Rohling, E.J., Den Dulk, M., Pujol, C., Vergnaud-Grazzini, C., 1995. Abrupt hydrographic change in the Alboran Sea (western Mediterranean) around 8000 yrs BP. Deep-Sea Research Part I: Oceanographic Research Papers 42, 1609-1619.

Rohling, E.J., Hilgen, F.J., 1991. The eastern Mediterranean climate at times of sapropel formation: a review. Geologie en Mijnbouw 70, 253-264.

Rohling, E. J., Mayewski, P. A., Challenor, P., 2003. On the timing and mechanism of millennial-scale climate variability during the last glacial cycle. Climate Dynamics 20, 257-267.

Rölh, U., Abrams, L.J., 2000. High-resolution, downhole, and nondestructive core measurements from Sites 999 and 1001 in the Caribean Sea: application to the late Paleocene Thermal Maximum. In Leckie, R.M., Sigurdsson, H., Acton, G.D., and Draper, G. (Eds.), Proc. ODP, Sci. Results, 165: College Station, TX (Ocean Drilling Program), 191-203.

Rossignol-Strick, M., Nesteroff, W.D., Olive, P., Vergnaud-Grazzini, C., 1982. After the deluge: Mediterranean stagnation and sapropel formation. Nature 295, 105-110.

Rossignol-Strick, M., 1985. Mediterranean Quaternary sapropels: an immediate response of the African monsoon to variation of insolation. Palaeogeography, Palaeoclimatology, Palaeoecology 49, 237-265.

Roucoux, K.H., Abreu, L., Shackleton, N.J., Tzedakis, P.C., 2005. The response of NW Iberian vegetation to North Atlantic climate oscillations during the last 65kyr. Quaternary Science Reviews 24, 1637-1653.

Rutten, A., de Lange, G.J., 2003. Sequential extraction of iron, manganese and related elements in S1 sapropel sediments, eastern Mediterranean. Palaeogeography, Palaeoclimatology, Palaeoecology 190, 79-101.

Rutten, A., de Lange, G.J., Hayes, A., Rohling, E.J., de Jong, A.F.M., Van der Borg, K., 1999. Deposition of sapropel S1 sediments in oxic pelagic and anoxic brine environments in the eastern Mediterranean: differences in diagenesis and preservation. Marine Geology 153, 319-335.

Sageman, B.B., Lyons, T.W., (2003) Geochemistry of fine-grained sediments and sedimentary rocks, pp. 115-148. In: Sediments, diagenesis, and sedimentary rocks (ed. F.T. Mckenzie) Vol. 7 Treatise on Geochemistry (eds. H.D. Holland and K.K. Turekian), Elsevier-Pergamon, Oxford.

Sakamoto, T., Kuroki, K., Sugawara, T., Aoike, K., Iijima, K., Sugisaki, S., 2006. Non-Destructive X-ray Fluorescence (XRF) Core Imaging Scanner (TATSCAN-F2). IODP science, Scientific Drilling 37-39.

Sanchez de las Heras (coord) 2004. Sociedades recolectoras y primeros productores. Actas de las jornadas temáticas andaluzas de arqueología. Junta de Andalucía, Conserjería de Cultura.

Sanchez-Goñi, M.F., Cacho, I., Turon, J.L., Guiot, J., Sierro, F.J., Peypouquet, J.P., Grimalt, J.O., Shackleton, N.J., 2002. Synchroneity between marine and terrestrial responses to millennial scale climatic variability during the last glacial period in the Mediterranean region. Climate Dynamics 19, 95–105.

Sánchez-Goñi, M.F., Loutre, M.F., Crucifix, M., Peyron, O., Santos, L., Duprat, J., Malaize, B., Turon, J.L., Peypouquet, J.P., 2005. Increasing vegetation and climate gradient in Western Europe over the Last Glacial Inception (122-110 ka): data-model comparison. Earth and Planetary Science Letters 231, 111-130.

Sánchez-Goñi, M.F., Turon, J.L., Eynaud, F., Gendreau, S., 2000. European climatic reponse to millenial-scale changes in the atmosphere-ocean system during the Last Glacial period. Quaternary Research 54, 394-403.

Sanchez-Vidal, A., Collier, R.W., Calafat, A., Fabres, J., Canals, M., 2005. Particulate barium fluxes on the continental margin: a study from the Alboran Sea (Western Mediterranean). Marine Chemistry 93, 105-117.

Schönfeld, J., Zahn, R., 2000. Late glacial to Holocene history of the Mediterranean Outflow: Evidence from benthic foraminiferal assemblages and stable isotopes at the Portuguese margin. Palaeogeography, Palaeoclimatology, Palaeoecology, 159, 85-111.

Schulz, M., Paul, A., 2002. Holocene climate variability on centennial-to-millennial time scales: 1. In: Wefer, G. et al., (Eds.), Climate records from the North-Atlantic realm. Springer-Verlag, Berlin, Heidelberg. 41-54.

Seidov, D., Barron, E.J., Haupt, B.J., 2001. Meltwater and the global ocean conveyor: northern versus southern connections. Global and Planetary Change 30, 257-270.

Send, U., Font, J., Krahmann, G., Millot, C., Rhein, M., Tintore, J., 1999. Recent advances in observing the physical oceanography of the western Mediterranean Sea. Progress in Oceanography 44, 17-64.

Serrano, F.J., González-Donoso, J.M., Palmqvist, P., Guerra-Merchán, A., Linares, D., Pérez-Claros, J.A., 2007. Estimating Pliocene sea-surface temperatures in the Mediterranean: An approach based on the modern analogs technique. Palaeogeography, Palaeoclimatology, Palaeoecology 243, 174-188.

Shackleton, N.J., Hall, M.A., Vincent, E., 2000. Phase relationships between millennial-scale events 64,000-24,000 years ago, Paleoceanography 15, 565-569.

Sierro, F.J., Hodell, D.A., Curtis, J.H., Flores, J.A., Reguera, I., Colmenero-Hidalgo, E., Barcena, M.A., Grimalt, J.O., Cacho, I., Frigola, J., Canals, M., 2005. Impact of iceberg melting on Mediterranean thermohaline circulation during Heinrich events. Paleoceanography 20 PA2019, 1-13.

Skliris, N., Sofianos, S., Lascaratos, A., 2006. Hydrological changes in the Mediterranean Sea in relation to changes in the freshwater budget: A numerical modelling study. Journal of Marine Systems *In press*.

Sprovieri, F., Pirrone, N., Gardfeldt, K., Sommar, J., 2003. Mercury speciation in the marine boundary layer along a 6000 km cruise path around the Mediterranean Sea. Atmospheric Environment 37 (SUPPL. 1), 63-S71.

Stewart, J.R., 2004a. Neanderthal-modern human competition? a comparison between the mammals associated with middle and upper Palaeolithic industries in Europe during OIS 3 . International Journal of Osteoarchaeology 14, 178-189.

Stewart, J.R., 2004b. The Fate of Neanderthals a special case or simply part of the broader Late Pleistocene megafaunal extinctions? The Upper Palaeolithic. Acts of th XIVth UISPP Congress, Liege, Belgium. BAR International Series 1240, 261-273.

Stewart, J.R., 2005. The ecology and adaptation of Neanderthals during the non-analogue environment of Oxygen Isotope Stage 3: armageddon or entente? The demise of the European Neanderthals in Isotope Stage 3. Quaternary International 137, 35-46.

Stewart, J.R., Lister, A.M., 2001. Cryptic northern refugia and the origins of modern biota. Trends in Ecology and Evolution 16, 608-613.

Stewart, J.R., Van Kolfschoten, M., Markova, A., Musil, R., 2003a. The mammalian faunas of Europe during Oxygen Isotope Stage three. In: van Andel, T.H., Davies, W. (Eds.), Neanderthals and modern humans in the European landscape during the Last Glaciation 60,000 to 20,000 years ago: Archaeological results of the Stage Three Project. McDonald Institute monograph series, 103-129.

Stewart, J.R., Van Kolfschoten, M., Markova, A., Musil, R., 2003b. Neanderthals as part of the broader Late Pleistocene megafaunal extinctions? In: van Andel, T.H., Davies, W. (Eds.), Neanderthals and modern humans in the European landscape during the Last Glaciation 60,000 to 20,000 years ago: Archaeological results of the Stage Three Project. McDonald Institute monograph series, 221-231.

Stringer, C., Andrews, P., 1988. Genetic and fossil evidence for the evolution of modern humans. Science 239, 1263-1268.

Stringer, C., Pälike, H., Van Andel, T.H., Huntley, B., Valdez, P., Allen, J.R.M., 2003. Climatic stress and the extinction of the Neanderthals. In: van Andel, T.H., Davies, W. (Eds.), Neanderthals and Moderns Humans in the European Landscape during the Last Glaciation, 60,000 to 20,000 years ago: Archaeological Results of the Stage Three Project. McDonalds Institute Monograph Series, 233-240.

Stuiver, M., Reimer, P.J., 1993. Extended $^{14}C$ data base and revised CALIB 3.0 14C Age calibration program. Radiocarbon 35, 215-230.

Stuivert, M., Reimer, P.J., 1993. Radiocarbon calibration program. Radiocarbon 125-230.

Taberlet, P., Fumagalli, L., Wust-Saucy, A.G., Cosson, J.F., 1998. Comparative phylogeography and postglacial colonization routes in Europe. Molecular Ecology 7, 453-464.

Taylor, K.C., White, J.W.C., Severinghaus, J.P., Brook, E.J., Mayewski, P.A., Alley, R.B., Steig, E.J., Spencer, M.K., Meyerson, E., Meese, D.A., 2004. Abrupt climate change around 22 ka on the Siple Coast of Antarctica. Quaternary Science Reviews 23, 7-15.

Thompson, L.G., Davis, M.E., Mosley-Thompson, E., et al., 1998. A 25,000 year tropical climate history form Bolivian ice cores. Science 282, 1858-1864.

Thomson, J., Higgs, N.C., Wilson, T.R.S., Croudace, I.W., De Lange, G.J., Van Santvoort, P.J.M., 1995. Redistribution and geochemical behaviour of redox-sensitive elements around S1, the most recent eastern Mediterranean sapropel. Geochimica et Cosmochimica Acta 59, 3487-3501.

Tipper, E.T., Galy, A., Gaillardet, J., Bickle, M.J., Elderfield, H., Carder, E.A., 2006. The magnesium isotope budget of the modern ocean: Constraints form riverine magnesium isotope ratios. Earth and Planetary Science Letters 250, 241-253.

Toucanne, S., Mulder, T., Schonfeld, J., Hanquiez, V., Gonthier, E., Duprat, J., Cremer, M., Zaragosi, S., 2006. Contourites of the Gulf of Cadiz: A high-resolution record of the paleocirculation of the Mediterranean outflow water during the last 50,000 years. Palaeogeography, Palaeoclimatology, Palaeoecology doi: 10.1016/j.paleo.2006.10.007.

Trinkaus, E., 1995. Neanderthal mortality patterns. Journal of Archaeological Science 22, 121-142.

Turney, C.S.M., Roberts, R.G., Jacobs, Z., 2006. Progress and pitfalls in radiocarbon dating. Arising from: P. Mellars. Nature 439, 931–935.

Turon, J.L., Lezine, A.M., Denefle, M., 2003. Land-sea correlations for the last glaciation inferred from a pollen and dinocyst record from the portuguese margin. Quaternary Research 59, 88-96.

Tzedakis, P.C., Lawson, I.T., Frogley, M.R., Hewitt, G.M., Preece, R.C., 2002. Buffered tree population changes in a Quaternary refugium: evolutionary implications. Science 297, 2044-2047.

UN-Nairobi conference meeting, 2006: http://unfccc.int/meetings/cop_12/items/3754.php mma:http://www.mma.es/portal/secciones/cambio_climatico/areas_tematicas/organismos_lucha_cc/index.htm.

Van Geel, B., Shinde, V., Yasuda, Y., 2001. Solar forcing of climate change and a monsoon-related cultural shift in Western India around 800 cal BC, in: Monsoon and Civilisation, edited by: yasuda,Y., Shinde, V., Asian Lake Drilling Programme 35-39.

Van Santvoort, P.J.M., de Lange, G.J., Thomson, J., Cussen, H., Wilson, T.R.S., Krom, M.D., Strohle, K., 1996. Active post-depositional oxidation of the most recent sapropel (S1) in sediments of the eastern Mediterranean Sea. Geochimica et Cosmochimica Acta 60, 4007-4024.

Vega Toscano, L.G., 2005. El final del Paleolitico Medio y el inicio del Paleolitico Superior: más allá de los datos Cantábricos. In: Barquín, R. M., Lasheras, J.A., (Coord.) Neandertales Cantábricos: estado de la cuestión. Museo de Altamira. Monogr. nº 20. Santander 541-556

Voelker, A.H.L., et al., 2002. Global distribution of centennial-scale records for Marine Isotope Stage (MIS) 3: a database. Quaternary Science Reviews 21, 1185-1212.

Voelker, A.H.L., Lebreiro, S.M., Schönfeld, J., Cacho, I., Erlenkeuser, H., Abrantes, F., 2006. Mediterranean outflow strengthening during northern hemisphere coolings: A salt source for the glacial Atlantic?. Earth and Planetary Science Letters 245, 39-55.

Walker, M.J.C., 1995. Climatic changes in Europe during the Last Glacial/Interglacial transition. Quaternary International 28, 63-76.

Wehausen, R., Brumsack, H.J., 1998. The formation of Pliocene Mediterranean sapropels: constraints from high-resolution major and minor elements studies. In: Robertson, A.A.F., et al., (Eds.), Proceedings ODP, Leg 160, Scientific Results, Mediterranean I: College Station, Texas, Ocean Drilling Program, 207-218.

Wehausen, R., Brumsack, H.J., 1999. Cyclic variations in the chemical composition of eastern Mediterranean Pliocene sediments: a key for understanding sapropel formation. Marine Geology 153, 161-176.

Weiss, H., Bradley, R.S., 2001. What drives societal collapse?. Science 291, 609-610.

Weiss, H., 2001. Prehistoric and early historic West Asian responses to abrupt climate change. Monsoon 3, 108.

Weldeab, S., Siebel, W., Wehausen, R., Emeis, K.C., Schmiedl, G., Hemleben, C., 2003. Late Pleistocene sedimentation in the Western Mediterranean Sea: implications for productivity changes and climatic conditions in the catchment areas. Palaeogeography, Palaeoclimatology, Palaeoecology 190, 121-137.

Willis, K.J., 1996. Where did all the flowers go? The fate of temperate European flora during the glacial periods. Endeavour 20, 110-114.

Wilson, R.C.L., Drury, S.A., Chapman, J.L., 2000. The great ice age. The Open University, 271 pp.

Wirtz, K.W., Lemmen, C., 2003. A global dynamic model for the Neolithic transition, Climatic Change 59, 333-367.

Wolpoff, M., 1989. Multiregional evolution: the fossil alternative to Eden. In: Mellars, P., Stringer, C. (Eds.), The Human Revolution. Edinburgh University Press, Edinburgh. pp. 62-108.

Woodward, F.I., 1987. Climate and plant distribution. Cambridge University Press, 174 pp.

Wroe, S., Field, J., Grayson, D.K., 2006. Megafaunal extinction: climate, humans and assumptions. Trends in Ecology & Evolution 21, 61-62.

Wunsam, S., Schmidt, R., Muller, J., 1999. Holocene lake development of two Dalmatian lagoons (Malo and Veliko, Isle of Mljet) in respect to changes in Adriatic sea level and climate. Palaeogeography, Palaeoclimatology, Palaeoecology 146, 251-281.

Yarincik, K.M., Murray, R.W., Lyons, T.W., Peterson, L.C., Haug, G.H., 2000. Oxygenation history of bottom waters in the Cariaco Basin, Venezuela, over the past 578,000 years: Results from redox-sensitive metals (Mo, V, Mn, and Fe). Paleoceanography 15, 593-604.

Yll, R., Carrión, J.S., Marra, A.C., Bonfiglio, L., 2006. Vegetation on the basis of pollen in Late Pleistocene hyena coprolites from San Teodoro Cave (Sicily, Italy). Palaeogeography, Palaeoclimatology, Palaeoecology 237, 32-39.

Young, J.R., 1994. Functions of coccoliths. Coccolithophores. In: Winter, A., Sissier, W. (Eds.). Cambridge University Press, Cambridge, 63-82.

Zavaleta, E.S., Thomas, B.D., Chiariello, N.R., Asner, G.P., Shaw, M.R., Field, C.B., 2003. Plants reverse warming effect on ecosystem water balance. Proceedings of the National Academy of Sciences of the United States of America 100, 9892-9893.

Zilhao, J., 1996. The extinction of Iberian Neanderthals and its implications for the origins of Modern Humans in Europe. Actes du XIII Congres des Sciences Prehistoriques et Protohistoriques 2, 299-312. Forli, Abaco.

Zuñiga, D., Garcia-Orellana, J., Calafat, A., Price, N.B., Adatte, T., Sanchez-Vidal, A., Canals, M., Sanchez-Cabeza, J.A., Masque, P., Fabres, J., 2006. Late Holocene fine-grained sediments of the Balearic Abyssal Plain, Western Mediterranean Sea. Marine Geology. doi:10.1016/j.margeo.2006.10.034

Zvelebil, M., (ed.), 1986. Hunters in transition . Cambridge: Cambridge University Press

# CORE TTR-268G

# BASACALB 1999

**R/V PROFESSOR LOGACHEV CRUISE TTR-9**

LITHOLOGY

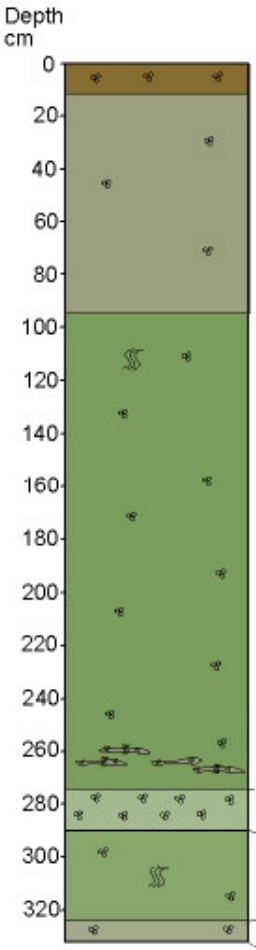


Brownish muddy, estructureless, water saturated.

Grey clay, estructureless. Foraminferal rich, Slighty bioturbation.
Colour: 5Y 6/1

Grey-greenwish clay, structureless, with foraminifers.
Sligh bioturbated.
Colour: 5Y 5/2

Grey-greenwish sand-silty, with foraminifers and shells fragments, and siliciclastics. Colour: 5Y 3/2

Grey-greenwish clay, structureless, with foraminifers.
Sligh bioturbated.
Colour: 5Y 5/2

Grey marl, with foraminifers and bioturbation

**R/V Professor Logachev TTR-12** **CORE 290G**

**Location:** Pelagic core

**Latitude:** 35°34.612' N **Date:** 23.07.02

**Longitude:** 4°34.004' W **Recovery:** 284 cm

**Water Depth:** 854 m

AGE:
EP - Late Pleistocene
EP - Early Pleistocene
H - Holocene

SUBSAMPLING CODES:
1- Express analysis 3- Geochemistry 5- Other
2- Sedimentology 4- Paleontology

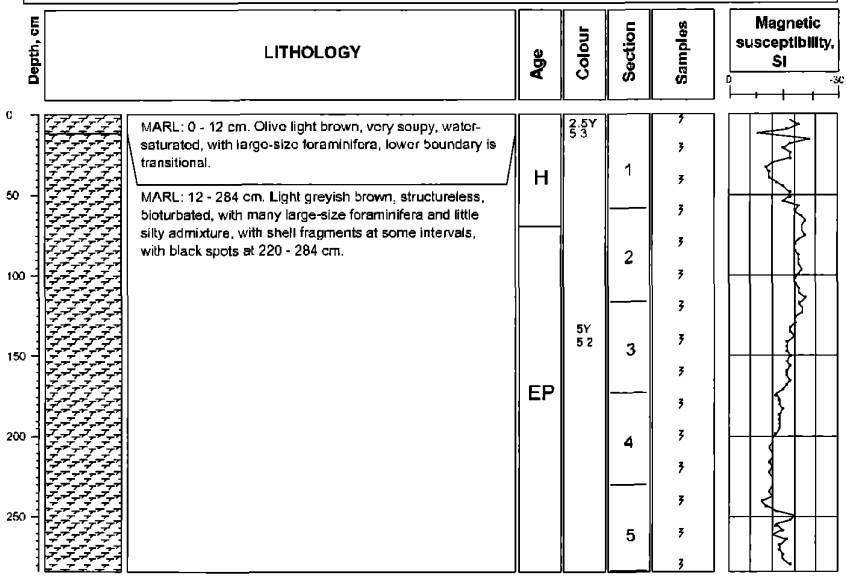

**R/V Professor Logachev TTR-12** **CORE 291G**

**Location:** Pelagic core

**Latitude:** 35°40.952' N

**Longitude:** 4°13.970' W

**Date:** 23.07.02

**Recovery:** 351 cm

**Water Depth:** 1520 m

**AGE:**

LP - Late Pleistocene
EP - Early Pleistocene
H - Holocene

**SUBSAMPLING CODES:**

1- Express analysis 3- Geochemistry 5- Other
2- Sedimentology 4- Palaeontology



MARL: 0 - 2 cm. Light olive brown, very water-saturated, with foraminifera, lower boundary is transitional.

MARL: 2 - 351 cm. Light greyish brown, structureless, intensively bioturbated, with foraminifera, with some visible silty admixture at 60 cm. At interval 70 - 72 cm - sand - fine to medium grained, with large amount of foraminifera, upper boundary is very sharp, lower boundary - transitional (posible contourite?). At interval 306 - 314 cm - planar lamination of clayey silt, silty clay and clayey sand. Black spots are randomly distributed at interval 181- 351 cm.

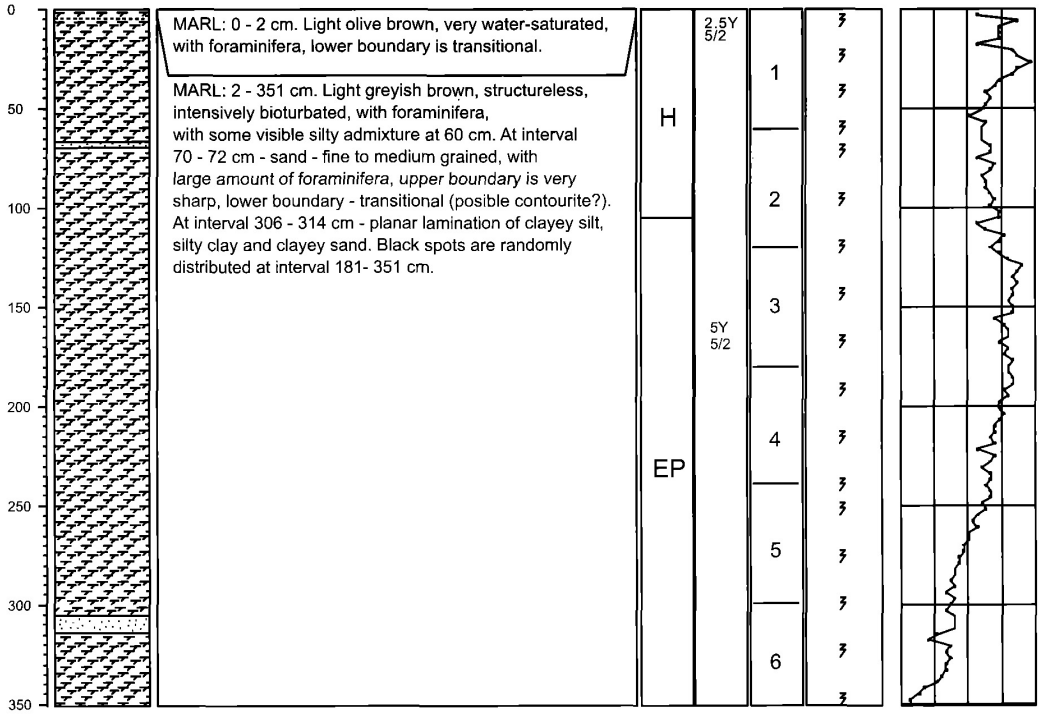

**R/V Professor Logachev TTR-14** **CORE MS-299G**

**Location:** East Alboran sea; Pelagic core

**Latitude:** 36°13,897' N **Date:** 13.08.2004

**Longitude:** 2°03,350' W **Recovery:** 469 cm

**Water Depth:** 1938 m

AGE:
LP - Late Pleistocene
EP - Early Pleistocene
H - Holocene

SUBSAMPLING CODES:
1- Excess analysis 3- Geochemistry 5- Other
2- Sedimentology 4- Paleontology

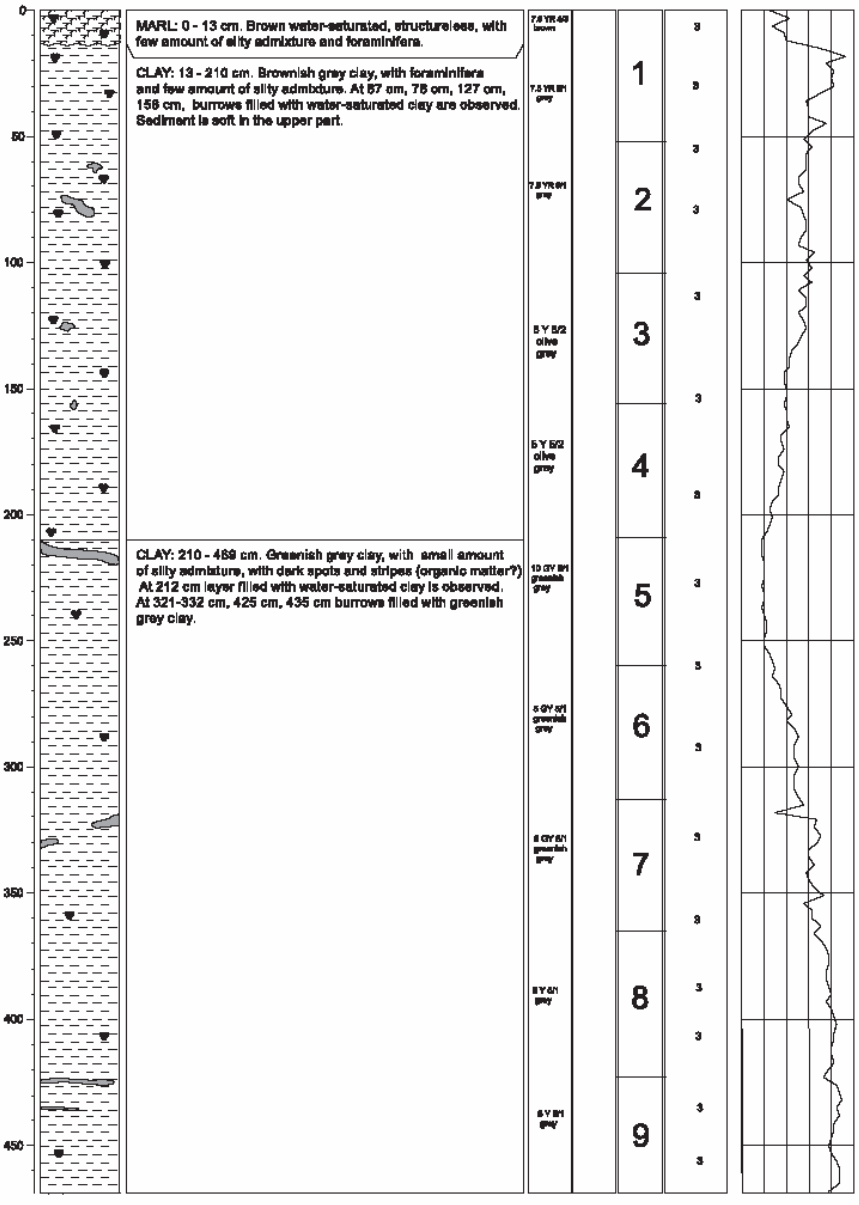

**R/V Professor Logachev TTR-14** **CORE MS-300G**

**Location:** East Alboran sea; Pelagic core

**Latitude:** 36°21,532' N **Date:** 13.08.2004

**Longitude:** 1°47,507' W **Recovery:** 456 cm

**Water Depth:** 1860 m

AGE:
LP – Late Pleistocene
EP – Early Pleistocene
H – Holocene

SUBSAMPLING CODES:
1- Express analysis 3- Geochemistry 5- Other
2- Sedimentology 4- Paleontology

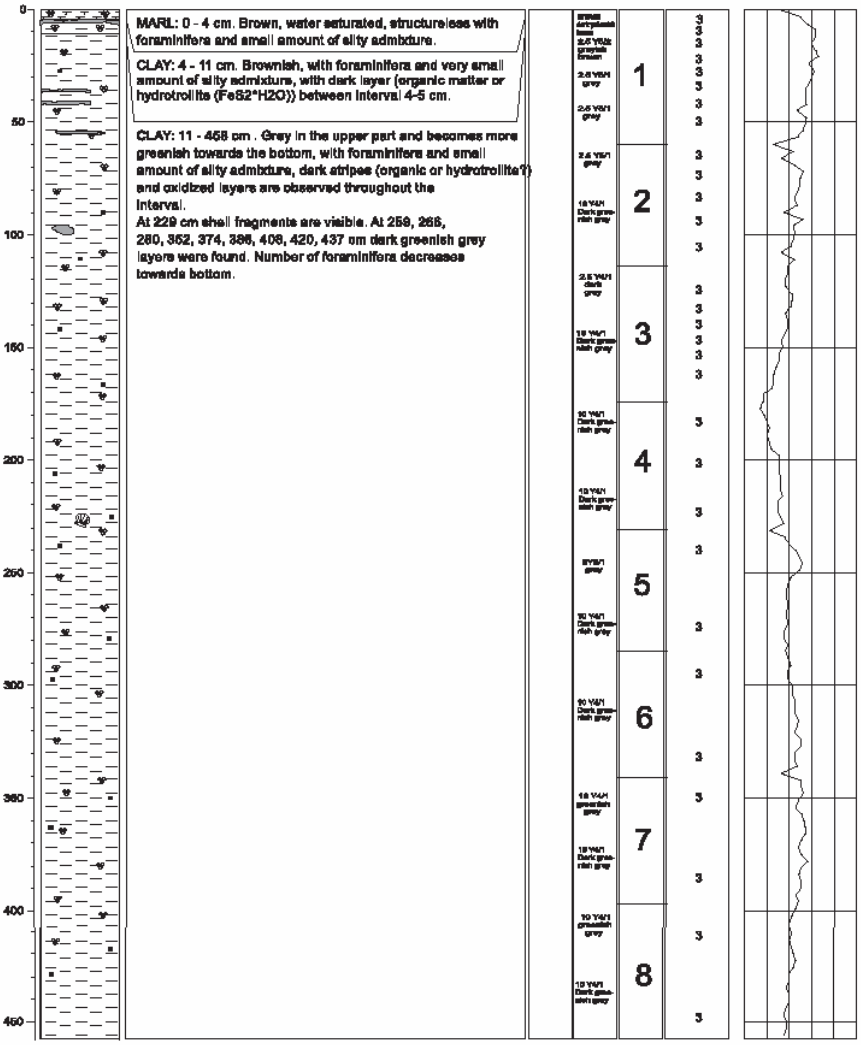

**R/V Professor Logachev TTR-14** **CORE MS-301G**

**Location:** East Alboran sea; Pelagic core

**Latitude:** 36°14,813' N **Date:** 13.06.2004

**Longitude:** 1°45,342' W **Recovery:** 487 cm

**Water Depth:** 1985 m

AGE:
LP - Late Pleistocene
EP - Early Pleistocene
H - Holocene

SUBSAMPLING CODES:
1- Express analysis 3- Geochemistry 5- Other
2- Sedimentology 4- Paleontology

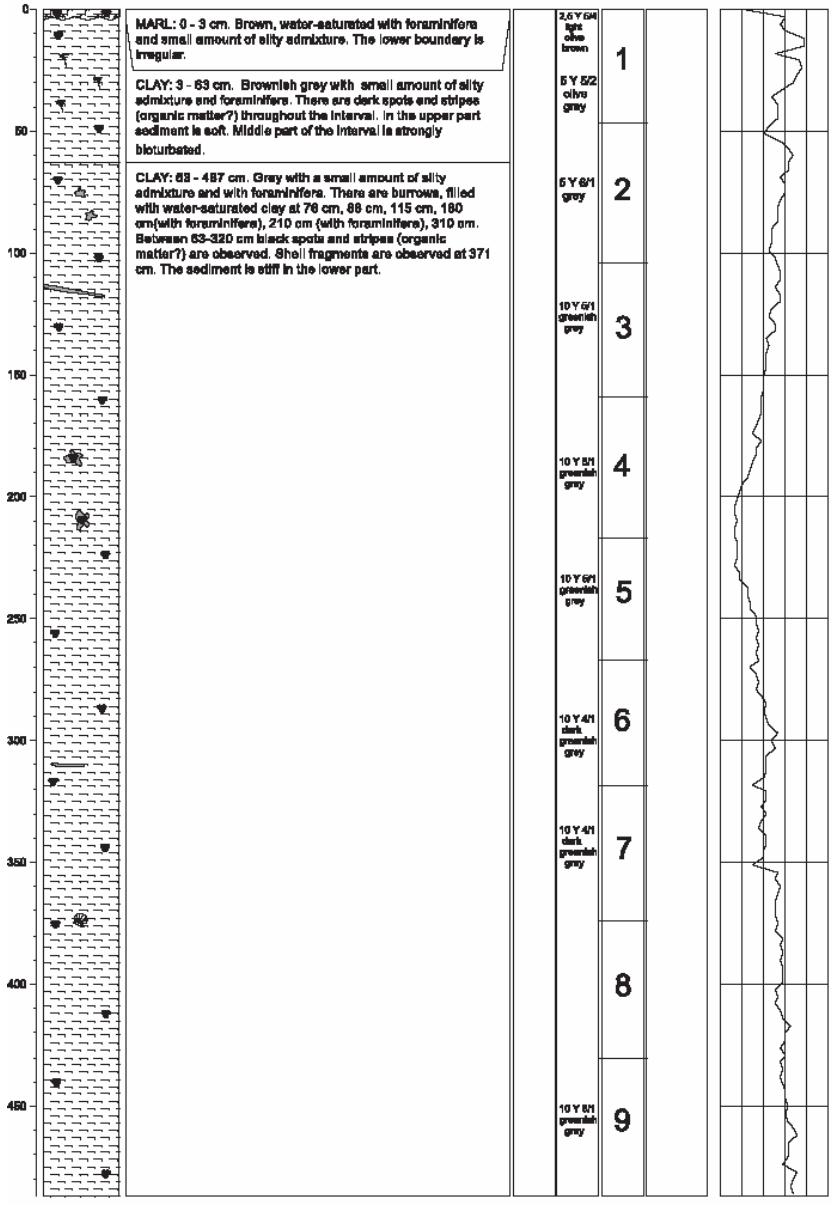

**R/V Professor Logachev TTR-14** **CORE MS-302G**

**Location:** East Alboran sea; Pelagic core

**Latitude:** 36°01,906' N

**Longitude:** 1°57,317' W

**Water Depth:** 1989 m

**Date:** 13.06.2004

**Recovery:** 420 cm

AGE:
LP - Late Pleistocene
EP - Early Pleistocene
H - Holocene

SUBSAMPLING CODES:
1- Express analysis 3- Geochemistry 5- Other
2- Sedimentology 4- Paleontology

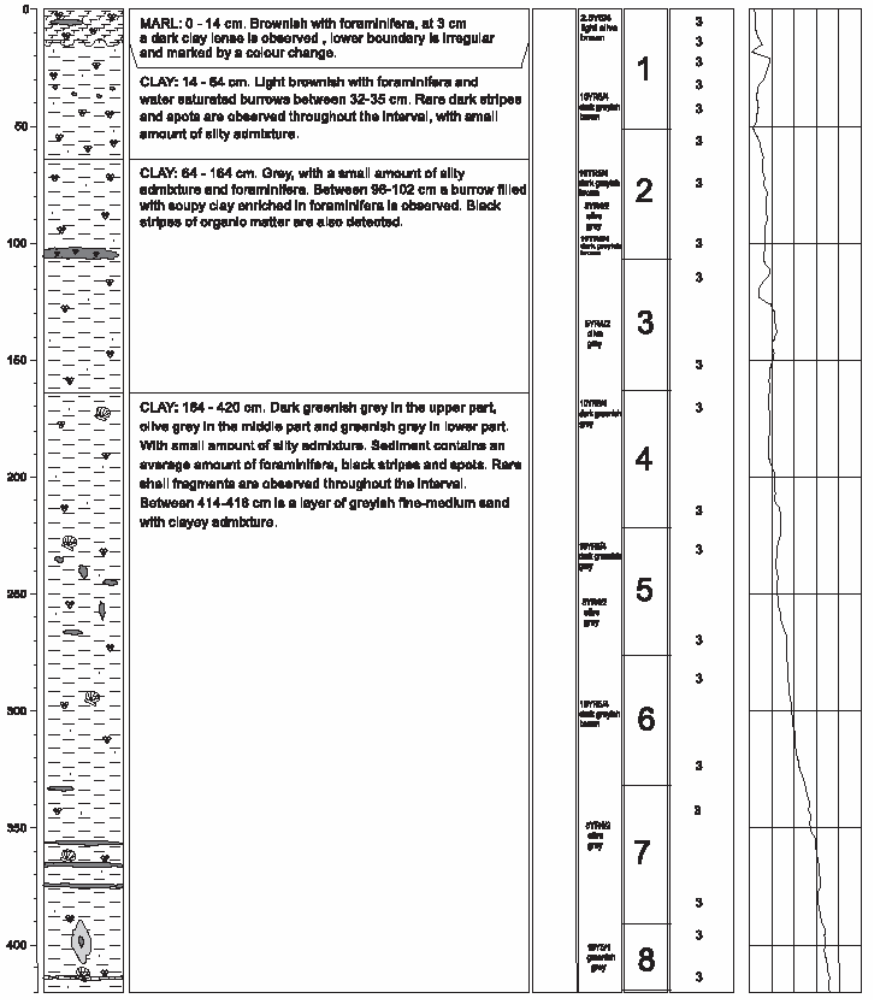

**R/V Professor Logachev TTR-14** — **CORE MS-303G**

**Location:** East Alboran sea; Pelagic core

**Latitude:** 36°17,429' N

**Date:** 13.08.2004

**Longitude:** 1°37,380' W

**Recovery:** 461 cm

**Water Depth:** 2094 m

AGE:
LP - Late Pleistocene
EP - Early Pleistocene
H - Holocene

SUBSAMPLING CODES:
1- Express analysis 3- Geochemistry 5- Other
2- Sedimentology 4- Paleontology

| Depth, cm | LITHOLOGY | Age | Colour | Section | Samples | Magnetic susceptibility, SI |
|---|---|---|---|---|---|---|

MARL: 0 - 6 cm. Brown soupy, rich in foraminifera.

CLAY: 6 - 57 cm. Brownish stiff clay with few foraminifera, with dark (organic?) layer in the upper 2 cm. Between 6-20 cm sediment is brownish in colour. There is oxidised patch at 14 - 16 cm

CLAY: 57 - 98 cm. Grey with some silty admixture and foraminifera throughout the interval. At 20 - 24 cm burrows filled with water-saturated clay are observed. There are spots and stripes (organic matter?). Sediment is strongly bioturbated.

CLAY: 98 - 292 cm. Grey clay with a small amount of silty admixture and foraminifera. Black spots and stripes (organic matter?) are observed throughout the interval. At 100 cm, 106 cm, 108 cm, 153 cm burrows filled with water-saturated clay are observed. At 249 cm, 256 cm, 260 cm, 266 cm greenish grey layers of clay are visible.

CLAY: 292 - 461 cm. Grey with stripes and spots (organic matter?). At 292 - 307 cm sediment is more greenish and at 369 cm and 371cm layers of greenish grey clay are observed. There are shell fragments between 307 - 318 cm and at 364 cm. Between 418-428 cm, 445-452 cm inclusions with large amount of foraminifers are observed.

| Colour | Section | Samples |
|---|---|---|
| 2.5 YR 4/3 brown | 1 | 3 |
| 10 YR 6/2 grayish brown | | 3 |
| | | 3 |
| 5 Y 5/1 grey | 2 | 3 |
| 5 Y 5/2 olive grey | | 3 |
| | 3 | 3 |
| 5 Y 5/1 grey | | 3 |
| | 4 | 3 |
| 5 Y 5/1 grey | | 3 |
| | 5 | 3 |
| | | 3 |
| 5 Y 5/1 grey | 6 | 3 |
| | | 3 |
| | 7 | 3 |
| | | 3 |
| 5 Y 5/1 grey | 8 | 3 |
| | | 3 |

**R/V Professor Logachev TTR-14** **CORE MS-304G**

**Location:** East Alboran sea; Pelagic core

**Latitude:** 36°19,873' N

**Longitude:** 1°31,631' W

**Date:** 13.08.2004

**Recovery:** 454 cm

**Water Depth:** 2382 m

**AGE:**

LP - Late Pleistocene
EP - Early Pleistocene
H - Holocene

**SUBSAMPLING CODES:**

1- Express analysis 3- Geochemistry 5- Other
2- Sedimentology 4- Palaeontology

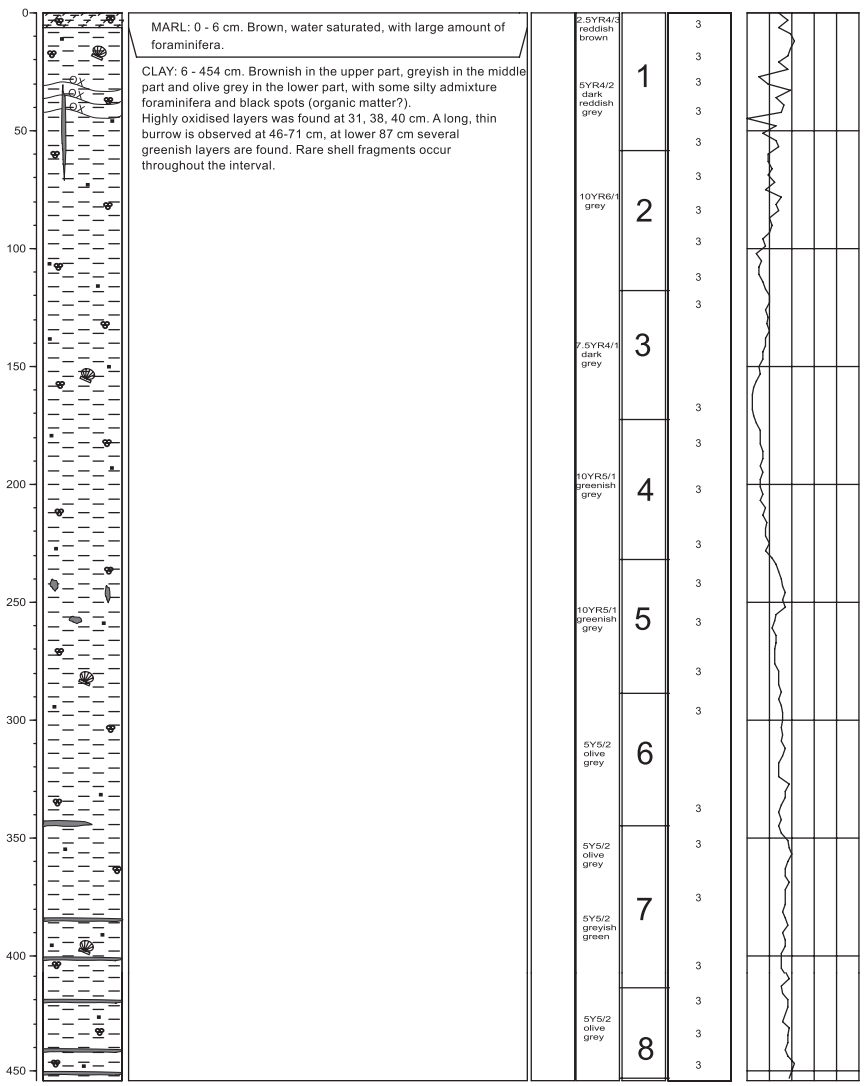

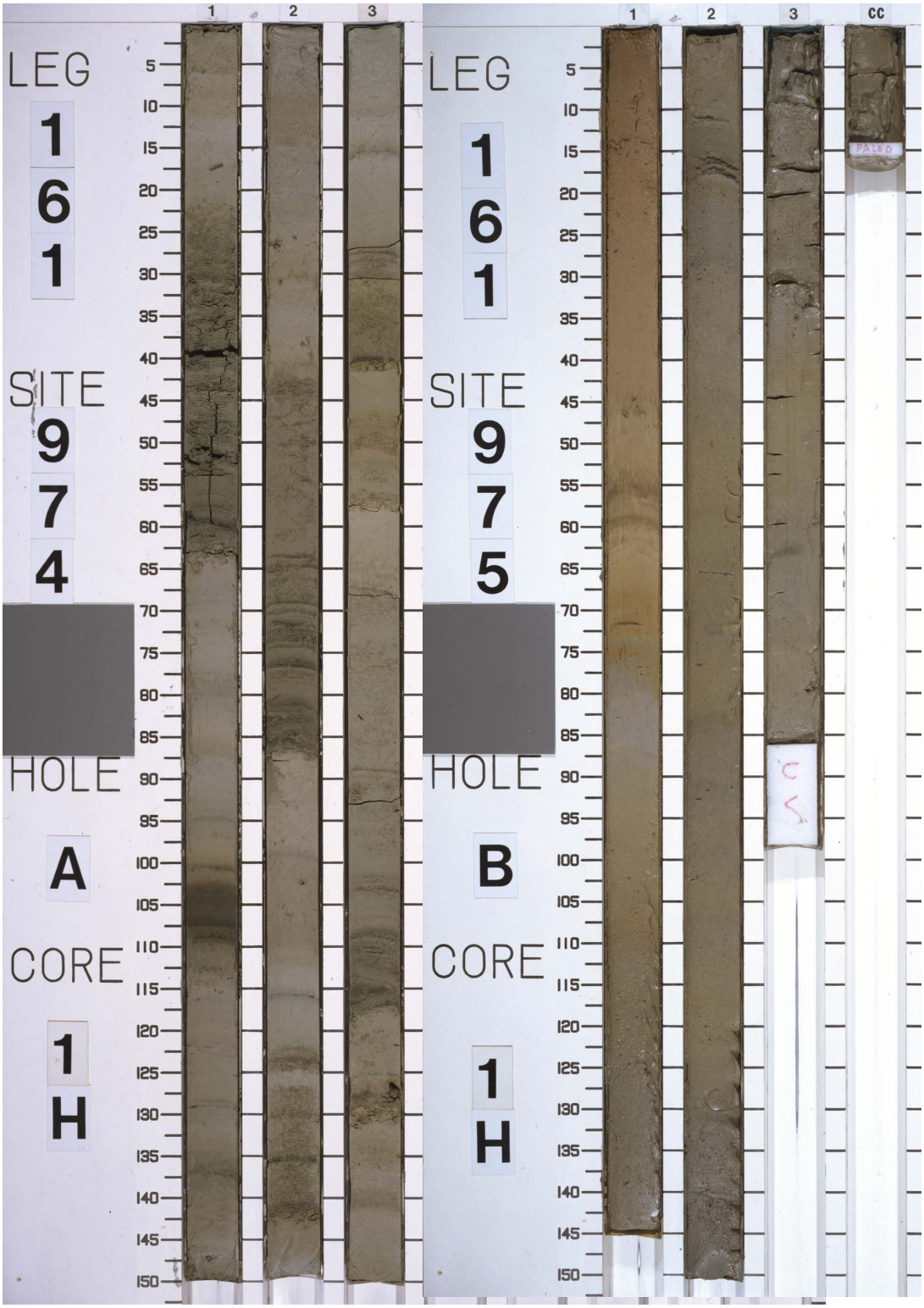
LEG
161
SITE
974
HOLE
A
CORE
1
H
1
2
3
LEG
161
SITE
975
HOLE
B
CORE
1
H
1
2
3
CC
PALEO

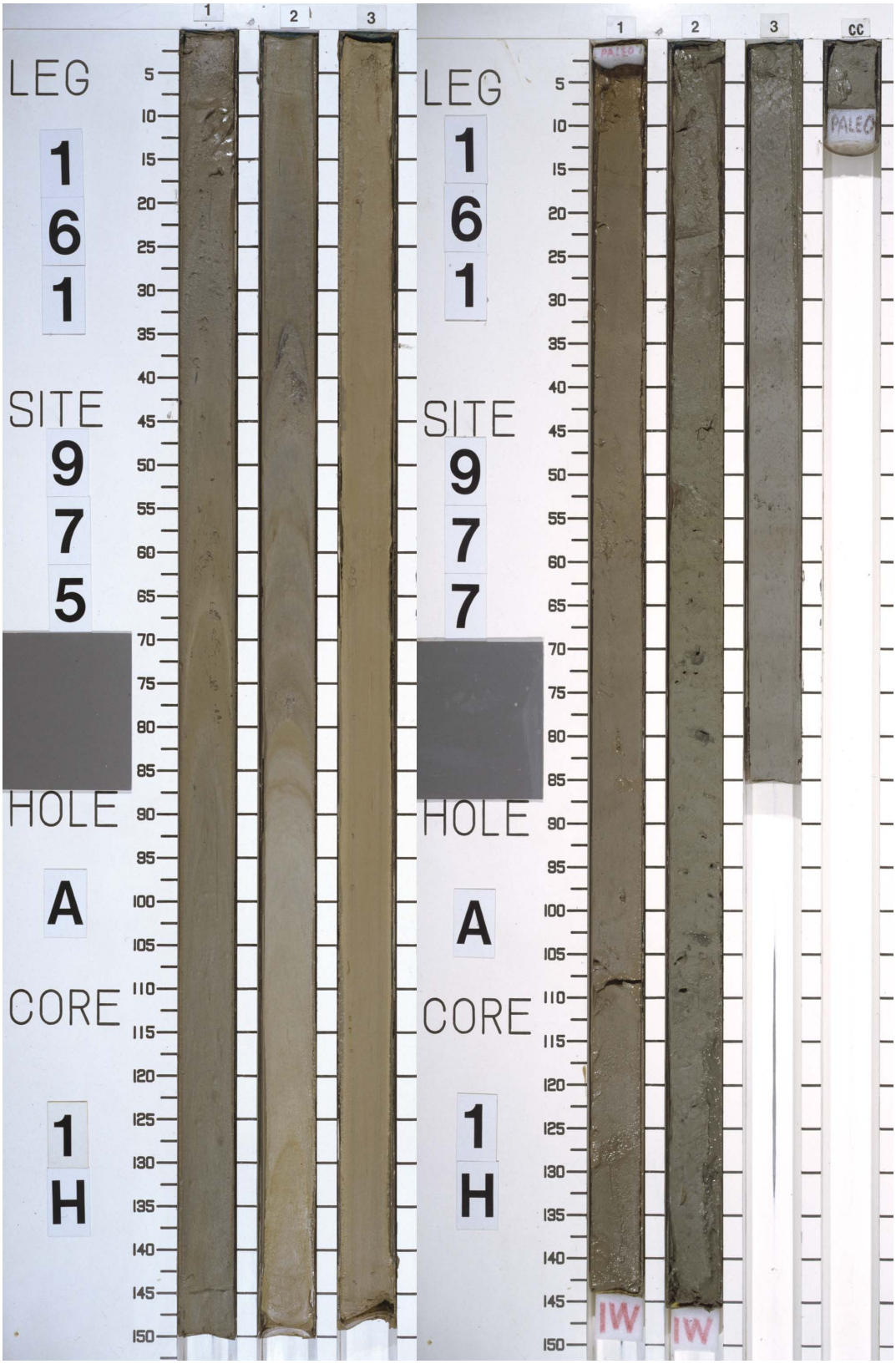
LEG
161
SITE
975
HOLE
A
CORE
1
H
1
2
3
LEG
161
SITE
977
HOLE
A
CORE
1
H
1
2
3
CC
PALEO
PALEO
IW
IW

# "Filtration method" for semi-quantitative powder X-ray diffraction analysis of clay minerals in marine sediments

Koichi Iijima[1], Francisco J. Jiménez-Espejo[2] and Tatsuhiko Sakamoto[1]

[1] Research Program for Paleoenvironment, Institute for Research on Earth Evolution (IFREE)
[2] Instituto Andaluz de Ciencias de la Tierra, University of Granada, Spain

## 1. Introduction

Several methods for clay minerals using semi-quantitative powder X-ray diffraction (XRD) analysis produces unique result due to its preparation procedure and XRD devices [*McManus*, 1991; *Moore and Reynolds*, 1989]. "Filtration method" and "air-dry method" are commonly used to prepare specimens of clay fraction for XRD, in particular to apply clay minerals to tracers in marine sediment. Relative contents of clay minerals are often utilized for spatial dispersal pattern or temporal fluctuation. These arguments founded on content values depend on reliable quantification process with less error. Filtration method theoretically provides uniform specimens; beside air-dry method latently involves specimens to enlarge the error within its preparation process. Accordingly, we made some examinations on preparation of clay fraction and filtration method to make sure which of two methods have preferable reproducibility. Firstly the process of filtration method we achieved, which is generally followed after *Petschick et al*. [1996], is described in detail. Subsequently, reproducibility of specimens made by two methods and application for marine sediments are discussed based on the operation that we validated.

## 2. Clay preparation for XRD

### 2.1 Separation of clay fraction from bulk sediments

Wet sediments were soaked in 30 ml of tap water and disaggregated for more than 24 hours. Sediments were not treated by hydrogenperoxide to dissolve organic materials and by acids to remove carbonates, on behalf of requirement to other operations. After removing of sand fraction (>63 μm φ) with wet sieve, supernatant of suspension contains tap water were removed by centrifuging at 3400 rpm for 1 hour. For deflocculation of particles, 0.001 mol/l sodium hexametaphosphate solutions were added. At this time, three dispersing agents, 1% sodium polyphosphate [*Petschick et al*., 1996], 0.0005 mol/l sodium hexametaphosphate [e.g., *Shirozu*, 1988] and 0.0005 mol/l sodium pyrophosphate [e.g., *Moore and Reynolds*, 1989], were attempted to compare effectiveness for particle separation and influence for clay minerals. Although sodium polyphosphate shows better ability for dispersion than that of sodium hexametaphosphate, it obviously attacked carbonate minerals (calcite peak was disappeared). Thus we selected sodium hexametaphosphate as the most efficient, non-destructive dispersing agent for clay mineral grains.

Silt fraction (2-63 μm φ) and clay fraction (<2 μm φ) were separated by centrifuging at 700 rpm three times using modified Stoke's law [*Shirozu*, 1988]. At each cycle, to correct centrifuging duration, we measured water temperature and distance to sink 2 μm particles. All extracted clay fraction were gathered in one tube and then washed by pure water for three times to remove dispersing agent. At last clay fraction was freeze dried before making XRD specimen.

### 2.2 Filtration method for XRD specimen

1 ml of 0.5% molybdenite suspension (0.3 μm grain-diameter) was added as internal standard to 40 mg of clay fraction in tube that preliminarily softly ground in an agate mortar. After addition of 2 ml of pure water, to avoid destruction of clay and molybdenite grains, ultrasonic dispersion of suspension was limited within 1 minute. Nevertheless talc and corundum are frequently adopted as internal standard for quantitative XRD analysis, molybdenite has many advantages such as; acute diffraction peak and substantial intensity with few amount, suitable peak position for clay minerals around 6.15 Å, and uncommon mineral in marine sediments [*Quakernaat*, 1970]. Disadvantages of molybdenite are difficulty to create powder of ordered particle size and to disperse in water, due to its high flexibility and electric charge. We persevered in development of fine molybdenite fraction and stock suspension.

After withdrawal from ultrasonic bath, whole suspension was immediately put into funnel of a vacuum filtration system with Millipore© membrane filter (JHWP04700, 0.45 μm pore diameter). The filter in this examination did not pass through particles. First filtration to drain all fluid was carried out within 5 minutes to avoid grain sedimentation on the filter. If it takes longer, suspension was stirred to keep homogenous. Molybdenite density is heavier than that of common clay minerals, which represents that molybdenite grains will concentrate near the filter, and clay cake homogeneity cannot be ensured. In succession, 1 ml of 0.1 mol/l magnesium chloride solution were followed to replace all free cations with Mg ions, and washed by pure water to remove excess cation and chloride ion. After filtration was completed entirely, "clay cake" on the filter was carefully transferred onto a glass slide. At this time, one drop of pure water was previously put on the slide to remove air bubble between the clay cake and the slide. Finally, the clay cake was dried for 15 minutes at 50 °C with the filter. The filter was slowly removed after it became white from semitransparent.

## 3. Comparison between filtration method and air-dry method

Although both filtration method and air-dry method have advantages and disadvantages, respectively, we preferred the former because of its convincing merits with low fractionation and definable thickness in the clay cake, for quantitative XRD analysis [*Moore and Reynolds*, 1989]. By grain-sized segregation in the

suspension, fine homogeneity in clay cake cannot be ensured by air-dry method [*Drever*, 1973]. In addition, clay cakes made by filtration method have all equivalent shape so we can easily control the thickness (mg/cm$^2$), while those made by air-dry method has difficulty to keep certain thickness. It is impossible to compare directly between specimens with different thickness since thinner clay cake thickness induces more loss of incident X-ray at high diffraction angles, which provides less diffraction and incorrect quantification. In other words, to contrast distinct samples, all specimens are required to be arranged in same thickness or to be mounted sufficient thickness called "infinite thickness" [e.g., *Moore and Reynolds*, 1989]. Furthermore, for quantitative XRD analysis, internal standard must have entirely been mixed and homogenized with crystals at certain ratio [*Alexander and Klug*, 1948; B*rindley and Brown*, 1980]. Molybdenite internal standard solution allows us to take fine mixture on the process of making specimen.

### *3.1 Reproducibility of specimen from the identical clay sample*

We have attempted to evaluate the precision of relative content of four clay mineral groups calculated from specimens adopted both in filtration and air-dry methods. Five specimens were made by each two methods and were measured by XRD to estimate a reproducibility of specimen. One air-dried specimen was measured five times to estimate a measurement error. Air-dried specimens were made from 0.8 ml of clay suspensions dispersed 8 mg clay. Suspensions were carefully smeared in 2.6 cm diameter round shape (5.31 cm$^2$) as possible. In this case, clay cake thickness of air-dry method specimen was 1.5 mg/cm$^2$ and that of filtration method specimen was 7.5 mg/cm$^2$ (40 mg clay). Marine sediment samples for this examination were collected by Ocean Drilling Program Leg160 in eastern Mediterranean Sea.

XRD measurements were carried out using Mac Science MXP3 HF diffractometer equipped with Cu target (40kV, 20mA, K$\alpha$1=1.54056Å), automatic goniometer and graphite monochromator, by a step scan with 2 seconds of counting time. "Normal scan" was firstly measured through 2-40° 2θ with 0.02° step, and subsequently "slow scan" was measured through 24-26° 2θ with 0.006° step to confirm kaolinite and chlorite content ratio. Then specimens were exposed in ethylene glycol vapor in small desiccator at 50°C for more than 24 hours. After saturation of ethylene glycol molecule, each "glycolated scan" was measured through 2-20° 2θ with 0.02° step, as soon as it was taken out from desiccator, one by one. Representative diffraction patterns of normal and glycolated measurements of one filtration specimen are shown in Figure 1.

All diffraction data were transferred to Apple Macintosh computer and were computed using MacDiff software [*Petschick et al*., 1996]. After peak correction of profile using molybdenite peak (without slow scan data), profiles were smoothed and fixed the baseline, and then d-value, peak intensity, peak area of four clay mineral groups (smectite 17Å, illite 10Å, kaolinite 3.58Å, and chlorite 3.54Å) were counted. Finally relative contents of four groups were determined by empirical coefficients; smectite peak area multiply by 1, illite peak area multiply by 4, and 7Å of kaolinite-chlorite doublet peak area multiply by 2 [*Biscaye*, 1965]. Relative content of kaolinite and chlorite were computed from respective peak areas arithmetically separated by peak fitting program [*Elverhøi and Rønningsland*, 1978].

Average value, standard deviation and relative error of relative contents (wt %) calculated from five distinct specimens are shown in Table 1. It is impossible to compare peak height or peak area intensity directly between two methods because clay cake thickness is quite different between them. All four standard deviation values of filtration method specimens are lower than that of air-dry method specimens, as well as lower than measurement repetition error of air-dried specimen measurements. This phenomenon definitely represents the uniformity of specimens made by filtration method. We did not verify whether quantification process is proper using artificial clay mixture of known content ratio, but in this examination we do consider only precision to estimate reproducibility of specimens, so we do not deal with accuracy of calculated relative content values. To make sure of it, according to relative error values, three group's values shows positive than measurement error except illite group. The other significant fact is inconsistency of smectite and illite contents between two methods. We interpreted it as difference in degree of orientation. Air-dried specimens were settled in stable atmosphere and they had needed almost 1 day to accomplish drying. During this period, illite grains were well oriented, and they provided high diffracted intensity in measurement.

### *3.2 Practical application for marine sediments*

Two methods were applied to 12 discrete samples collected by ODP leg161 in western Mediterranean Sea. Procedures for XRD measurement and calculation were same as mentioned above. Four correlation plots for relative content of clay mineral groups between two methods are shown in Figure 2. Smectite group content estimated from air-dried specimens are mostly higher than filtration specimens. This trend represents that fine particles of smectite grains were accumulated on the surface of specimens. The other deduction of this phenomenon is high orientation of smectite through drying of air-dried specimens, similarly observed in illite at former experiment. However, because smectite is scarcely contained in these sediments (~10 wt %) and the range of contents are restricted, it could not determine whether miscalculation of diffraction data or smectite grain's behavior on the specimens. Chlorite group content of air-dried specimens are slightly under-estimated in comparison with filtration specimens, which deduced from over-estimation of smectite group. Illite content and kaolinite content of filtration specimens are almost consistent with air-dried specimens, except one sample.

## *4. Summary*

Since individual method produces respective consequence, it is precarious to make immediate approach one another. As observed in this paper, semi-quantification of clay minerals using air-dry method specimens involves unexpected problems and complications, such as low reproducibility of specimen, particular orientation of specific minerals and grain segregation. Especially for quantitative analysis, therefore, we recommend the filtration method to utilize clay minerals precisely for marine sediments.

## *References*

Alexander, L.E. and H.P. Klug, Basic aspects of x-ray absorption in quantitative diffraction analysis of powder mixtures, *Anal. Chem*., 20, 886-889, 1948.

Biscaye, P.E., Mineralogy and sedimentation of recent deep-sea clay

in the Atlantic Ocean and adjacent seas and oceans, *Geol. Soc. Am. Bull*., 76, 803-832, 1965.

Brindley, G.W. and Brown, G. (Editors), Crystal Structures of Clay Minerals and their X-ray Identification, Miner. Soc. Monogr., London, 495pp, 1980.

Drever, J.I., The preparation of oriented clay mineral specimens for X-ray diffraction analysis by a filter-membrane peel technique, *Am. Miner*., 58, 553-554, 1973.

Ehrmann, W.U., M. Melles, G. Kuhn and H. Grobe, Significance of clay mineral assemblages in the Antarctic Ocean, *Mar. Geol*., 107, 249-273, 1992.

Elverhøi, A. and T.M. Rønningsland, Semiquantitative calculation of the relative amounts of kaolinite and chlorite by X-ray diffraction, *Mar. Geol*., 27, M19-M23, 1978.

McManus, D.A., Suggestions for authors whose manuscripts include quantitative clay mineral analysis by X-ray diffraction, *Mar. Geol*., 98, 1-5, 1991.

Moore, D.M. and R.C. Reynolds Jr., (Editors), X-Ray Diffraction and the Identification and Analysis of Clay Minerals, Oxford Univ. Press, 322pp, 1989.

Petschick, R., G. Kuhn and F. Gingele, Clay mineral distribution in surface sediments of the South Atlantic: sources, transport, and relation to oceanography, *Mar. Geol*., 130, 203-229, 1996.

Quakernaat, J., Direct diffractometric quantitative analysis of synthetic clay mineral mixtures with molybdenite as orientation-indicator, *J. Sediment. Petrol*., 40, 506-513, 1970.

Shirozu, H. (Editor), Introduction to Clay Mineralogy -Fundamentals for Clay Science-, Asakura Pub., Japan, 185pp, 1988.

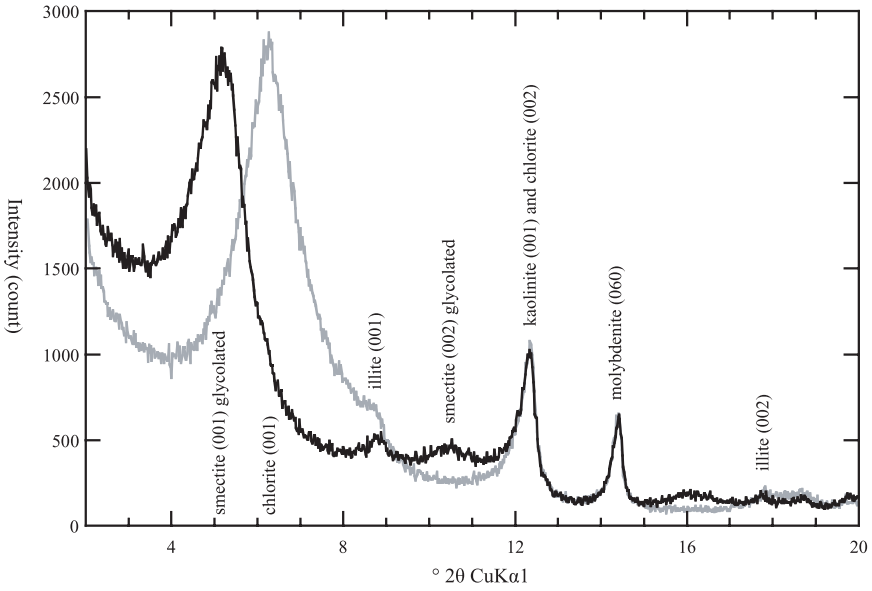


**Figure 1**. Typical diffraction profiles of a filtration method specimen. Black line represents glycolated scan and gray line represents normal scan. Mineral name and Miller's indices are based on glycolated scan.

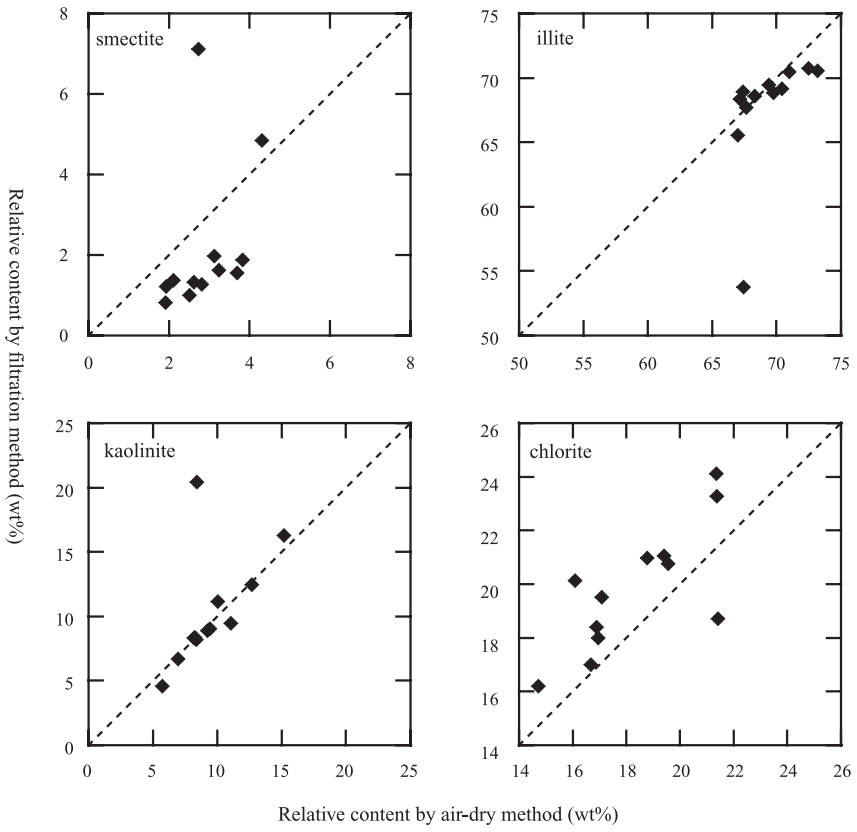


**Figure 2**. Correlation plots of relative content values derived from filtration method and air-dry method. Dotted line means equal.

**Table 1.** Relative content values of filtration and air-dry method averaged from five specimens for each method. Measurement error was derived from five measurement repetition of one air-dried specimen.

| | | smectite | illite | kaolinite | chlorite |
|---|---|---|---|---|---|
| Filtration method | Relative content (wt%) | 59.0 | 29.0 | 6.4 | 5.6 |
| | Standard deviation | 2.0 | 2.4 | 0.4 | 0.5 |
| | Relative error (%) | 3.5 | 8.1 | 6.5 | 8.2 |
| Air-dry method | Relative content (wt%) | 50.5 | 37.8 | 6.7 | 4.9 |
| | Standard deviation | 4.9 | 4.8 | 0.5 | 0.7 |
| | Relative error (%) | 9.8 | 12.7 | 6.8 | 13.3 |
| Measurement error | Relative content (wt%) | 50.6 | 38.5 | 6.2 | 4.7 |
| | Standard deviation | 2.3 | 2.8 | 0.6 | 0.8 |
| | Relative error (%) | 4.6 | 7.2 | 9.5 | 16.7 |

LETTERS

# Late survival of Neanderthals at the southernmost extreme of Europe

Clive Finlayson[1,2], Francisco Giles Pacheco[3], Joaquín Rodríguez-Vidal[4], Darren A. Fa[1], José María Gutierrez López[5], Antonio Santiago Pérez[3], Geraldine Finlayson[1], Ethel Allue[6], Javier Baena Preysler[7], Isabel Cáceres[6], José S. Carrión[8], Yolanda Fernández Jalvo[9], Christopher P. Gleed-Owen[10], Francisco J. Jimenez Espejo[11], Pilar López[12], José Antonio López Sáez[13], José Antonio Riquelme Cantal[14], Antonio Sánchez Marco[9], Francisco Giles Guzman[15], Kimberly Brown[16], Noemí Fuentes[8], Claire A. Valarino[1], Antonio Villalpando[15], Christopher B. Stringer[17], Francisca Martinez Ruiz[11] & Tatsuhiko Sakamoto[18]

**The late survival of archaic hominin populations and their long contemporaneity with modern humans is now clear for southeast Asia[1]. In Europe the extinction of the Neanderthals, firmly associated with Mousterian technology, has received much attention, and evidence of their survival after 35 kyr BP has recently been put in doubt[2]. Here we present data, based on a high-resolution record of human occupation from Gorham's Cave, Gibraltar, that establish the survival of a population of Neanderthals to 28 kyr BP. These Neanderthals survived in the southernmost point of Europe, within a particular physiographic context, and are the last currently recorded anywhere. Our results show that the Neanderthals survived in isolated refuges well after the arrival of modern humans in Europe.**

The association between Neanderthals and Gibraltar dates to 1848 when a Neanderthal cranium was discovered at Forbes's Quarry[3]. The excavation of the Devil's Tower rock shelter in 1925–26 by Dorothy Garrod produced a second Neanderthal cranium with associated Mousterian industry[4]. It has since been established beyond doubt that the Neanderthals were the makers of the Mousterian in western Europe[5]. In Gibraltar there are currently eight Neanderthal occupation sites on the 6-km-long 426-m-high rock. The presence of Mousterian technology in Gorham's Cave, Gibraltar, was established during excavations made between 1948 and 1954 (ref. 6). The site was revisited from 1995 with a view to establishing the timing of the Middle to Upper Palaeolithic transition. A date of $32.28 \pm 0.42$ kyr BP (OxA-7857) was obtained for the uppermost Mousterian levels[7]. Before 1997 all excavations and soundings had been made in the external part of the cave. Problems of contamination of radiocarbon samples from wet, unprotected, exterior, parts of caves have recently been brought to light[2]. Here we describe the results of a series of excavations deep within Gorham's Cave between 1999 and 2005.

Excavations have been made of 29 $m^2$ of cave floor. The stratigraphy is composed of four levels (Fig. 1). Level I corresponds to Phoenician and Carthaginian (eighth to third century BC) horizons; level II corresponds to a brief occupation during the Neolithic. The two levels of interest in this paper are levels III and IV. The technology associated with level III, from which 240 artefacts have been recovered so far, is Upper Palaeolithic. The raw materials are predominantly flints, cherts and some quartzites. Three horizons have been identified, two corresponding to occupation during the Solutrean (Supplementary Information) and a higher horizon that corresponds to the Magdalenian (Supplementary Information). Aurignacian and Gravettian are absent. The technology associated with level IV, with 103 artefacts recovered so far, is exclusively Mousterian with flints, cherts and quartzites (Supplementary Information). Previous excavations by Waechter[6] also attributed the Upper Palaeolithic to the Solutrean and Magdalenian. Barton[7] and Pettit & Bailey[8] found only a few, undiagnostic, Upper Palaeolithic pieces in their profiles.

Figure 1 and Table 1 present 30 accelerator mass spectrometry (AMS) dates in stratigraphic position for levels III and IV in the deepest part of the cave. The samples were identified as individual pieces of charcoal under a microscope before being dated. The 22 AMS dates from the upper part of level IV span a 10-kyr period between 33 and 23 kyr BP. We have not attempted to calibrate the dates in view of the uncertainty surrounding calibration beyond 26 kyr cal BP[9]. The dates suggest a favoured location that was visited repeatedly over many thousands of years. Its situation, where natural light penetrates deep into the cave and where a high ceiling permits ventilation of smoke, is unique within the cave system, and hearths were made in the same location many times. This repeated use is confirmed by the stratigraphic distribution of the dates within level IV that indicate localized alterations due to use and reuse (for example trampling and cleaning) in the area around the position of the hearths but dates in stratigraphic sequence within the location of the hearths themselves. Thus, three samples (16, 17 and 20; Fig. 1) came from *in situ* Mousterian superimposed hearths. These three dates provide a stratigraphic sequence from $24{,}010 \pm 320$ to $30{,}560 \pm 720$ yr BP. Taken together, all the dates show that Neanderthals occupied the site until 28 kyr BP and possibly as recently as 24 kyr BP. The evidence in support of the 24 kyr BP date is more limited than for 28 kyr BP, which is taken as the latest well-supported

[1]The Gibraltar Museum, 18–20 Bomb House Lane, Gibraltar. [2]Department of Social Sciences, University of Toronto at Scarborough, Toronto, Ontario M1C 1A4, Canada. [3]Museo Arqueologico de El Puerto Santa María, 11500 El Puerto Santa María, Spain. [4]Departamento de Geodinámica y Paleontología, Facultad de Ciencias Experimentales, Universidad de Huelva, 21071 Huelva, Spain. [5]Museo Municipal, 11650 Villamartín, Spain. [6]Institut Catala de Paleoecologia Humana i Evolucio Social, Area de Prehistoria, Universidad Rovira i Virgili, 43003 Tarragona, Spain. [7]Departamento de Prehistoria y Arqueología, Universidad Autonoma, 28049 Madrid, Spain. [8]Department of Plant Biology, Universidad de Murcia, 30100 Murcia, Spain. [9]Museo Nacional de Ciencias Naturales (CSIC), 28006 Madrid, Spain. [10]The Herpetological Conservation Trust, Bournemouth, Dorset BH1 4AP, UK. [11]Instituto Andaluz de Ciencias de la Tierra, CSIC-UGR, 18002 Granada, Spain. [12]Department of Geography, Royal Holloway College, University of London, Egham, Surrey TW20 0EX, UK. [13]Laboratorio de Arqueobotánica, Instituto de Historia (CSIC), 28014 Madrid, Spain. [14]Departamento de Prehistoria y Arqueologia, Universidad de Granada, 18071 Granada, Spain. [15]Area de Prehistoria, Facultad de Filosofía y Letras, Universidad de Cádiz, 11003 Cádiz, Spain. [16]Department of Biological Anthropology, University of Cambridge, Cambridge CB2 3DZ, UK. [17]Department of Palaeontology, The Natural History Museum, London SW7 5BD, UK. [18]Institute for Research on Earth Evolution, Japan Agency for Marine-Earth Science and Technology, Yokosuka 237-0061, Japan.



©2006 Nature Publishing Group

occupation date. The level III dates represent a different occupation pattern and are consistent with sporadic visits to the cave during the Solutrean and Magdalenian and are separated from the Mousterian occupation by a stratigraphic gap of at least 5 kyr (Fig. 1 and Table 1).

Geochemical detrital ratios such as K/Al and Mg/Al are constant within each level at Gorham's Cave and different from each other. Level IV has a particular composition that differs from the rest of the sequence (Supplementary Information). Representative samples from all levels were analysed geochemically and mineralogically (Supplementary Information). The resulting data have been used as proxies to establish a sedimentary regime for the deep part of the cave, geochemical ratios acting as fingerprints in each level[10]. The sediments sampled were predominantly composed of clay minerals, calcite and quartz, with small quantities of dolomite, ankerite and feldspars. Levels III and IV are clearly differentiated. Level IV has a geochemical characterization that is clearly different from other levels that contain Mg/Al and K/Al ratios that are almost twice as high (Supplementary Information). A sharp change in concentration of most of the elements analysed was detected between levels III and IV, suggesting a sudden change in environmental conditions and/or occupational pattern. Together with the absence of Upper Palaeolithic tools in level IV and of any dates older than 19 kyr BP in level III, the geochemical results confirm that there is no contamination of level IV from the upper levels and that the boundary between levels III and IV is sharp and clear.

Taphonomic study (Supplementary Information) indicated that all taxa and animal sizes, according to weight, showed evidence of human-induced damage (for example cut-marks, percussion scars and conchoidal breakage), affecting 14.4% of identified specimens. This is in agreement with other Middle Palaeolithic sites[11,12].

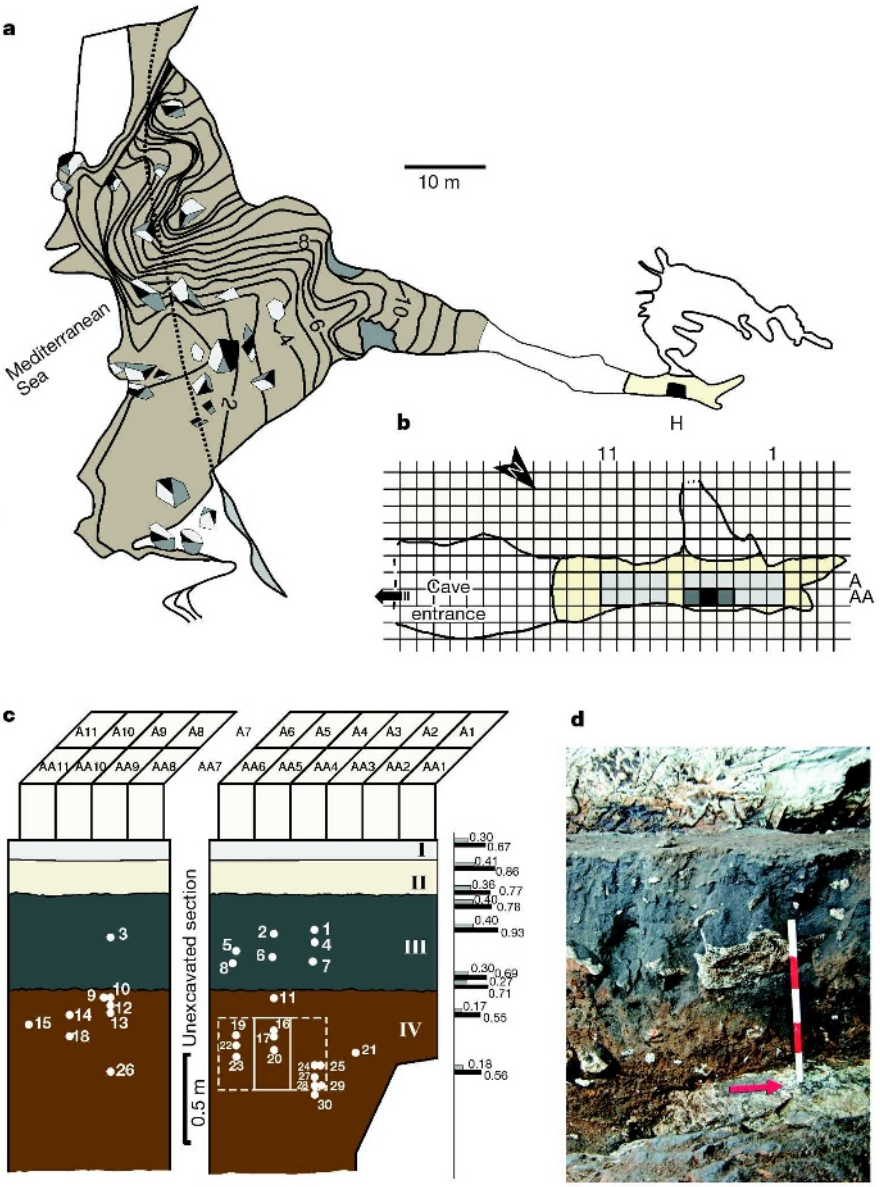


**Figure 1 | Plan of Gorham's Cave including the section excavated.** **a**, General plan of Gorham's Cave showing, at the right, the excavated area in the deep part of the cave (yellow) and the location of the hearth site (black). **b**, Detail of the excavated area (light grey) with the hearth site (black) and the hearth radius of influence (dark grey; see **c**). **c**, Stratigraphy of the excavated inner part of Gorham's Cave described in the text. Numbered dots indicate the positions of charcoal samples; the corresponding AMS dates are given in Table 1. The white rectangle marks the position of the Mousterian hearth site (see also Supplementary Information). Hatched lines indicate the hearth's radius of influence indicated by charcoal concentrations. The column on the right gives K/Al (black bars) and Mg/Al (grey bars) values for specific points in the stratigraphy (see Supplementary Information for details). The grid above the figure shows the $1 \times 1$ m squares excavated. **d**, Photograph showing the section at AA2–AA3. Level IV (brown, below) is clearly differentiated from level III (grey, above). The red arrow indicates north.



©2006 Nature Publishing Group

**Table 1 | The 30 AMS dates in the sequence illustrated in Fig. 1**

| Sample no.* | Laboratory reference | AMS radiocarbon age (yr)† | $^{13}C/^{12}C$ ratio (‰) |
|---|---|---|---|
| 1 | Beta-181896 | 13,870 ± 80 | −24.0 |
| 2 | Beta-185343 | 10,880 ± 80 | −25.4 |
| 3 | Beta-181895 | 12,460 ± 100 | −24.0 |
| 4 | Beta-184047 | 12,640 ± 100 | −25.4 |
| 5 | Beta-196780 | 13,820 ± 100 | −24.6 |
| 6 | Beta-196777 | 12,540 ± 100 | −24.9 |
| 7 | Beta-181893 | 16,420 ± 120 | −25.5 |
| 8 | Beta-184042 | 18,440 ± 160 | −21.7 |
| 9 | Beta-196785 | 26,070 ± 360 | −25.6 |
| 10 | Beta-196784 | 28,360 ± 480 | −26.1 |
| 11 | Beta-185344 | 27,020 ± 480 | −25.0 |
| 12 | Beta-196786 | 29,910 ± 600 | −24.7 |
| 13 | Beta-196787 | 31,480 ± 740 | −23.7 |
| 14 | Beta-196792 | 30,310 ± 620 | −24.7 |
| 15 | Beta-185345 | 23,780 ± 540 | −25.0 |
| 16 | Beta-196775 | 24,010 ± 320 | −24.0 |
| 17 | Beta-196773 | 26,400 ± 440 | −23.2 |
| 18 | Beta-196791 | 28,570 ± 480 | −25.2 |
| 19 | Beta-196779 | 29,400 ± 540 | −25.4 |
| 20 | Beta-196776 | 30,560 ± 720 | −24.5 |
| 21 | Beta-184045 | 31,110 ± 460 | −23.7 |
| 22 | Beta-196778 | 29,720 ± 560 | −24.8 |
| 23 | Beta-196782 | 23,360 ± 320 | −22.4 |
| 24 | Beta-196768 | 31,290 ± 680 | −25.8 |
| 25 | Beta-196772 | 31,780 ± 720 | −23.1 |
| 26 | Beta-196789 | 32,100 ± 800 | −24.5 |
| 27 | Beta-196769 | 31,850 ± 760 | −23.5 |
| 28 | Beta-196770 | 28,170 ± 480 | −25.9 |
| 29 | Beta-184048 | 29,210 ± 380 | −25.2 |
| 30 | Beta-196771 | 32,560 ± 780 | −25.1 |

Level III dates are numbered 1 to 8; level IV dates are numbered 9 to 30. Three dates from the hearth position are numbered 16, 17 and 20.
* Sample numbers are those used in Fig. 1.
† Errors shown are $2\sigma$.

Carnivore activity is present, but it is not conspicuous (only 5.7% of the remains were affected by carnivore tooth-marks). Post-depositional alterations are not especially destructive; trampling, which produced surface scratches, was the principal factor (7.8%). No bone fragments or artefacts could be refitted. Evidence of re-sedimentation or reworking was not observed either. This confirms that most taxa represented at Gorham's Cave were brought from the surrounding environments by humans and butchered inside the cave with a subsequent negligible access to scavengers.

The sequence of radiocarbon dates presented, including 14 dates at or statistically younger than 30 kyr BP, are the only currently reliable ones that establish the persistence of Neanderthals and associated Mousterian technology after 30 kyr BP. Earlier claims are now dismissed or are uncertain for a variety of reasons and in particular after the revision of dates on bone with the use of ultrafiltration treatment, a treatment only meaningful for dates on bone[13]. Hyaena Den (UK) is now considered older than 30 kyr BP[2]; the Vindija (Croatia) Neanderthals have been re-dated to between 32 and 33 kyr BP or older[14]; Zafarraya (Spain) is now discarded for several reasons[15]; the Mezmaiskaya, Russia, Neanderthal is now dated to at least 36 kyr BP[16]. The single AMS date on *Cervus* bone for Caldeirão (Portugal)[17] will require revision and is likely, given the result for Hyaena Den of similar age[2], to be older than 30 kyr BP. Finally, the single $^{14}C$ date, from *Patella* shells, from Figueira Brava, Portugal, is not statistically younger than 30 kyr BP[17].

The last Neanderthals that occupied Gorham's Cave had access to a diverse community of plants and vertebrates on the sandy plains, open woodland and shrubland, wetlands, cliffs and coastal environments surrounding the site. Such ecological diversity might have facilitated their long survival. The overall pattern of fauna and vegetation in the late Mousterian level IV is consistent with that occurring outside the cave for the greater part of the Late Pleistocene and indicates Mediterranean glacial refugium conditions with a Thermo/Meso-Mediterranean, subhumid climate (Supplementary Information). It consisted of a broad mosaic of mesothermophilous plant communities, open parkland habitats and seasonal fresh and brackish water sources (Supplementary Information).

The Neanderthals therefore persisted in Mediterranean environments that had acted as glacial refugia for many species throughout the Quaternary period[18]. The presence of Aurignacian technology in Bajondillo, Málaga, about 100 km east of Gibraltar at around 32 kyr BP (ref. 19) and of sporadic Gravettian sites after this[20] indicates that the late survival of Neanderthals and the arrival of modern humans was a mosaic process in which pioneer groups of moderns and remnant groups of Neanderthals together occupied a highly heterogeneous region for several thousand years. The low density of early Upper Palaeolithic sites in southern Iberia[20] and the late presence of Neanderthals, reported in this paper, indicate that for a long time populations of both Neanderthals and modern humans were thinly scattered across the region. The absence of transitional industries that have been attributed to Neanderthal–modern cultural contact[21], as are found in northern Iberia and France (Châtelperronian), adds weight to the view of limited contact between Neanderthals and moderns in southern Iberia. The transition from the Middle to the Upper Palaeolithic was not, in southern Iberia at least, a sudden rupture but instead took the form of a long and diffuse spatio-temporal mosaic involving populations at low density.

## METHODS

Cave deposits often have a complex sedimentation and the possibility of mixing of sediments cannot be discounted. Representative samples were therefore taken from each level at Gorham's Cave and were analysed, both geochemically and mineralogically, with the aim of checking the homogeneity of the stratigraphic levels and the conditions in the cave. The resulting data have been used as proxies to establish a sedimentary regime and conditions within the cavity. The four stratigraphical levels (I–IV) were sampled. Sediment samples were dried and homogenized in an agate mortar for mineralogical and geochemical analyses.

Bulk mineral compositions were obtained by X-ray diffraction (XRD) in accordance with international recommendations[22]. X-ray diffractograms were obtained with a Philips PW 1710 diffractometer with CuK$\alpha$ radiation and an automatic slit. Resulting diffractograms were interpreted with Xpowder software[23]. Major element measurements (Mg, Al, K, Ca, Mn and Fe) were obtained by atomic absorption spectrometry (AAS; Perkin-Elmer 5100 spectrometer) with an analytic error of 2% in the Analytical Facilities (CIC) of the University of Granada. Al, K, Ca, Ti, Mn, Fe, Cu and Sr have also been quantified with an X-ray fluorescence scanner in the Japan Agency for Marine-Earth Science and Technology (JAMSTEC) laboratories. The XRF-core scanner TATSCAN-F2 (ref. 24) was set to determine bulk intensities of major elements on split sediment sections at intervals of 0.5 cm with an accuracy in standard powder samples of better than 0.20 wt%. A depth correction was performed to compare AAS and XRF-scanner data, indicating a high correlation between techniques. Analyses of trace elements including Ba were performed with inductively coupled plasma–mass spectrometry (ICPMS) after digestion with $HNO_3$ plus HF. Measurements were performed in triplicate by spectrometry (Perkin-Elmer Sciex Elan 5000), with Re and Rh as internal standards. Variation coefficients determined by the dissolution of ten replicates of powdered samples were more than 3% and 8% for analyte concentrations of 50 and 5 p.p.m., respectively[25].

High-resolution geochemical mapping was performed with an XRF scanner in sediments proceeding from level IV (Supplementary Information). Results indicate a sublaminar sedimentation slightly turbated by limestone dropstone, flint tools, fossil bones and carbonate nodules. This confirms that sedimentation in level IV does not correspond to 'breccia' or chaotic deposits.

The 30 AMS dates presented in this paper were analysed by Beta Analytic Inc. All samples were pretreated to eliminate secondary carbon components. The samples were first gently crushed and dispersed in deionized water. They were then given acid washes with hot HCl to eliminate carbonates, and alkali washes with NaOH to remove secondary organic acids. The alkali washes were followed by a final acid rinse to neutralize the solution before drying. Chemical concentrations, temperatures, exposure times and number of repetitions, were applied according to the scarcity of the sample. Each chemical solution was neutralized before application of the next. During these serial rinses, mechanical contaminants such as associated sediments and rootlets were eliminated. This type of pretreatment is considered a 'full pretreatment'.



©2006 Nature Publishing Group

**Received 12 April; accepted 25 August 2006.**
**Published online 13 September 2006.**

1. Brown, P. *et al.* A new small-bodied hominin from the Late Pleistocene of Flores, Indonesia. *Nature* **431**, 1055–1061 (2004).
2. Mellars, P. A. A new radiocarbon revolution and the dispersal of modern humans in Eurasia. *Nature* **439**, 931–935 (2006).
3. Busk, G. On a very ancient cranium from Gibraltar. *Report of the 34th Meeting of the British Association for the Advancement of Science (Bath, 1864)* 91–92 (1865).
4. Garrod, D. A. E., Buxton, L. H. D., Elliot Smith, G. & Bate, D. M. A. Excavation of a Mousterian Rock-shelter at Devil's Tower, Gibraltar. *J. R. Anthropol. Inst.* **58**, 91–113 (1928).
5. Mellars, P. *The Neanderthal Legacy* (Princeton Univ. Press, Princeton, 1996).
6. Waechter, J. D'A. The excavations at Gorham's Cave, Gibraltar, 1951–1954. *Bull. Inst. Archaeol. Lond.* **4**, 189–221 (1964).
7. Barton, N. in *Neanderthals on the Edge* (eds Stringer, C. B., Barton, R. N. E. & Finlayson, C.) 211–220 (Oxbow Books, Oxford, 2000).
8. Pettitt, P. B. & Bailey, R. M. in *Neanderthals on the Edge* (eds Stringer, C. B., Barton, R. N. E. & Finlayson, C.) 155–162 (Oxbow Books, Oxford, 2000).
9. Reimer, P. J. *et al.* Comment on 'Radiocarbon calibration curve spanning 0 to 50,000 years BP based on paired 230Th/234U/238U and 14C dates on pristine corals' by R. G. Fairbanks *et al*. (*Quaternary Science Reviews* **24** (2005) 1781–1796) and 'Extending the radiocarbon calibration beyond 26,000 years before present using fossil corals' by T.-C. Chin *et al*. (*Quaternary Science Reviews* **24** (2005) 1797–1808). *Quat. Sci. Rev.* **25**, 855–862 (2006).
10. Romano, F. P. *et al.* Quantitative non-destructive determination of trace elements in archaeological pottery using a portable beam stability-controlled XRF spectrometer. *XRay Spectrom.* **35**, 1–7 (2006).
11. Gaudzinski, S. (2004) A matter of high resolution? The Eemian Interglacial (OIS 5e) in North-central Europe and Middle Palaeolithic subsistence. *Int. J. Osteoarchaeol.* **14**, 201–211 (2004).
12. Grayson, D. K. & Delpech, F. Ungulates and the Middle-to-Upper Paleolithic transition at Grotte XVI (Dordogne, France). *J. Archaeol. Sci.* **30**, 1633–1648 (2003).
13. Higham, T. F. G., Jacobi, R. M. & Bronk Ramsay, C. AMS radiocarbon dating of ancient bone using ultrafiltration. *Radiocarbon* **48**, 179–195 (2006).
14. Higham, T., Bronk Ramsey, C., Karavanic, I., Smith, F. H. & Trinkaus, E. Revised direct radiocarbon dating of the Vindija $G_1$ Upper Palaeolithic Neanderthals. *Proc. Natl Acad. Sci. USA* **103**, 553–557 (2006).
15. Barroso Ruiz, C. (ed.) *El Pleistoceno Superior de la Cueva del Boquete de Zafarraya* (Junta de Andalucía, Arqueología Monografías, 2003).
16. Skinner, A. R. *et al.* ESR dating at Mezmaiskaya Cave, Russia. *Appl. Radiat. Isot.* **62**, 219–224 (2005).
17. Zilhao, J. in *Neanderthals on the Edge* (eds Stringer, C. B., Barton, R. N. E. & Finlayson, C.) 111–119 (Oxbow Books, Oxford, 2000).
18. Finlayson, C. Biogeography and evolution of the genus *Homo*. *Trends Ecol. Evol.* **20**, 457–463 (2005).
19. d'Errico, F. & Sánchez Goñi, M. F. Neanderthal extinction and the millennial scale climatic variability of OIS 3. *Quat. Sci. Rev* **22**, 769–788 (2003).
20. Finlayson, C. *Neanderthals and Modern Humans* (Cambridge Univ. Press, Cambridge, 2004).
21. Mellars, P. The Neanderthal problem continued. *Curr. Anthropol.* **40**, 341–364 (1999).
22. Kirsch, H. J. Illite crystalinity: recommendations on sample preparation, X-ray diffraction settings, and interlaboratory samples. *J. Metamorphic Geol.* **9**, 665–670 (1991).
23. Martin, J. D. Qualitative and quantitative powder X-ray diffraction analysis. <http://www.xpowder.com> (2004).
24. Sakamoto, T. *et al.* 2006 non-destructive X-ray fluorescence (XRF) core imaging scanner, 'TATSCAN-F2' for the IODP science, scientific drilling. *Integrated ODP* **2**, 37–39 (2006).
25. Bea, F., Montero, P., Stroh, A. & Baasner, J. Microanalysis of minerals by an Excimer UV-LA-ICP-MS system. *Chem. Geol.* **133**, 145–156 (1996).

**Supplementary Information** is linked to the online version of the paper at www.nature.com/nature.

**Acknowledgements** We thank all those who have participated in this project. The project Palaeomed was co-funded by the Government of Gibraltar and the European Union Interreg IIIB Programme Medocc. Palynological and geochemical investigations were funded by Fundación Séneca, Murcia, Spain, and Ministerio de Educación y Ciencia, DGI, Spain, respectively. Geomorphological work was funded by Ministerio de Educación y Ciencia, DGI, Spain.

**Author Contributions** C.F., F.G.P., J.R.-V. and C.B.S. were responsible for project direction and management. C.F. coordinated the writing. Multidisciplinary work was divided as follows: archaeology and curation—F.G.P., J.M.G.L., A.S.P., J.B.P., F.G.G., K.B., C.A.V. and A.V.; geomorphology and sedimentology—J.R.-V., F.J.J.E., F.M.R. and T.S.; taphonomy—I.C. and Y.F.J.; palaeoecology—C.F., D.A.F. (general), G.F. (palaeolandscape), E.A. (anthracology), J.S.C., P.L., J.A.L.S., N.F. (palaeobotany), C.P.G.-O. (herpetological taxonomy), J.A.R.C. (mammalian taxonomy) and A.S.M. (avian taxonomy). All authors discussed and interpreted the results and commented on the manuscript.

**Author Information** Reprints and permissions information is available at www.nature.com/reprints. The authors declare no competing financial interests. Correspondence and requests for materials should be addressed to C.F. (jcfinlay@gibraltar.gi).



©2006 Nature Publishing Group